
Supplementary information

A species-level timeline of mammal evolution integrating phylogenomic data

In the format provided by the
authors and unedited

Supplementary Information for A Species-Level Timeline of Mammal Evolution Integrating Phylogenomic Data

Sandra Álvarez-Carretero^{†,1,2}, Asif U. Tamuri^{†,3,4}, Matteo Battini⁵, Fabrícia F. Nascimento⁶, Emily Carlisle⁵, Robert J. Asher⁷, Ziheng Yang², Philip C.J. Donoghue^{*5}, and Mario dos Reis^{*1}.

¹ School of Biological and Behavioural Sciences, Queen Mary University of London, London, UK.

² Department of Genetics, Evolution, and Environment, University College London, London, WC1E 6BT, UK.

³ Centre for Advanced Research Computing, University College London, Gower St, London, WC1E 6BT, UK.

⁴ EMBL-EBI, Wellcome Genome Campus, Hinxton, Cambridgeshire, CB10 1SD, UK

⁵ School of Earth Sciences, University of Bristol, Life Sciences Building, Tyndall Avenue, Bristol, BS8 1TQ, UK.

⁶ MRC Centre for Global Infectious Disease Analysis, School of Public Health, Imperial College London, London, UK.

⁷ Department of Zoology, University of Cambridge, Downing Street, Cambridge, CB2 3EJ, UK.

[†] Contributed equally to this work

^{*} Corresponding authors

Table of Contents

Data Collection and Filtering.....	2-7
Divergence Time Estimation	8-31
Integrity of time estimates across dating steps and data partitions	31
Technical comment on the sequential Bayesian-subtree approach	32-33
Benchmarking.....	33-34
Supplementary data structure.....	34-35
References	35
ANNEX: Justification for Fossil Calibrations.....	36-70
References for “Justification for Fossil Calibrations”	71-85

Data Collection and Filtering

Tables and Figures cited in the “Methods” section “*Data Collection and Filtering*” can be found below. They are shown in the same order in which they are cited in the corresponding subsections.

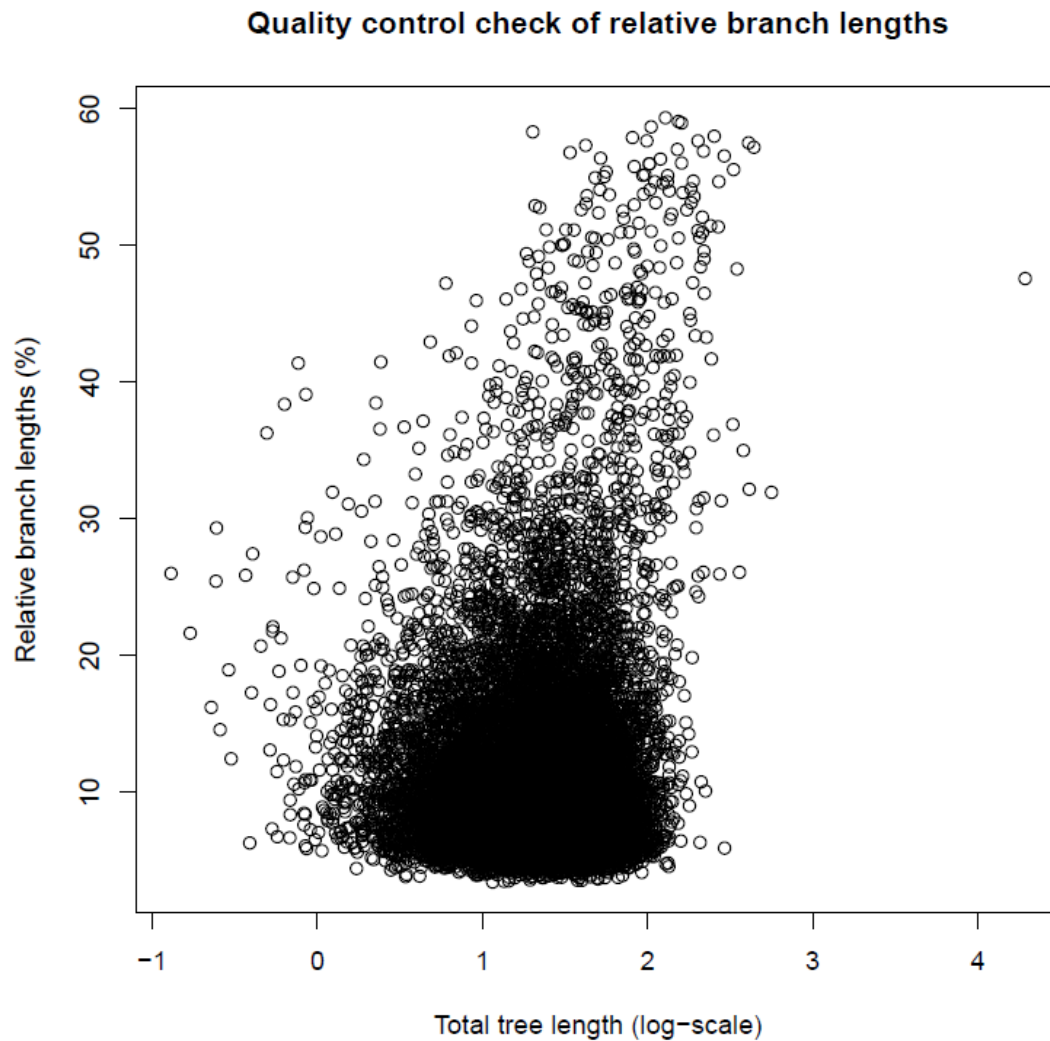


Figure S1: Quality control check of the estimated relative branch lengths (%) for each gene tree in comparison to the corresponding total tree length (log-scale). One of the criteria we had to keep a gene alignment was that the relative branch lengths (x-axis) could not be larger than or equal to 60% of the total length of the tree (y-axis). This plot shows how most of the gene trees have relative branch lengths that are 10-30% of the length of the tree, while few gene trees have relative branch lengths very close to the threshold (60%). Nevertheless, there is one outlier whose tree length in the log-scale is 4 units despite the relative branch length not accounting for more than 60% of the tree; there are at least two very long branch lengths in this gene tree. This plot is useful to visually identify which gene trees should be deleted according to the total log tree length that the relative branch lengths of each gene tree account for with regards to a specific threshold.

Table S1. Summary statistics for the 72-taxon gene alignments after each filtering step.

Filtering step	Raw	Initial filtering	Relative branch test	Pairwise distances	HMMER (dataset 2)
Number of genes left	15,904	15,569	15,436	15,431	15,268
Genes removed	0	335	133	5	163
% Removed	0	2.11	0.85	0.03	1.06
Cumulative genes removed	0	335	468	473	636
% Cumulative removed	0	2.11	2.94	2.97	4.00

Table S2. Number of taxa and orthologs, alignment length, corresponding site pattern counts, and missing data for each data subset and partition scheme. Partitions go from fastest-evolving (1) to slowest-evolving (4).

Data subset	No. taxa	No. orthologs	Alignment length (base pairs)	Site pattern counts	% Missing data
Partition 1	72	3,817	8,926,316	3,613,711	60.17
Partition 2	72	3,817	8,339,196	2,941,508	50.78
Partition 3	72	3,817	8,605,264	2,416,624	48.49
Partition 4	72	3,817	7,302,398	1,521,894	45.92

Table S3. Content of the mammal dataset after bioinformatics filtering.

Dataset	Data source	Data type	Dataset extended?	Range of taxa	No. genes
Dataset 1	Ensembl	Nuclear protein-coding	No	10-72	15,268
	ENA/HMM-profile RefSeq	Nuclear protein-coding	Yes, homology search	48-1,242	168
	RefSeq	Mitochondrial protein-coding	No	767	3
Dataset 2	ENA / HMM-profile		Yes, homology search	805-3,986	9
	ENA / HMM-profile	Mitochondrial non-coding rRNA	Yes, homology search	1,542-2,114	2

Table S4. Number of taxa (alignment length | site pattern counts) for mitochondrial subtrees and partitions. Monotremata is an outgroup in all subtrees.

Data subset	mit-12CP	mit-3CP	mit-RNA
Afrotheria	34 (7,226 2,298)	34 (3,613 3,352)	32 (2,786 1,486)
Euarchonta	452 (7,260 4,549)	452 (3,630 3,630)	289 (3,087 2,274)
Lagomorpha	82 (7,198 1,326)	82 (3,599 3,034)	46 (2,634 928)
Artiodactyla	419 (7,240 3,430)	419 (3,620 3,614)	293 (2,817 1,828)
Chiroptera (I)	216 (7,202 1,932)	216 (3,601 3,457)	133 (3,287 1,993)
Chiroptera (II)	566 (7,240 3,020)	566 (3,620 3,590)	328 (4,117 3,033)
Rest of Laurasiatheria	598 (7,320 3,710)	598 (3,660 3,640)	386 (3,402 2,436)
Marsupialia	260 (7,278 3,131)	260 (3,639 3,610)	215 (3,366 2,342)
Ctenohystica	174 (7,224 2,535)	174 (3,612 3,375)	125 (2,897 1,709)
Sciuridae and related	215 (7,200 2,068)	215 (3,600 3,398)	100 (2,958 1,727)
Rest of Rodentia (I)	602 (7,366 3,712)	602 (3,694 3,663)	167 (3,072 2053)
Rest of Rodentia (II)	636 (7,320 2,826)	636 (3,662 3,568)	127 (2,927 1,581)
Xenarthra	32 (7,210 1,980)	32 (3,605 3,404)	33 (2,655 1,190)

Table S5. Number of taxa (alignment length | site pattern counts) for nuclear subtrees and partitions. Monotremata is an outgroup in all subtrees.

Data subset	nuc-12CP	nuc-3CP
Afrotheria	52 (166,190 6,853)	52 (83,095 6,786)
Euarchonta	253 (193,708 40,599)	253 (96,854 42,084)
Lagomorpha	43 (130,746 1,845)	43 (65,373 2,070)
Artiodactyla	189 (191,394 19,451)	189 (95,697 20,472)
Chiroptera (I)	163 (222,499 8,057)	163 (80,524 9,316)
Chiroptera (II)	448 (234,986 9,407)	448 (117,248 10,205)
Rest of Laurasiatheria	453 (198,006 45,479)	453 (177,439 43,565)
Marsupialia	249 (171,898 10,417)	249 (85,949 9,322)
Ctenohystrica	116 (33,287 8,980)	116 (16,778 7,043)
Sciuridae and related	118 (24,890 2,967)	118 (12,445 3,115)
Rest of Rodentia (I)	379 (423,700 11,881)	379 (94,825 12,671)
Rest of Rodentia (II)	505 (206,736 8,285)	505 (95,950 7,878)
Xenarthra	20 (102,226 2,513)	20 (51,113 2,487)

Table S6. Total number of taxa and alignment length (across all partitions) for each subtree. Monotremata is an outgroup in all subtrees.

Data subset	Number of taxa	Total alignment length
Afrotheria	60	262,910
Euarchonta	486	304,539
Lagomorpha	88	209,550
Artiodactyla	431	300,768
Chiroptera (I)	256	317,113
Chiroptera (II)	634	367,211
Rest of Laurasiatheria	659	389,827
Marsupialia	307	272,130
Ctenohystrica	210	63,798
Sciuridae and related	267	51,093

Rest of Rodentia (I)	630	532,657
Rest of Rodentia (II)	691	316,595
Xenarthra	33	166,809

Table S7. Missing data (%) for each subtree partition before (top) and after (bottom) removing missing taxa. The percentage of missing data is calculated by dividing the number of gaps in the alignment by the number of taxa times the alignment length. The number of taxa is shown within brackets. We note missing taxa are not used by MCMCtree during likelihood calculation.

Data subset	mit-12CP	mit-3CP	mit-RNA	nuc-12CP	nuc-3CP
Afrotheria	70.66 (60)	70.66 (60)	55.44 (60)	93.16 (60)	93.16 (60)
	48.22 (34)	48.22 (34)	16.46 (32)	92.11 (52)	92.11 (52)
Euarchonta	51.51 (486)	51.51 (486)	58.28 (486)	96.02 (486)	96.02 (486)
	47.86 (452)	47.86 (452)	29.84 (289)	92.35 (253)	92.35 (253)
Lagomorpha	65.24 (88)	65.24 (88)	68.55 (88)	96.57 (88)	96.57 (88)
	62.69 (82)	62.69 (82)	39.84 (46)	92.98 (43)	92.98 (43)
Artiodactyla	35.83 (431)	35.83 (431)	43.86 (431)	97.85 (431)	97.85 (431)
	33.99 (419)	33.99 (419)	17.42 (293)	95.10 (189)	95.10 (189)
Chiroptera (I)	82.48 (256)	82.48 (256)	69.59 (256)	98.33 (256)	97.69 (256)
	79.23 (216)	79.23 (216)	41.47 (133)	97.37 (163)	96.37 (163)
Chiroptera (II)	82.84 (634)	82.84 (634)	71.68 (634)	99.16 (634)	99.16 (634)
	80.78 (566)	80.78 (566)	45.26 (328)	98.81 (448)	98.81 (448)
Rest of Laurasiatheria	59.35 (659)	59.35 (659)	66.98 (659)	97.84 (659)	98.80 (659)
	55.20 (598)	55.20 (598)	43.62 (386)	96.86 (453)	98.25 (453)
Marsupialia	61.52 (307)	61.52 (307)	57.51 (307)	97.39 (307)	97.39 (307)
	54.56 (260)	54.56 (260)	39.33 (215)	96.79 (249)	96.79 (249)
Ctenohystrica	83.33 (210)	83.33 (210)	76.03 (210)	93.96 (210)	94.01 (210)
	79.88 (174)	79.88 (174)	59.74 (125)	89.06 (116)	89.15 (116)
Sciuridae and related	84.83 (267)	84.83 (267)	85.37 (267)	96.57 (267)	96.57 (267)
	81.16 (215)	81.16 (215)	60.95 (100)	92.24 (118)	92.24 (118)

Rest of Rodentia (I)	81.15 (630)	81.21 (630)	87.69 (630)	99.51 (630)	98.90 (630)
	80.27 (602)	80.33 (602)	53.54 (167)	99.18 (379)	98.16 (379)
Rest of Rodentia (II)	84.02 (691)	84.03 (691)	90.69 (691)	98.96 (691)	98.88 (691)
	82.64 (636)	82.65 (636)	49.35 (127)	98.57 (505)	98.46 (505)
Xenarthra	3.30 (33)	3.30 (33)	4.67 (33)	90.04 (33)	90.04 (33)
	0.28 (32)	0.28 (32)	4.67 (33)	83.57 (20)	83.57 (20)

Divergence Time Estimation

Tables and Figures cited in the “Methods” section “*Divergence Time Estimation*” can be found below. They are shown in the same order in which they are cited in the corresponding subsections.

Figure S2 (a) - T1

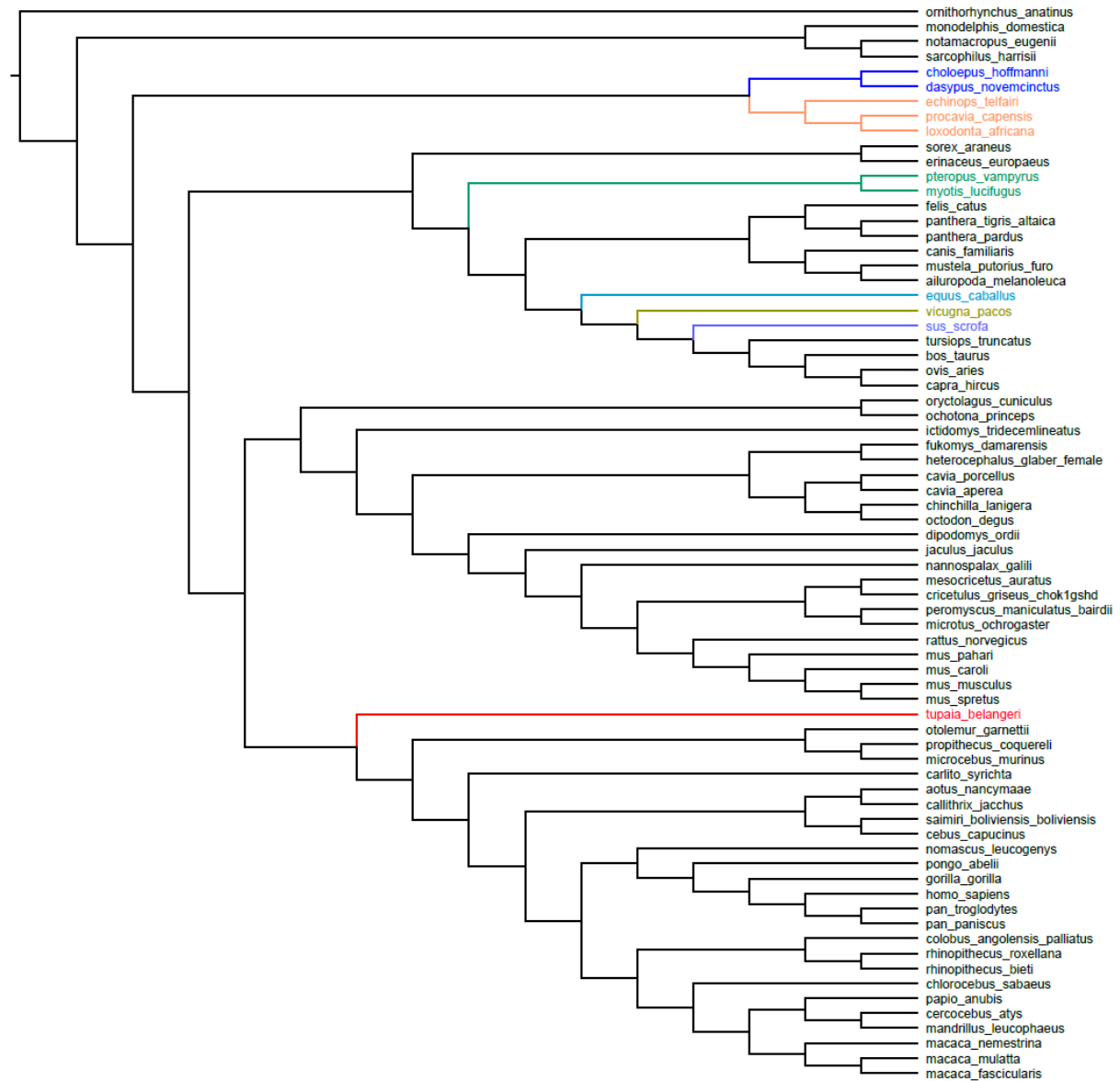


Figure S2 (b) - T2 (main tree)

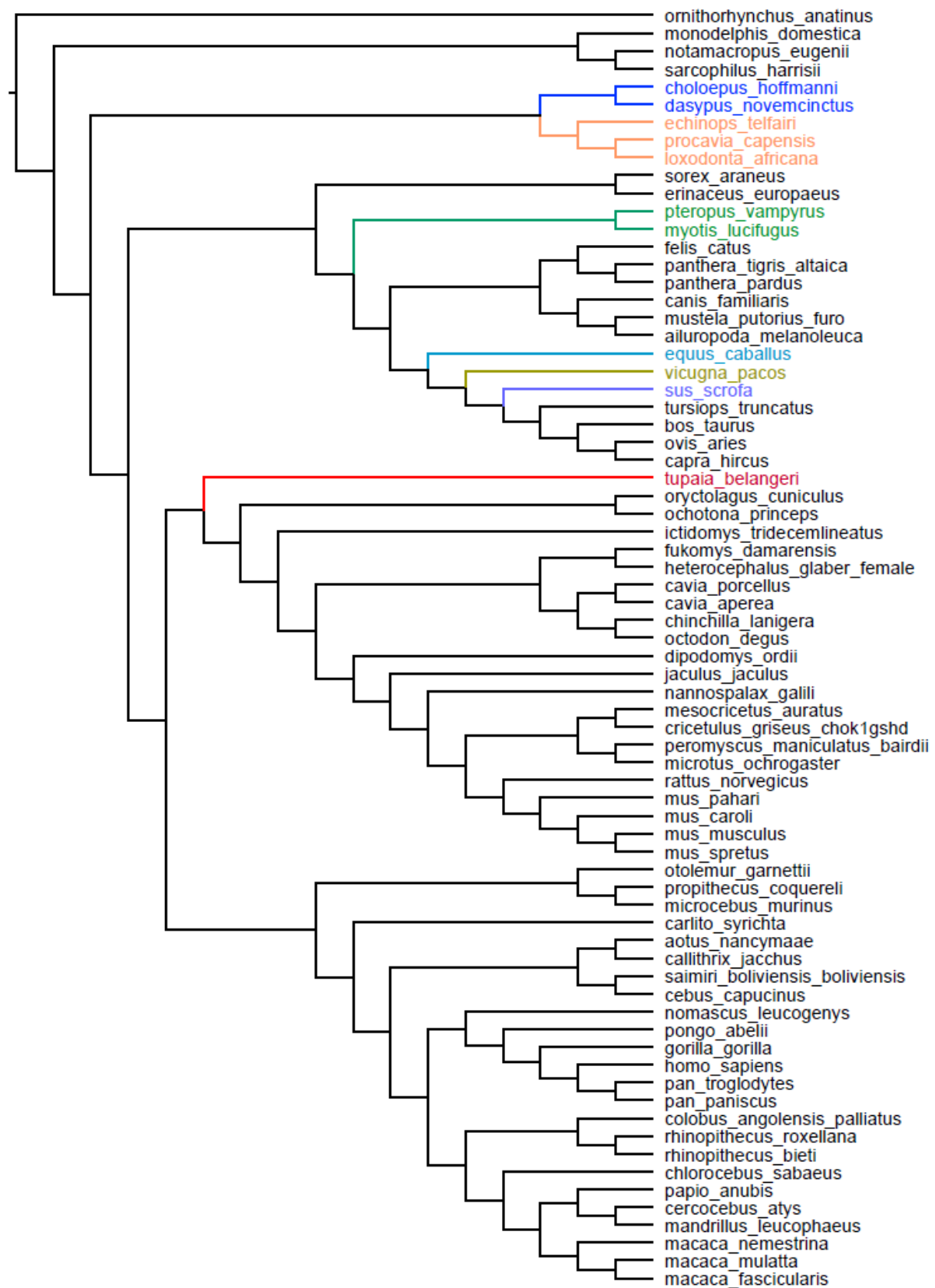


Figure S2 (c) - T3

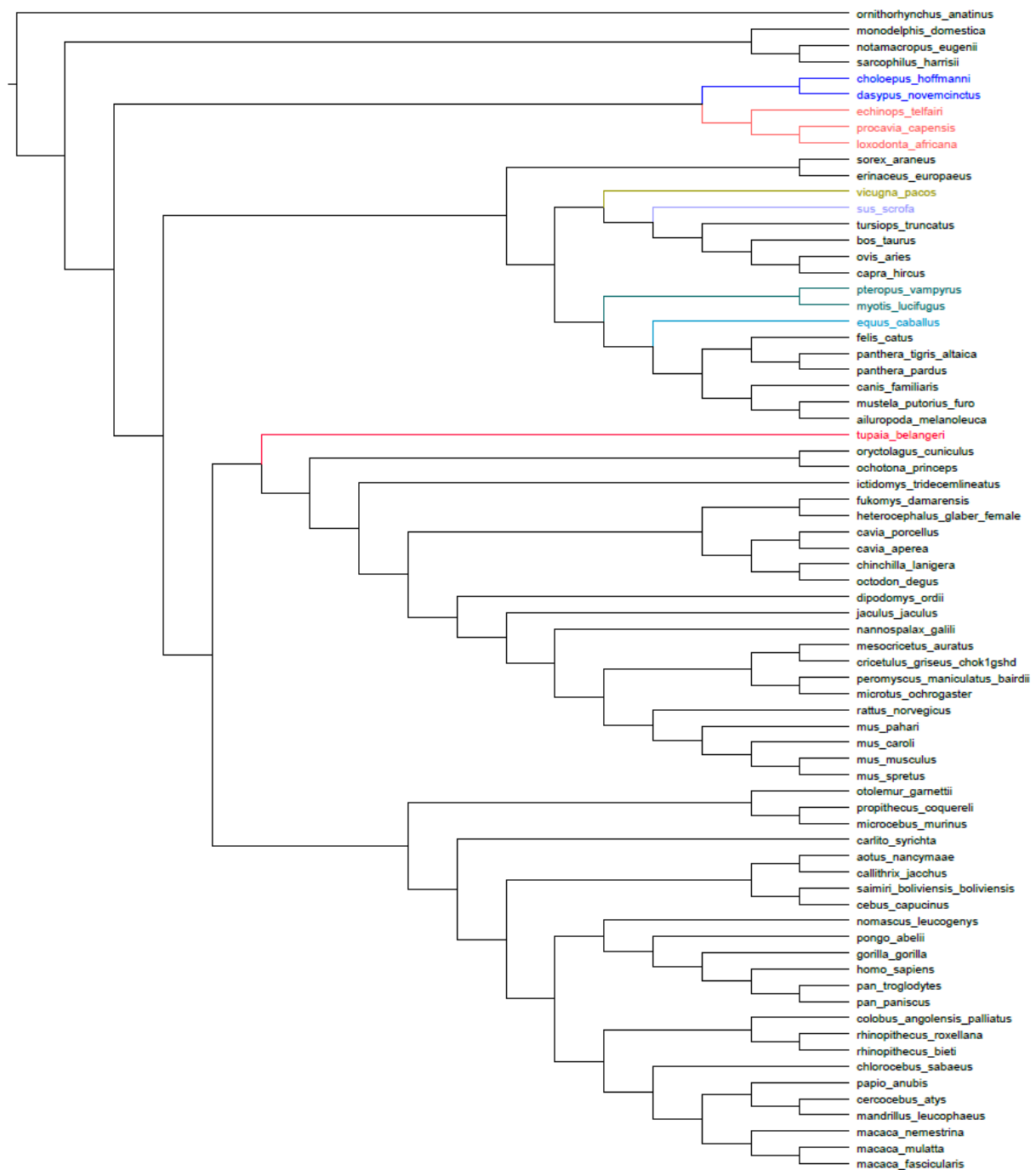


Figure S2 (d) - T4

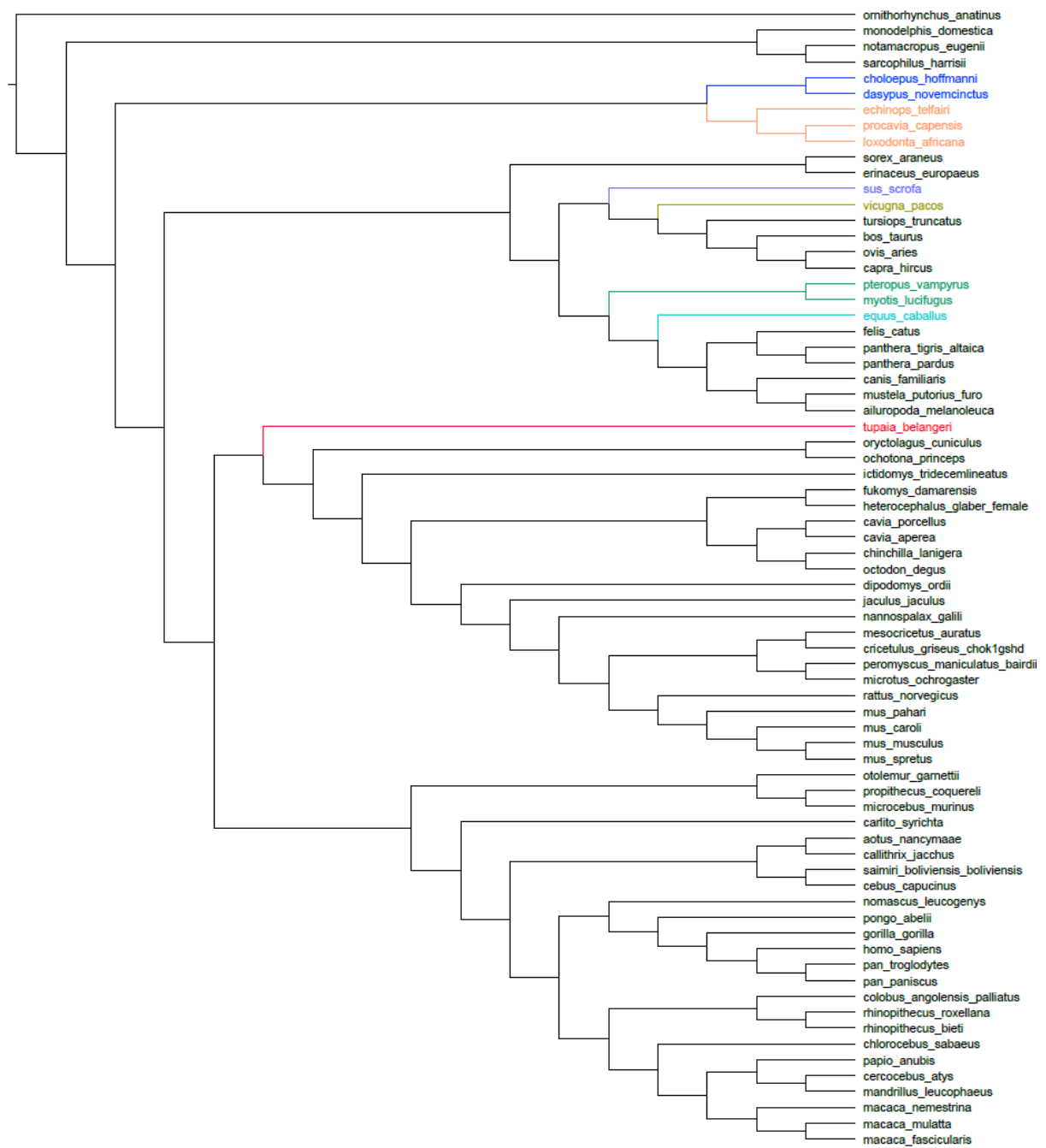


Figure S2 (e) - T5

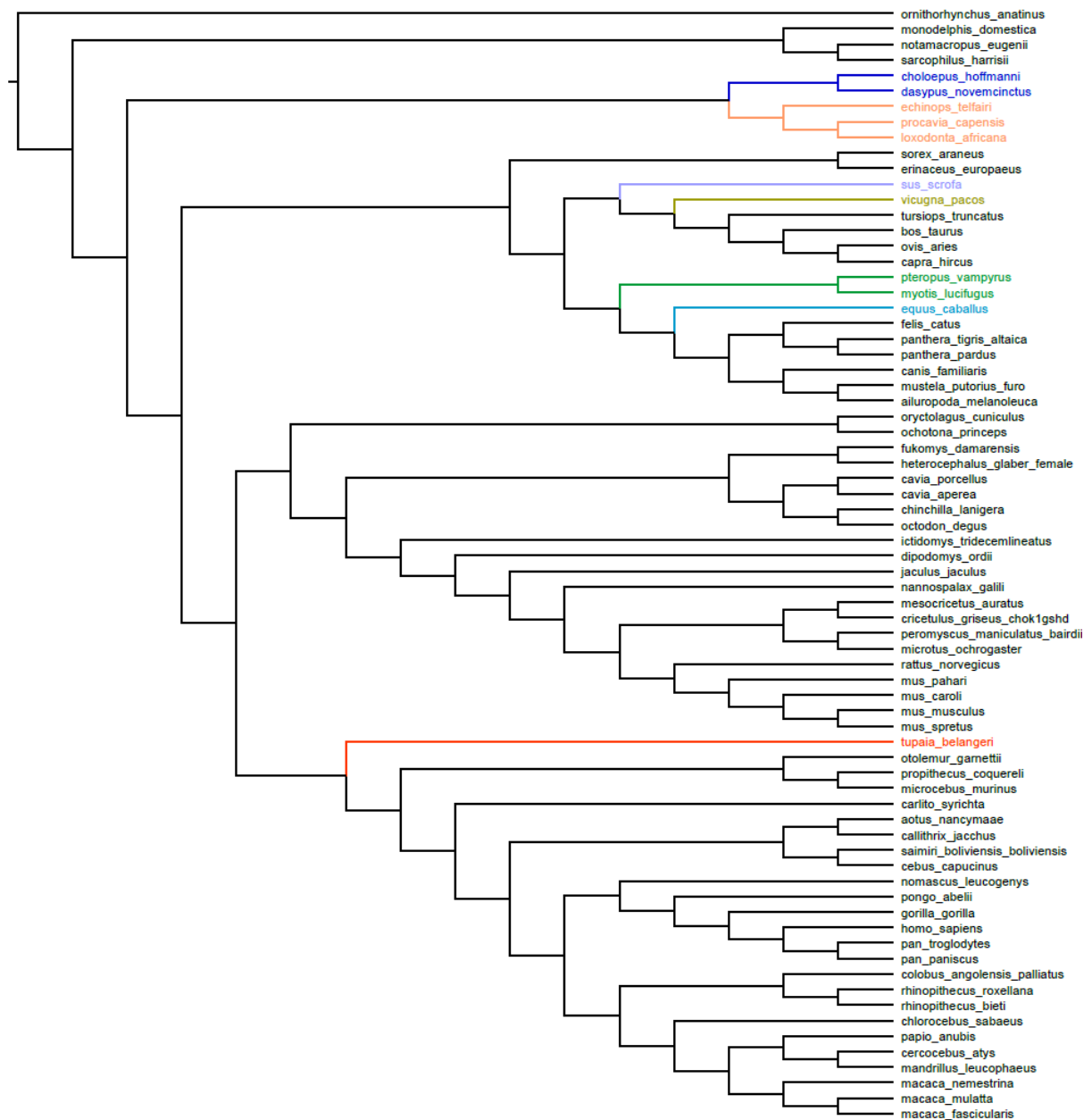


Figure S2 (f) - T6

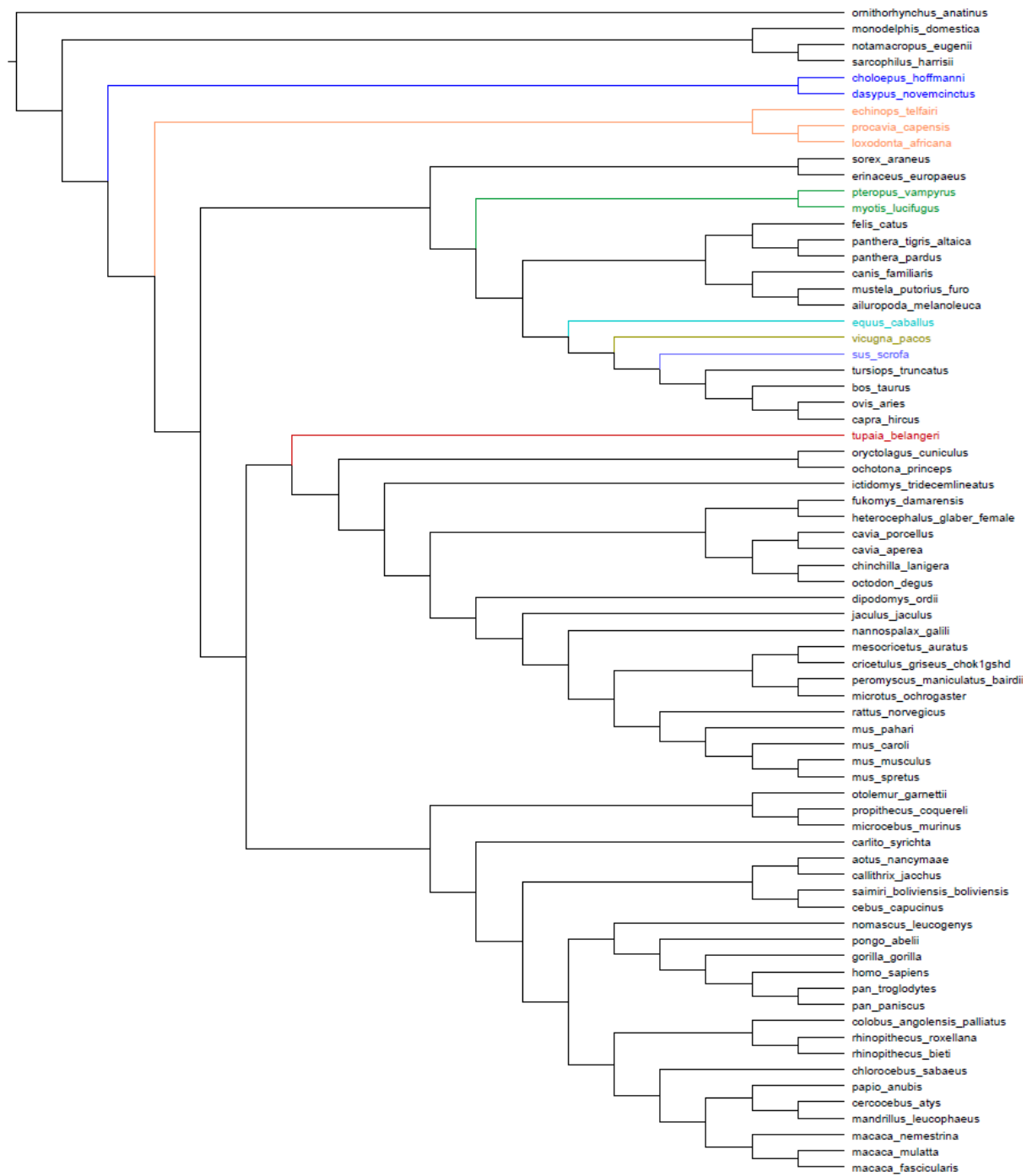


Figure S2 (g) - T7

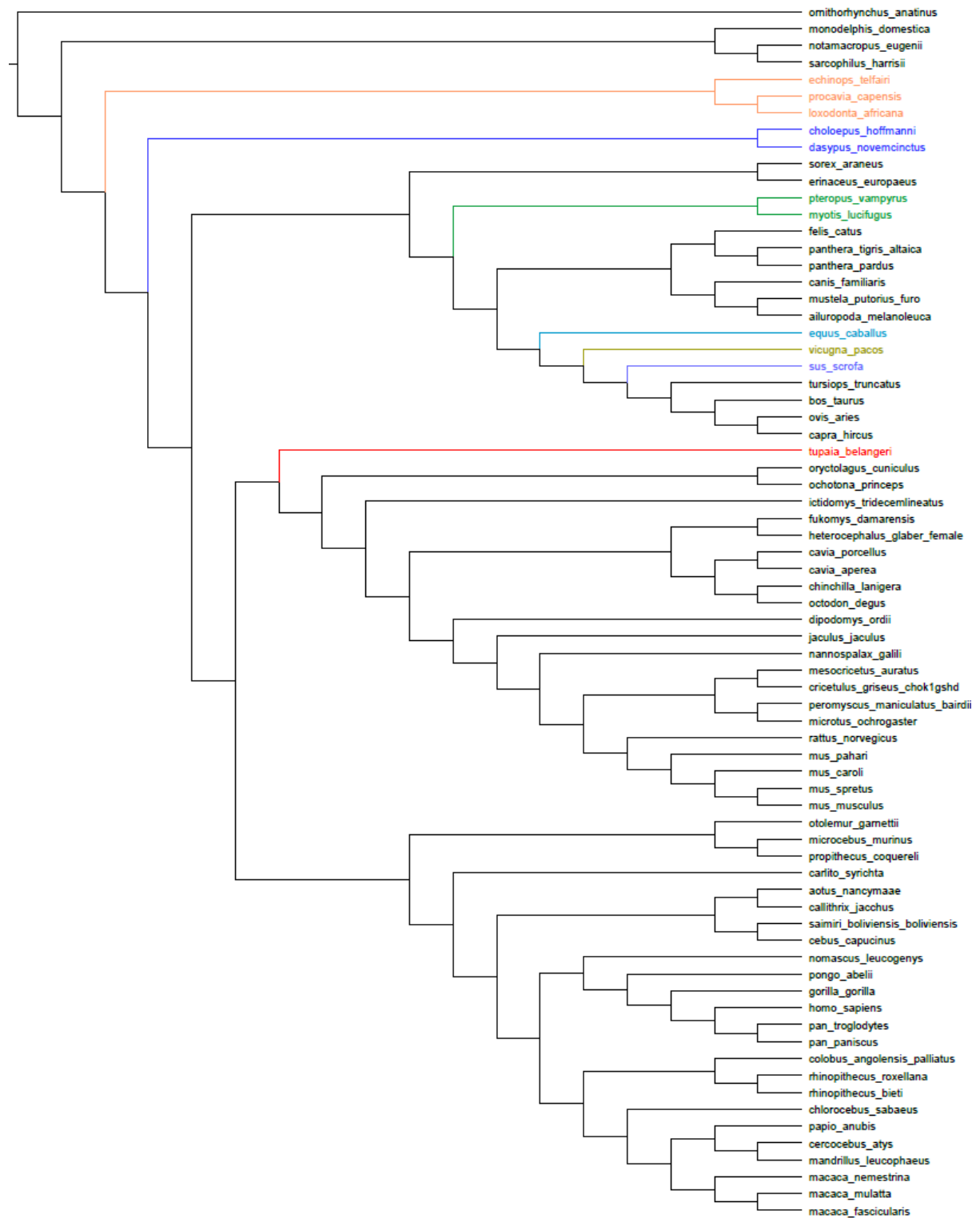


Figure S2: The seven mammal tree topologies analysed. **a-T1**, Atlantogenata rooting and *Tupaia belangeri* sister clade to Primates; **b-T2**, Atlantogenata rooting and *Tupaia belangeri* sister clade to Glires; **c-T3**, same as T1 but Chiroptera and *Equus caballus* are placed as sister clades to Carnivora; **d-T4**, same as T3 but *Vicugna pacos* and *Sus scrofa* exchange their placement; **e-T5**, same as T4 but *Tupaia belangeri* is sister clade to Primates; **f-T6**, Epitheria rooting and same placement for the other taxa as T2; **g-T7**, Exafroplacentalia rooting and same placement for the other taxa as T2. Taxa which topological placement changed are colored: (1, blue) Xenarthra, (2, orange) Afrotheria, (3, green) Chiroptera, (4, blue) *Equus caballus*, (5, yellow) *Vicugna pacos*, (6, purple) *Sus scrofa*, (7, red) *Tupaia belangeri*. The topologies in Newick format are available in the supplementary data.

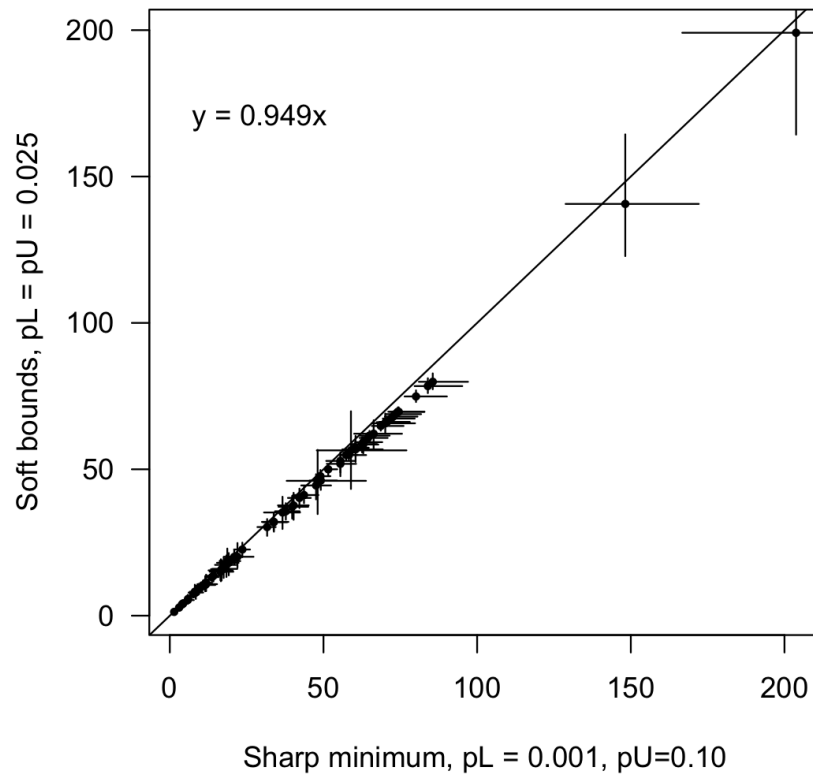


Figure S3: Comparison of posterior mean times (Ma) for the 72-genome phylogeny estimated using two different sets of bound violation probabilities. Points are plotted at the posterior mean ages. Error bars are 95% credibility intervals from the MCMC sample.

Table S8. Summary of the 32 fossil calibrations used in the 72-genome phylogeny.

Calibrated node	Old calibrations	Updated calibrations
Mammalia	B(1.649, 2.51254)	B(1.641 , 2.522)
Theria	B(1.2156, 1.696)	B(1.2156, 1.694)
Placentalia	B(0.616, 1.646)	B(0.6166 , 1.625)
Euarchontoglires	B(0.616, 1.646)	B(0.6166 , 1.625)
Primates	B(0.56, 0.6611)	B(0.56, 0.6609)
Anthropoidea	B(0.339, 0.6611)	B(0.339, 0.6609)
Catarrhini	B(0.2444, 0.339)	B(0.2444, 0.339)
Hominidae	B(0.1163, 0.339)	B(0.1165 , 0.339)
Homininae	B(0.0533, 0.339)	B(0.0533, 0.339)
Hominini	B(0.065, 0.1)	B(0.065, 0.1)
Cercopithecinae	B(0.0533, 0.34)	B(0.0533, 0.339)
Papionini	B(0.053, 0.339)	B(0.0533 , 0.339)

Strepsirrhini	B(0.339, 0.6611)	B(0.339, 0.6609)
Glires	B(0.56, 1.646)	B(0.56, 1.625)
Rodentia	B(0.56, 0.6611)	B(0.56, 0.6609)
Nonsquirrel rodents ^a	B(0.476, 0.592)	B(0.4807 , 0.5924)
Dipodidae-Muroidea	B(0.407, 0.592)	B(0.4103 , 0.5924)
Murinae	B(0.072, 0.16)	B(0.0725 , 0.1599)
Lagomorpha	B(0.476, 0.6611)	B(0.4807 , 0.6609)
Euungulata ^b	B(0.524, 0.6611)	B(0.507 , 0.6609)
Artiodactyla	B(0.505, 0.6611)	B(0.507 , 0.6609)
Cetruminantia	B(0.505, 0.6611)	B(0.507 , 0.6609)
Bovidae	B(0.16, 0.281)	B(0.1599 , 0.2729)
Carnivora	B(0.373, 0.6611)	B(0.3771 , 0.6609)
Caniformia	B(0.373, 0.6611)	B(0.3771 , 0.6609)
Chiroptera	B(0.4760, 0.6611)	B(0.4807 , 0.6609)
Lipotyphla	B(0.6160, 1.6460)	B(0.6166 , 1.625)
Xenarthra	B(0.476, 1.646)	B(0.4807 , 1.625)
Afrotheria	B(0.56, 1.646)	B(0.56, 1.625)
Paenungulata	B(0.56, 1.646)	B(0.56, 1.625)
Marsupialia	B(0.4760, 1.313)	B(0.4807 , 1.272)
Eometatheria	B(0.2303, 0.56)	B(0.2304 , 0.56)

Note: Calibrations are given in time unit = 100 Ma. Prior calibrations: soft-bound distributions are specified in *MCMCtree* format. The first number corresponds to the minimum age and the second to the maximum age in the soft-bound calibration, “B(max,min)”. The second column, “Old calibrations”, contains the calibrations used initially after the beginning of this project in 2016. The third column, “Updated calibrations”, contains the geochronologically updated calibrations as of September 2021 (see changes in bold).

^aNot included in tree hypothesis 5 due to taxa clustering differently.

^bNot included in tree hypotheses 3, 4, and 5 due to taxa clustering differently.

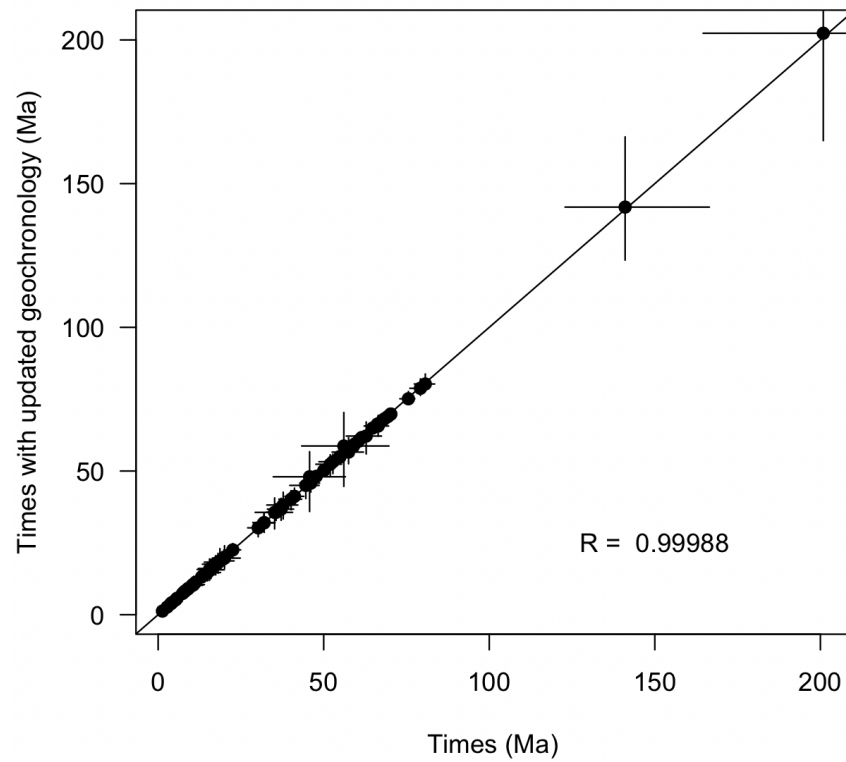


Figure S4: Comparison of posterior mean times (Ma) for the 72-genome phylogeny when using the original calibrations vs. the new calibrations with update geochronology (as of September 2021). Points are plotted at the posterior mean of node ages. Error bars are 95% credibility intervals from the MCMC. Solid line is $x = y$.

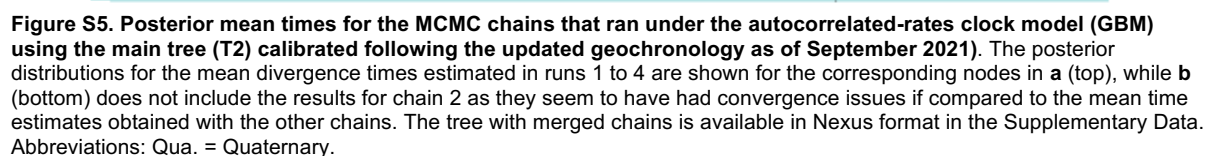
Table S9. Measures of effective sample size (ESS). For each tree (T1-T7), the ESS for bulk and tail quantiles together with the Rhat were measured for each parameter with the R package `rstan::monitor`. In addition, the ESS calculated with the `coda::effectiveSampleSize` has been included for comparison.

	MAIN (upd) ¹	MAIN (old) ²	T1	T3	T4	T5	T6	T7
tail-ESS times (median)	232	929	2074	1839	2007	1118	2721	1362
tail-ESS times (min)	61	216	507	503	451	361	442	196
tail-ESS times (max)	3884	11669	22442	28525	27303	15411	29174	21129
bulk-ESS times (median)	180	374	1062	949	968	709	1295	751
bulk-ESS times (min)	22	56	142	98	177	125	193	103
bulk-ESS times (max)	2888	8358	16211	18054	19469	11241	19324	14015
Rhat (min)	0.9999884	1.000024	0.9999901	0.999998	0.9999954	0.9999916	0.9999919	1.000035
coda-ESS times (median)	426	1255	2495	2141	2301	1765	2634	2147
coda-ESS times (min)	62	179	285	353	373	330	355	266
coda-ESS times (max)	5722	9868	31305	34459	39686	21647	16136	28988
Number of samples	60003	160008	180009	200010	200010	180009	200010	160008

Note: An ESS for bulk and tail quantiles > 100 per chain is considered good. If $Rhat \leq 1.05$, convergence is assumed. The ESS estimated with the coda package needs to be larger than or equal to 200.

¹ Values calculated with the posterior time estimates obtained when using the calibrations according to the geochronology updated as of September 2021.

² Values calculated with the posterior time estimates obtained when using the calibrations prior to September 2021.



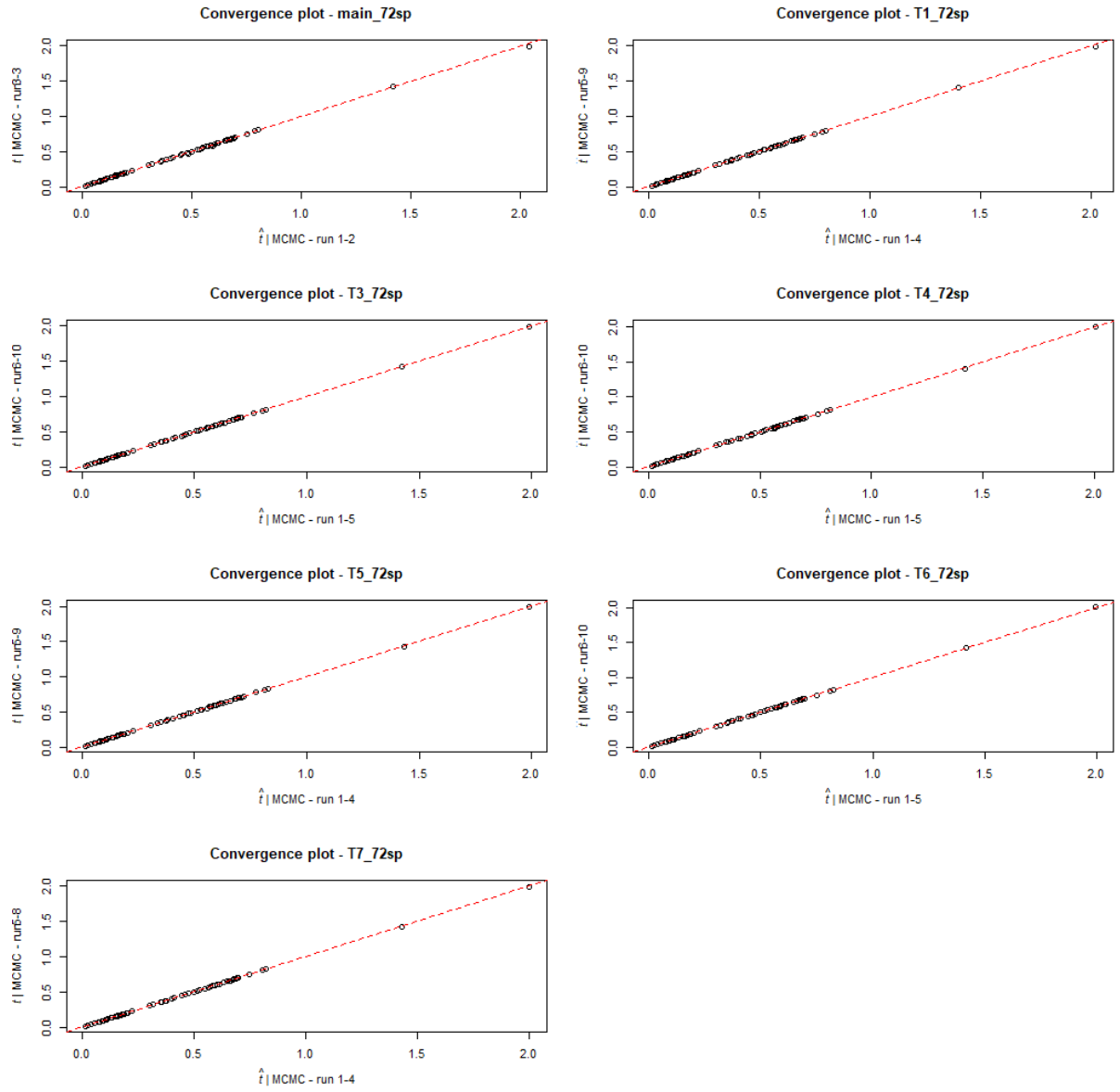


Figure S6. Scatterplot of the estimated posterior mean times for the MCMC runs under the autocorrelated-rates relaxed-clock model (GBM) model for each tree hypothesis. When comparing the mean estimates for half of the chains against the other half, they fall almost in a straight line (i.e., $x \approx y$), thus visually showing that the chains have converged.

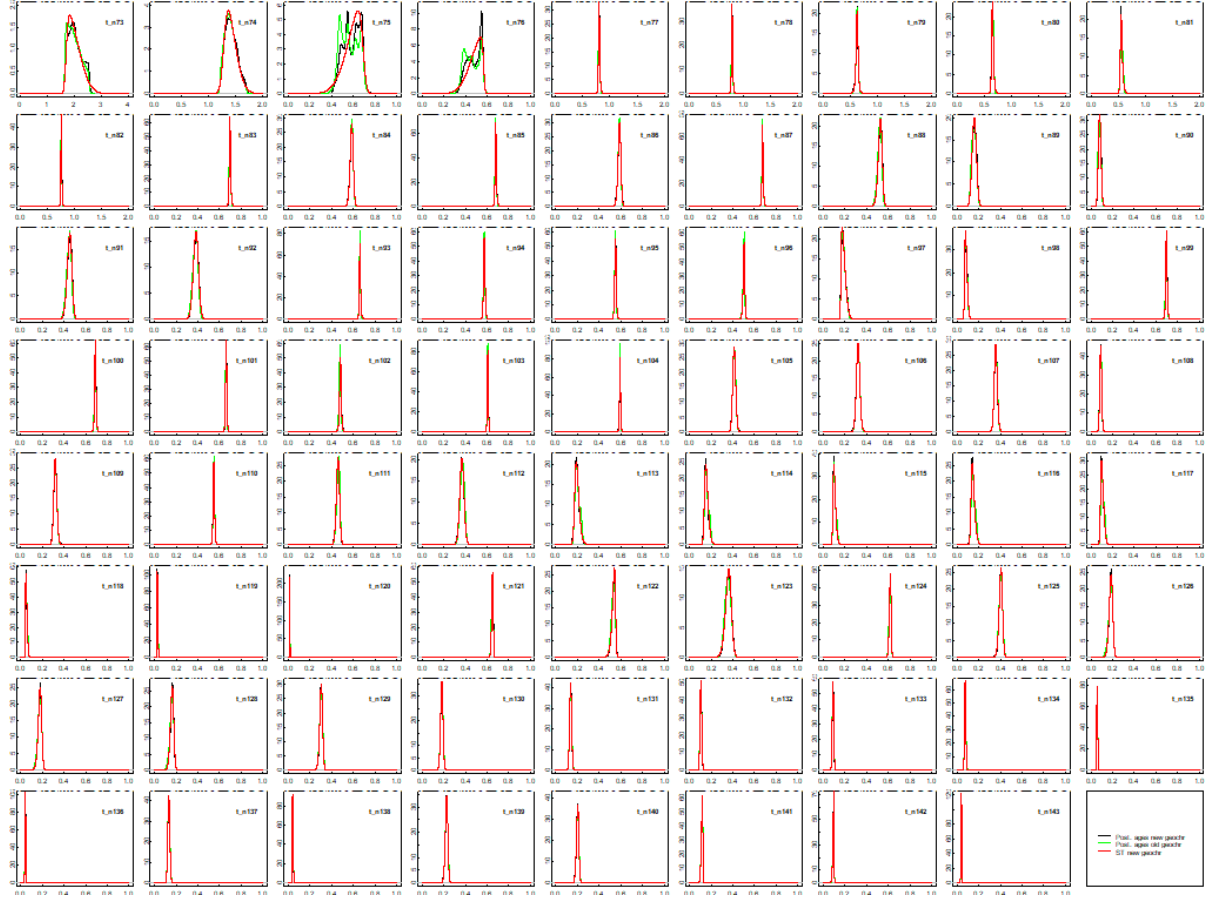


Figure S7. Assessment of the Skew-t (ST) distributions fitted to the internal nodes of the 72-species mammal tree. The ST distributions estimated with the `sn::st.mple` R function are plotted in red, those estimated when sampling from the posterior with `MCMCtree` when using the old set of calibrations in light green, and when sampling from the posterior with `MCMCtree` when using the calibrations with geochronology updates (as of September 2021) in black.

Table S10. Summary of soft-bound and low-bound calibrations used in molecular-clock dating of subtrees.

Calibrated node	Old calibrations
Cingulata	B(0.3485, 0.56)
Chlamyphoridae	B(0.339, 0.56)
Pilosa	B(0.3117, 0.56)
Folivora	B(0.1599, 0.56)
Vermilingua	B(0.1736, 0.56)
<i>Chrysochloris asiatica</i> - other chrysochlorids	B(0.036, 0.339)
Macroscelidea	B(0.2304, 0.56)
Proboscidea	B(0.0533, 0.2304)
Sirenia	B(0.4103, 0.6609)
Hyracoidea	B(0.0533, 0.339)
Paucituberculata	B(0, 0.1597)
Didelphidae	B(0.11608, 0.281)
Dasyuromorphia	B(0.1597, 0.33) ¹
Peramelidae	B(0.0436, 0.238)
Vombatiformes	B(0.255, 0.33) ¹
Phalangeridae - Burramyidae	B(0.25, 0.33) ¹
Petauridae - Pseudocheiridae	B(0.255, 0.33) ¹
Macropodoidea	B(0.247, 0.33) ¹
Platyrrhini	B(0.2045, 0.377)
Primates	B(0.64645, 0.68)
Scandentia	B(0.38, 0.66)
Suina	B(0.347, 0.53) ¹
Whippomorpha	B(0.478, 0.507) / L(0.507, 0, 0.01) ²
Cetacea	B(0.3613, 0.56)
Mysticeti	B(0.1599, 0.48) ¹
Odontoceti	B(0.2304, 0.48) ¹
Delphinida	B(0.1599, 0.48) ¹
Phocoenidae - Monodontidae	B(0.076, 0.48) ¹

Hippopotamidae	B(0.0774, 0.48) ¹
Giraffidae	B(0.14, 0.48) ¹
Bovini	B(0.102, 0.16) ¹
Tragelaphini	B(0.0549, 0.16) ¹
Reduncini	B(0.05111, 0.16) ¹
Hippotragini - Alcelaphini	B(0.0648, 0.16) ¹
Alcelaphini	B(0.0505, 0.16) ¹
Caprinae	B(0.089, 0.16) ¹
Cervidae	B(0.17235, 0.284)
stem-Moschidae	B(0.195, 0.48) ¹
Neobalaeninae	B(0.2304, 0.339)
Balaenopteridae	B(0.073, 0.48) ¹
Physeteroidea	B(0.1382, 0.48) ¹
Perissodactyla	B(0.555, 0.6609)
Ceratomorpha	B(0.48078, 0.6609)
Prinodontidae - Felidae	B(0.281, 0.6609)
Herpestidae- Eupleridae	B(0.1597, 0.339)
Mustelidae-Procyonidae	B(0.2642, 0.33) ¹
Feliformia	B(0.19535, 0.48) ¹
Viverrinae - Genettinae	B(0.2044, 0.48) ¹
Lobodontini	B(0.0505, 0.33) ¹
Phocidae	B(0.1382, 0.33) ¹
Otarioidea	B(0.1597, 0.33) ¹
Pinnipedia	B(0.2045, 0.2729)
Hipposideridae - Rhinolophidae	B(0.38, 0.56)
Megadermatidae - Craseonycteridae	B(0.339, 0.478)
Molossidae - Vespertilionidae + Miniopteridae	B(0.38, 0.56)
Natalidae - Vespertilionidae + Miniopteridae + Molossidae	B(0.38, 0.56)
Sciuromorpha	B(0.4103, 0.5924)

Abrocomidae	B(0.01778, 0.1382)
Monotremata	B(0.24459, 1.332)
Tachyglossidae	B(0.0258, 1.332)

Note: Time unit is 100 Ma. Calibrations are specified in `MCMCtree` format, with “B(max, min)” giving the minimum and maximum bounds respectively and “L(min)” giving the minimum bound.

¹ The maximum ages of these calibrations are set to be the 2.5% quantile of the ST distributions on the corresponding ancestors. This adjustment is done to avoid truncation artefacts against the ST and soft-bound calibrations.

² The posterior age of the parent node, Cetruminantia (derived from the 72-taxon tree), is in conflict with its fossil calibration (Himalayacetus, 50.7 Ma, from the Ypressian deposits of the Subathu Formation, India), with the 2.5% quantile of the posterior close to ~48 Ma. This node, Whippomorpha, uses the same fossil constraint as its parent, thus creating a conflict with the ST calibration on its parent node. We deal with this conflict by dating the Artiodactyla subtree twice, once using the 50.7 Ma minimum, and again using a minimum of 47.8 Ma, which is the top of the Ypressian. The ‘B’ calibration results are used in the stitched tree of 4,705 taxa.

Table S11. Summary of ST/SN-fitted calibrations used in molecular-clock dating of subtrees.

Calibrated node	ST/SN calibrations	Subtree
Mammalia	ST(1.642, 0.425, 12.652, 1714.565)	Afrotheria
Afrotheria	ST(0.653, 0.017, 0.302, 11.274)	Afrotheria
Paenungulata	ST(0.55, 0.028, 1.247, 14.653)	Afrotheria
Mammalia	ST(1.642, 0.425, 12.652, 1714.565)	Euarchonta
Euarchontoglires	ST(0.695, 0.007, 0.32, 7.619)	Euarchonta
Primates	ST(0.655, 0.01, -1.355, 178.316)	Euarchonta
Strepsirrhini	ST(0.548, 0.026, -2.506, 66.983)	Euarchonta
Propithecus - Microcebus	ST(0.37, 0.033, -0.876, 275.655)	Euarchonta
Haplorrhini	ST(0.622, 0.011, -1.196, 166.803)	Euarchonta
Anthropoidea	ST(0.415, 0.021, -1.14, 156.796)	Euarchonta
Aotidae - Callitrichidae	ST(0.186, 0.033, -1.856, 48.135)	Euarchonta
Cebidae	ST(0.189, 0.021, -1.722, 40.505)	Euarchonta
Catarrhini	ST(0.314, 0.018, -1.23, 314.095)	Euarchonta
Cercopithecoidea	ST(0.182, 0.012, -0.054, 88.157)	Euarchonta
Cercopithecinae	ST(0.136, 0.009, -1.159e-07, 10)	Euarchonta
Papionini	ST(0.1, 0.009, 0.641, 145.414)	Euarchonta

Papio - Mandrillus	ST(0.087, 0.007, 0.195, 50.335)	Euarchonta
<i>Cercocebus atys</i> - <i>Mandrillus leucophaeus</i>	ST(0.073, 0.006, 0.229, 40.768)	Euarchonta
Genus Macaca	ST(0.053, 0.007, 1.101, 200.596)	Euarchonta
<i>Macaca fascicularis</i> - <i>Macaca mulatta</i>	ST(0.039, 0.005, 1.207, 108.063)	Euarchonta
Colobinae	ST(0.127, 0.011, 0.584, 209.998)	Euarchonta
Genus Rhinopithecus	ST(0.038, 0.007, 1.525, 104.388)	Euarchonta
Hominoidea	ST(0.236, 0.016, -1.223, 135.248)	Euarchonta
Hominidae	ST(0.21, 0.015, -1.248, 109.524)	Euarchonta
Homininae	ST(0.122, 0.012, -4.859, 295.449)	Euarchonta
Hominini	ST(0.101, 0.01, -7.603, 93.226)	Euarchonta
<i>Pan paniscus</i> - <i>Pan troglodites</i>	ST(0.038, 0.003, -0.337, 47.276)	Euarchonta
Mammalia	ST(1.642, 0.425, 12.652, 1714.565)	Lagomorpha
Lagomorpha	SN(0.474, 0.008, 0.293)	Lagomorpha
Mammalia	ST(1.642, 0.425, 12.652, 1714.565)	Artiodactyla
Artiodactyla	ST(0.577, 0.007, -0.634, 7.509)	Artiodactyla
Artiofabula	ST(0.554, 0.008, -0.964, 7.343)	Artiodactyla
Cetruminantia	ST(0.507, 0.009, -1.513, 6.294) / ST(0.479, 0.016, -1.513, 6.294)	Artiodactyla
Bovidae	ST(0.149, 0.025, 5.863, 624.148) / ST(0.149, 0.025, 5.863, 624.148)	Artiodactyla
<i>Ovis aries</i> - <i>Capra hircus</i>	ST(0.059, 0.016, 3.225, 169.672) / ST(0.058, 0.014, 3.225, 169.672)	Artiodactyla
Mammalia	ST(1.642, 0.425, 12.652, 1714.565)	Chiroptera (I and II)
Chiroptera	ST(0.596, 0.016, -1.239, 13.572)	Chiroptera (I and II)
Mammalia	ST(1.642, 0.425, 12.652, 1714.565)	Rest of Laurasiatheria
Laurasiatheria	ST(0.694, 0.006, 0.431, 4.953)	Rest of Laurasiatheria
Erinaceidae - Soricidae	ST(0.596, 0.017, -1.243, 19.856)	Rest of Laurasiatheria
Scrotifera	ST(0.678, 0.006, 0.37, 4.464)	Rest of Laurasiatheria

Chiroptera	ST(0.596, 0.016, -1.239, 13.572)	Rest of Laurasiatheria
Fereungulata	ST(0.671, 0.005, 0.355, 4.329)	Rest of Laurasiatheria
Carnivora	ST(0.538, 0.027, -2.115, 70.375)	Rest of Laurasiatheria
Felidae	ST(0.14, 0.02, 0.417, 367.218)	Rest of Laurasiatheria
Pantherinae	ST(0.067, 0.015, 1.12, 331.497)	Rest of Laurasiatheria
Caniformia	ST(0.467, 0.031, -1.966, 117.012)	Rest of Laurasiatheria
Arctoidea	ST(0.397, 0.031, -1.415, 427.391)	Rest of Laurasiatheria
Euungulata	ST(0.660, 0.005, 0.341, 4.207)	Rest of Laurasiatheria
Artiodactyla	ST(0.577, 0.007, -0.634, 7.509)	Rest of Laurasiatheria
Mammalia	ST(1.642, 0.425, 12.652, 1714.565)	Marsupialia
Didelphimorphia - Australidelphia	ST(0.562, 0.08, 0.035, 299.837)	Marsupialia
Eometatheria	ST(0.459, 0.068, 0.025, 623.433)	Marsupialia
Mammalia	ST(1.642, 0.425, 12.652, 1714.565)	Ctenohystrica
Rodentia	ST(0.606, 0.005, 0.178, 5.22)	Ctenohystrica
Caviomorpha - Phiomorpha	ST(0.414, 0.014, -0.164, 18.225)	Ctenohystrica
Phiomorpha	ST(0.324, 0.016, -0.255, 17.835)	Ctenohystrica
Caviomorpha (Cavioidea - Erethizontoidea)	ST(0.356, 0.014, 0.022, 18.214)	Ctenohystrica
<i>Cavia porcellus</i> - <i>Cavia aperea</i>	ST(0.086, 0.01, 0.671, 36.22)	Ctenohystrica
<i>Chinchilla lanigera</i> - <i>Octodon degus</i>	ST(0.317, 0.014, 0.203, 19.215)	Ctenohystrica
Mammalia	ST(1.642, 0.425, 12.652, 1714.565)	Rest of Rodentia (I and II)
<i>Dipodomys ordii</i> - Myomorpha	ST(0.55, 0.006, -0.171, 6.759)	Rest of Rodentia (I)
Dipodidae-Muroidea	ST(0.473, 0.017, -1.282, 13.044)	Rest of Rodentia (I)
<i>Nannospalax galili</i> - Muridae	ST(0.382, 0.022, -0.67, 36.812)	Rest of Rodentia (I)
Muridae	ST(0.174, 0.035, 3.117, 381.97)	Rest of Rodentia (I and II)
<i>Mesocricetus auratus</i> - <i>Cricetulus griseus</i>	ST(0.081, 0.022, 3.756, 209.065)	Rest of Rodentia (I)

<i>Peromyscus maniculatus</i> - <i>Microtus ochrogaster</i>	ST(0.128, 0.029, 3.532, 404.416)	Rest of Rodentia (I)
Murinae	ST(0.094, 0.027, 3.794, 547.445)	Rest of Rodentia (I)
Murinae	ST(0.086, 0.021, 3.794, 547.445)	Rest of Rodentia (II)
Cricetidae	ST(0.137, 0.03, 3.464, 240.317)	Rest of Rodentia (II)
<i>Mus pahari</i> - rest of <i>Mus</i>	ST(0.043, 0.013, 3.575, 94.222)	Rest of Rodentia (II)
<i>Mus caroli</i> - rest of <i>Mus</i>	ST(0.022, 0.007, 3.426, 86.245)	Rest of Rodentia (II)
<i>Mus spretus</i> - <i>Mus musculus</i>	ST(0.0104, 0.003, 3.38, 83.529)	Rest of Rodentia (II)
Mammalia	ST(1.642, 0.425, 12.652, 1714.565)	Xenarthra
Xenarthra	ST(0.628, 0.019, -0.389, 4.88)	Xenarthra

Note: Time unit is 100 Ma. Calibrations are specified in *MCMCtree* format. ST calibrations are given as “ST(a, b, c, d)”, with a, b, c, and d being the location, scale, shape and degrees of freedom respectively (see *MCMCtree*’s manual for details). Skew-normal distributions are given as “SN(a, b, c)”, with parameters to be the same as in ST but without the degrees of freedom. For Cetruminantia, Bovidae, and *Ovis-Capra*, two versions are provided corresponding to the B and L calibrations on Whippomorpha, respectively (Table S10).

Table S12. Effective sample sizes (ESS) for each subtree. The ESS for bulk and tail quantiles together with the Rhat were measured for each parameter with the R package `rstan::monitor`. In addition, the ESS calculated with the `coda::effectiveSampleSize` has been included for comparison (part I).

	Afro.	Eua.	Lag.	Art.	Chi-I	Chi-II	L.rest.
tail-ESS times (median)	130906	4651	36837	14401	65955	1958	1573
tail-ESS times (min)	27957	305	9338	1713	461	112	171
tail-ESS times (max)	278303	17309	251588	51125	211161	10379	6221
bulk-ESS times (median)	68429	1527	11006	6102	26290	419	523
bulk-ESS times (min)	16209	167	4679	1066	329	19	68
bulk-ESS times (max)	244573	14074	136426	47870	172817	9045	5870
Rhat (min)	0.9999971	0.9999437	0.9999968	0.999981	0.9999965	0.9999122	0.9998421
coda-ESS times (median)	138179	3397	22876	12623	59814	1622	1223
coda-ESS times (min)	29675	476	10151	2397	409	82	164
coda-ESS times (max)	519552	27388	263722	96251	343651	17425	11988
No. samples	640032	35507	600030	104802	493192	21725	12572
No. taxa	60	486	88	431	256	634	659

Note: An ESS for bulk and tail quantiles > 100 per chain is considered good. If $Rhat \leq 1.05$, convergence is assumed. The ESS estimated with the coda package needs to be larger than or equal to 200. **Abbreviations:** Afro. = Afrotheria, Eua. = Euarchonta, Lag. = Lagomorpha, Art. = Artiodactyla, Chi-I = Chiroptera (I), Chi-II = Chiroptera (II), L.rest. = Rest of Laurasiatheria. **No. taxa:** All subtrees include 3 taxa as outgroup. Some subtrees include common taxa in other subtrees to avoid issues with calibrations: Rest of Laurasiatheria = 4 repeated taxa, Chiroptera (I) = 1 repeated taxon, Chiroptera (II) = 1 repeated taxon.

Table S13. Effective sample sizes (ESS) for each subtree. The ESS for bulk and tail quantiles together with the Rhat were measured for each parameter with the R package `rstan::monitor`. In addition, the ESS calculated with the `coda::effectiveSampleSize` has been included for comparison (part II).

	Mar.	Cte.	Sci.	Rod-I	Rod-II	Xen.
tail-ESS times (median)	48352	94398	74820	1615	569	149875
tail-ESS times (min)	4047	13121	7537	247	40	28838
tail-ESS times (max)	135255	315674	260577	14387	2471	285304
bulk-ESS times (median)	20550	37585	29477	843	95	75308
bulk-ESS times (min)	123593	5727	7785	125	14	13837
bulk-ESS times (max)	4579	308325	201905	13662	2502	226337
Rhat (min)	0.999993	0.9999969	0.9999969	0.9999344	0.999821	0.999997
coda-ESS times (median)	43470	75039	61317	2113	329	150844
coda-ESS times (min)	7617	11372	13229	53	29	30200
coda-ESS times (max)	245808	634321	354877	26974	4951	439262
No. samples	284546	640032	639984	30169	11096	640032
No. taxa	307	210	267	630	691	33

Note: An ESS for bulk and tail quantiles > 100 per chain is considered good. If $Rhat \leq 1.05$, convergence is assumed. The ESS estimated with the coda package needs to be larger than or equal to 200. **Abbreviations:** Mar. = Marsupialia, Cte. = Ctenohystrica, Sci. = Sciuridae and related, Rod-I = Rest of Rodentia (I), Rod-II = Rest of Rodentia (II), Xen. = Xenarthra. **No. taxa:** All subtrees include 3 taxa as outgroup. Some subtrees include common taxa in other subtrees to avoid issues with calibrations: Rest of Rodentia (II) = 2 repeated taxa, Rest of Rodentia (I) = 2 repeated taxa, Ctenohystrica = 1 repeated taxon.

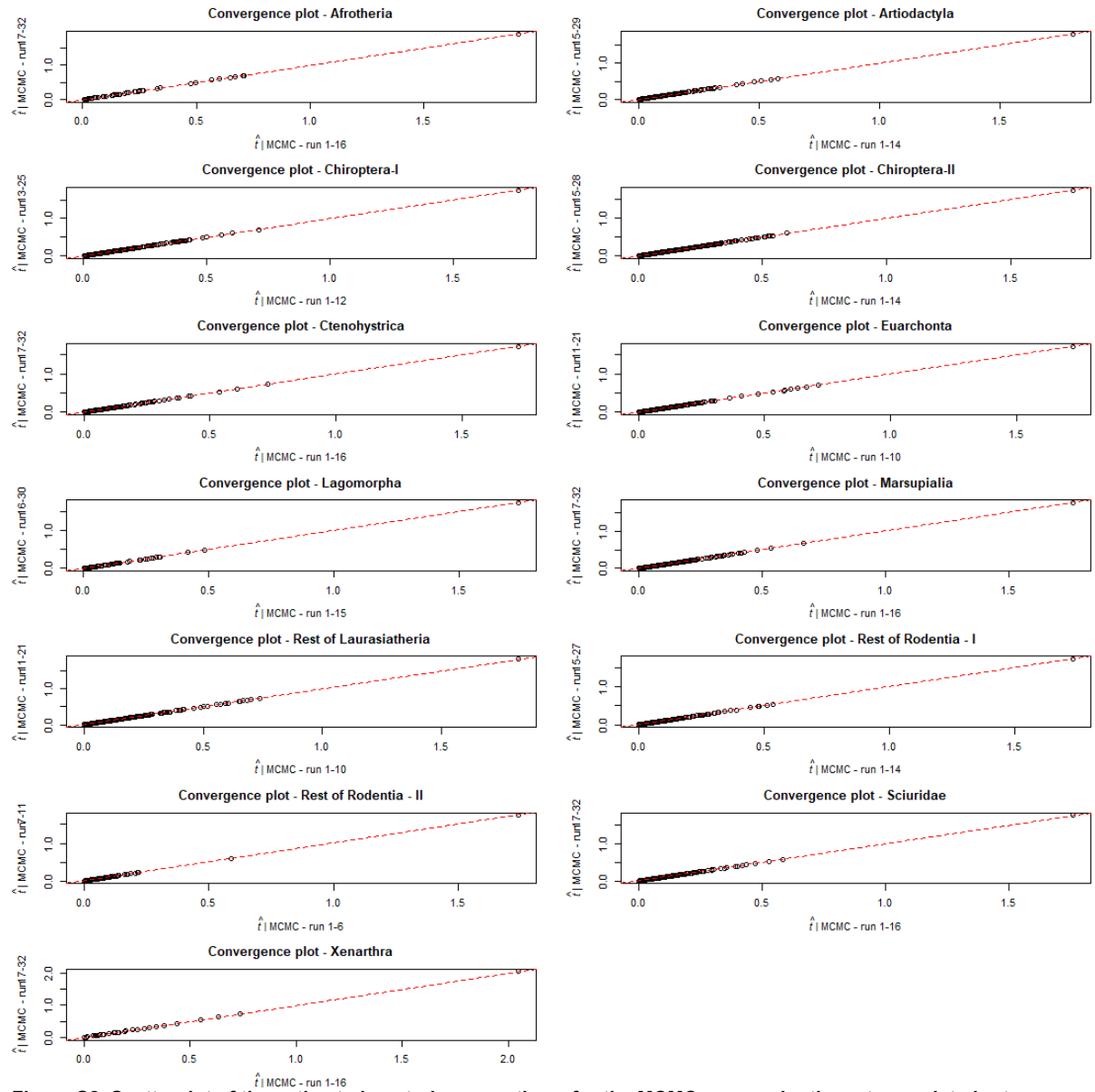


Figure S8. Scatterplot of the estimated posterior mean times for the MCMC runs under the autocorrelated-rates relaxed-clock model (GBM) model for each of the 13 subtrees. The mean estimates for half of the chains are plotted against the other half. They fall almost perfectly on the $x = y$ line, thus visually showing the two sets of chains have converged to the same distribution. Note that 32 MCMC chains were run for each subtree, but some of those did not pass quality filters (e.g., convergence) and were not included.

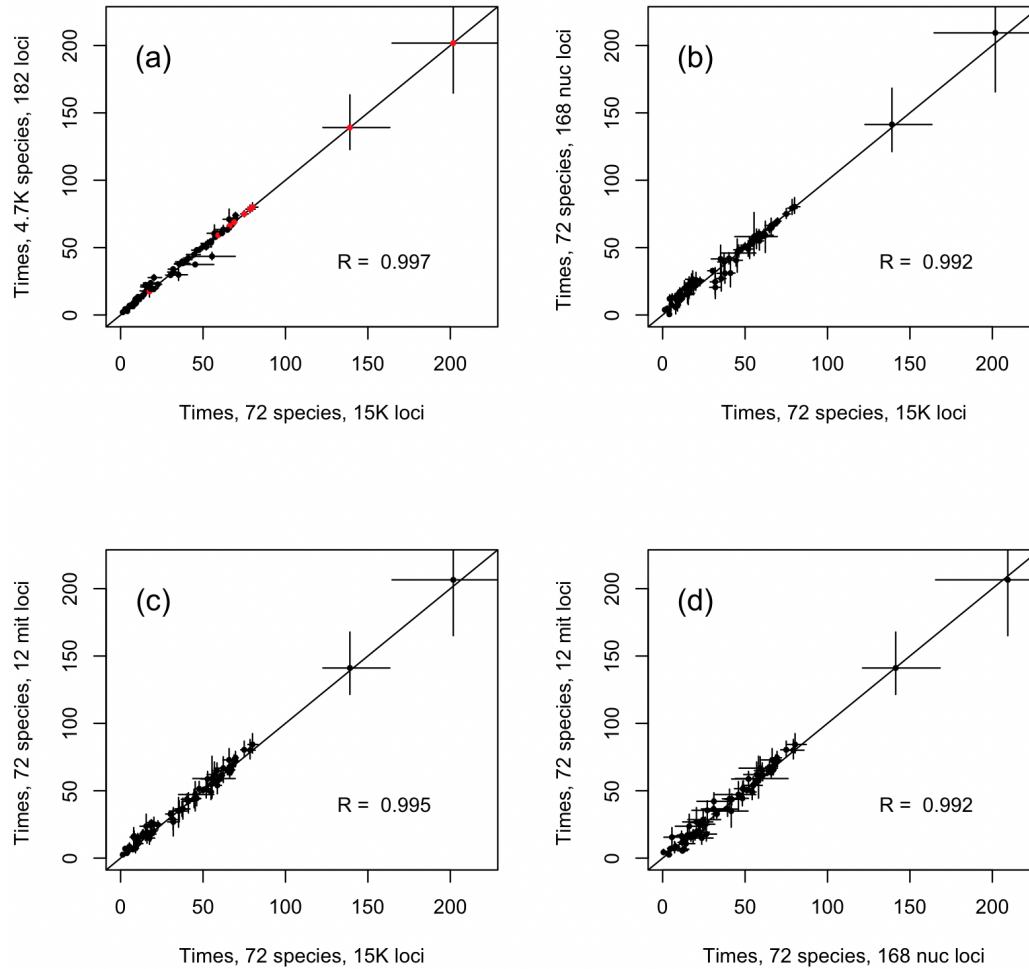


Figure S9. Integrity of divergence time estimates across dating steps and data partitions. **a**, Estimated posterior mean of divergence times from step I plotted against estimates from step II. Red dots are the nine nodes from the main 72-taxon tree that are not present in any subtree. The posterior time estimates for these nodes in the final stitched tree are the same as the estimates in the main tree. **b-c**, Estimates of posterior mean of divergence times on 72 taxa using the 182 loci step II dataset (with nuclear and mitochondrial loci analysed separately and using the original fossil calibrations), plotted against the estimates fusing 15K loci from step I. **d**, The estimates from the mitochondrial and nuclear loci plotted against each other. In all cases vertical and horizontal bars are the 95% CIs from the MCMC sample. Points are plotted at the posterior mean of node ages.

Integrity of time estimates across dating steps and data partitions

We assessed integrity of time estimates across dating steps and partitions. **Figure S9 a** shows the estimates of divergence times from step I (using the 72 genomes) vs those from step II (using 4,705 taxa) for the 71 nodes shared between the analyses. The posterior mean time estimates between the analyses are highly correlated. This does not appear surprising given the posterior of times in step I is used as the prior in step II. However, note the posterior means and 95% CIs do differ between the two analyses. This is a consequence of the increased taxon sampling in step II with corresponding use of additional fossil calibrations. We also assessed whether the nuclear and mitochondrial loci from the step II dataset produced similar time estimates. We extracted the 72 taxa from the 182 loci dataset and re-estimated the divergence times using the original fossil calibrations, with the mitochondrial and nuclear loci analysed separately (**Figure S10 b-d**). Time estimates are highly correlated and consistent when compared against the estimates from the 15K loci analysis (**Figure S10 b-c**) and when compared against each other (**Figure S10 d**).

Technical comment on the sequential Bayesian-subtree approach

The sequential Bayesian approach with subtree stitching used here is approximate. The joint posterior of divergence times on a phylogeny contains a correlation structure. This correlation structure is discarded when fitting the ST and SN densities to the marginal posteriors and when using these fitted densities as priors in the second step of the analysis¹. A potential source of correlation may emerge from the constraint that nodes cannot be older than their ancestors. In divergence dating, this means the joint density of ages of nodes and their parents are truncated along the $x = y$ diagonal². For example, consider the sample from two joint independent normals with mean = 0 and s.d. = 0.5. If a truncation along the $x = y$ line is applied so that samples in the $x < y$ region are discarded, a positive correlation is generated on the remaining samples in the $x > y$ region (**Figure S10, left panel**). On the other hand, if we sample from two joint independent normals with means 2 and -2, both with s.d. = 0.5, and apply the same truncation, no positive correlation is generated because the joint density is far from the $x = y$ line and no data are discarded (**Figure S10, right panel**).

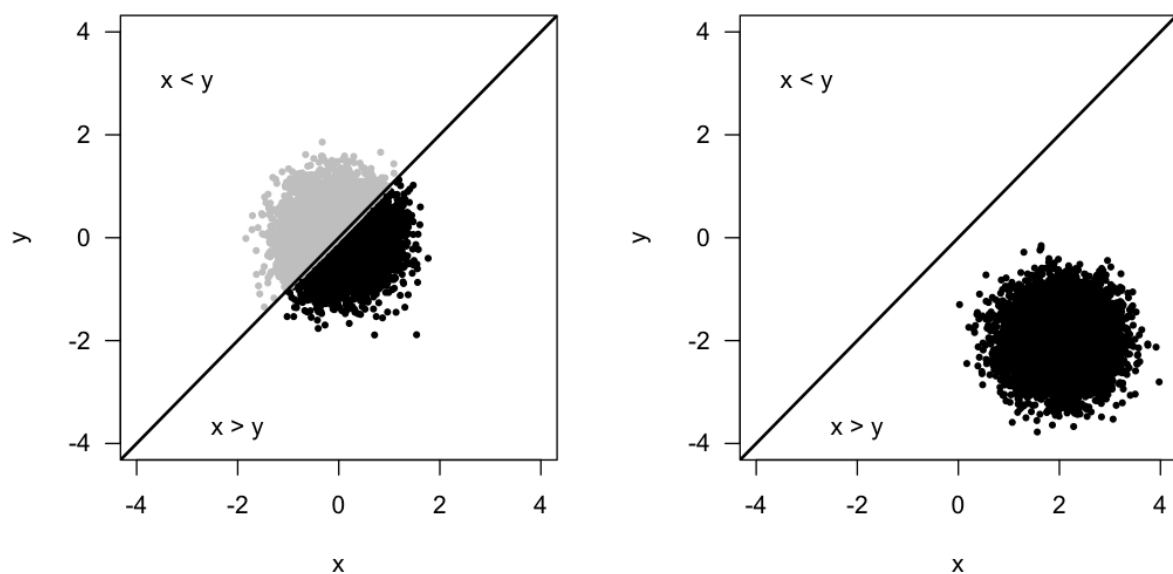


Figure S10. The effect of truncation on correlation. **Left**, a joint sample from two independent normal densities with mean = 0 and s.d. = 0.5 is generated, and a truncation along the $x < y$ is applied. **Right**, a joint sample from two independent normal densities with means 2 and -2 and s.d. = 0.5 is generated, and the same truncation is applied. However, in this case, the truncation $x = y$ line is far from the joint sample and no actual data are removed. Truncated (removed) samples are shown in light gray, and non-truncated samples are shown in black. Sample correlations after truncation are $R = 0.468$ (left) and $R = 0.0126$ (right).

If the marginal posterior densities on the ages of a node and its parent overlap, truncation means a positive correlation is present in the joint posterior, similar to the case of the **left panel of Figure S10**. Thus, when fitting ST or SN densities to the marginal posteriors, this correlation is discarded. In this case, the sequential Bayesian approach may not work well because the ST and SN calibrations will be a poorer approximation to the joint posterior of the corresponding node ages. On the other hand, if the marginal posterior densities of the ages of a node and its parent do not overlap (**as in the right panel of Figure S10**), then truncation is not an issue and the fitted ST and SN calibrations will provide an appropriate approximation.

Consequently, we recommend users examine the joint posterior of node ages in the first step of the sequential approach to assess whether truncation is present. If the marginal posterior density of the age of a node overlaps extensively with those of its ancestors, then truncation will be present and it will be substantial; using the sequential approach in this case may result in a poor approximation. In particular, if truncation is substantial and if the posterior of a daughter node's age is used to calibrate the root of a subtree, it may not be

possible to stitch the subtree back into the main tree because the mean posterior age of the subtree's root may, for example, be older than the posterior mean of the parent node in the main tree (a consequence of ignoring truncation and correlation).

Benchmarking

We performed a benchmarking analysis to calculate the computational time savings of our Bayesian sequential-subtree approach. We ran one MCMC chain for each subtree (using its appropriate fossil calibrations and rate prior, and approximate likelihood) with a burn-in of 150,000 iterations and a total of 10,000 samples collected every 100 iterations (note that, in MCMCtree, one iteration is one cycle in which all model parameters are sampled sequentially³). We then calculated the ESS of the divergence times per hour of computation (Figure S11). For example, the smallest subtree, Xenarthra (33 taxa), achieved a median ESS of 2,400 per hour. As the number of taxa increases, the computational efficiency decreases (Figure S11). The largest subtree, "Rest of Rodentia (II)" (691 taxa) has an expected median of only ESS of 0.903 per hour (Figure S11), a 2,657x reduction in sampling efficiency per time unit when compared to Xenarthra. Extrapolating these results to 4,705 taxa, we get an expected median ESS per hour of 7.8×10^{-3} (Figure S11). This means that obtaining a median ESS of 1,000 on the 4,705-taxon phylogeny would require running the MCMC chain for ~15 years (128K hours). Of course, the analysis could be parallelised, but this would require many months per chain and each chain would still need its own expensive burn-in period. In total, we estimate a 115x time saving when comparing the required MCMC lengths for our largest subtree against the full 4,705-taxon phylogeny.

Computational improvements are also due to the use of approximate likelihood calculation⁴, which a previous benchmarking study⁵ places very close to 1000x. Three of the most widely used Bayesian molecular-clock dating programs (MrBayes, BEAST, and PhyloBayes) implement exact likelihood only. Thus, if using exact likelihood, our largest subtrees would be expected to need over 1.12 M hours (126 years) of computation to achieve a median ESS of 1,000. This appears unfeasible, and thus subtrees would need to be made smaller (less taxa) and chains would have to run for shorter times to achieve an ESS in the order of 100 or less. Such small ESSs would sacrifice precision of MCMC parameter estimates. We note the ESS per hour may depend not only on the number of taxa in the tree, but also on the number of partitions, the clock model, the number of fossil calibrations used, the variance of the calibration densities, and whether the calibrations are in conflict or not. Thus, it may be possible to further adjust these to reduce computation time at the cost of information loss.

We estimate the totality of the approximate likelihood analysis here (excluding the clock model selection analysis which used exact likelihood) took ~80K hours or ~9 years of CPU time. Because 1 day of CPU computing emits ~5 Kg CO₂ (see ⁶), this means our analysis emitted roughly 16.7 metric tonnes of CO₂. Without the subtree approach (i.e., attempting to estimate the times on the whole 4,705-taxon tree directly), the analyses would have required over 115x more CPU time and thus would have emitted over 1.9 thousand tonnes of CO₂. Without the use of approximate likelihood, computation times and CO₂ emissions would have increased by 1,000-fold.

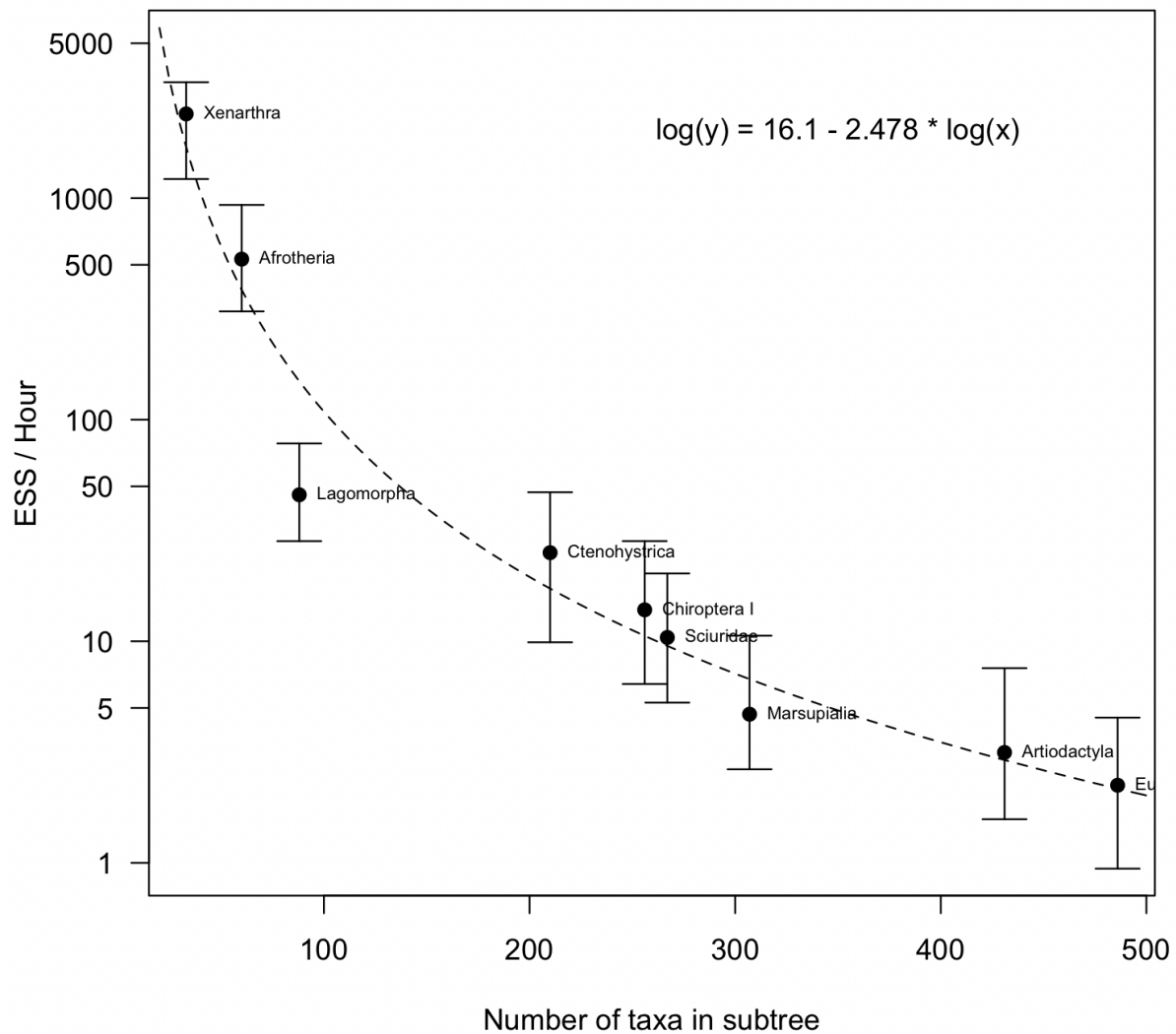


Figure S11. Benchmarking analyses. Each subtree was analysed with a single MCMC chain and the median ESS (for the divergence times, black circles) per hour calculated. The bars span the 25% and 75% quantiles of ESS values among the 71 node ages for the subtree. The dashed line is the fitted regression model $\log(y) = b + a \times \log(x)$. The four largest subtrees (all with >600 taxa) did not produce usable samples during the test period and thus are not included. However, the regression equation can be used to extrapolate to our largest subtree (Rest of Rodentia (II), 691 taxa) and also to the complete 4,705-taxon phylogeny, giving 0.903 ESS/h and 7.8×10^{-3} ESS/h, respectively.

Supplementary Data Structure

The data (available at DOI: [10.6084/m9.figshare.14885691](https://doi.org/10.6084/m9.figshare.14885691)) are released as a single zip file (~450 Mb) containing alignments, trees, and other files.

Alignments: Directory `aln/00_step_01/` contains the alignments for the 72 genomes in phylip format. Directory `aln/01_step_02/` contains the uncompressed, raw subtree alignments for the 4,705 taxa, with missing species represented as sequences of gaps (see [Table S7](#)). Directory `aln/01_step_02_patterns/` contains the same alignments after processing, that is, with missing species removed and with the alignments compressed into site patterns (see `MCMCtree` and `PAML` documentation for alignment formats). The processed alignments are the ones used by `MCMCtree` to calculate the likelihood during estimation of gradient and Hessian. Note each alignment file contains several alignment blocks, with each block corresponding to an alignment partition. If you load an alignment file into an alignment editor, make sure your editor allows you to see all partition blocks and not just the first one.

Approximate likelihood: Directory `inBV/` contains the estimated gradient and Hessian for each alignment partition, which are required to estimate the divergence times under the approximate likelihood method. This directory is subdivided into `step01` and `step02` subdirectories corresponding to the data for the 72 genomes and the 4,705-taxon subtrees respectively.

Phylogenetic trees: Directory `trees/` contains the trees with fossil calibrations in Newick format. As per above, subdirectories `step01` and `step02` contain the corresponding trees for the 72 genomes and 4,705 taxa respectively. These trees are required, together with the alignment and `in.BV` files to estimate the divergence times with `MCMCtree`. Directory `timetrees/` contains the estimated posterior timetrees in Nexus format. These are suitable for plotting with `FigTree` v1.3 (<http://tree.bio.ed.ac.uk/software/figtree/>). For the 4,705 taxa, both the separate subtrees and the fully stitched 4,705-taxon tree are provided.

Other files: Directory `clocktest/` contains the full results for the Bayesian selection of relaxed-clock model, while directory `paleodb/` contains the data mined from the Paleobiology Database. Note that all directories contain `README.md` files that provide additional information on the directory contents.

References

- 1 dos Reis M, Gunnell GF, Barba-Montoya J, Wilkins A, Yang Z, Yoder AD. Using phylogenomic data to explore the effects of relaxed clocks and calibration strategies on divergence time estimation: primates as a test case. *Syst Biol* 2018; **67**: 594–615.
- 2 Rannala B. Conceptual issues in Bayesian divergence time estimation. *Philos Trans R Soc Lond B Biol Sci* 2016; **371**. doi:10.1098/rstb.2015.0134.
- 3 Nascimento FF, dos Reis M, Yang Z. A biologist's guide to Bayesian phylogenetic analysis. *Nat Ecol Evol* 2017; **1**: 1446–1454.
- 4 dos Reis M, Yang Z. Approximate likelihood calculation on a phylogeny for Bayesian estimation of divergence times. *Mol Biol Evol* 2011; **28**: 2161–2172.
- 5 Battistuzzi FU, Billing-Ross P, Paliwal A, Kumar S. Fast and slow implementations of relaxed-clock methods show similar patterns of accuracy in estimating divergence times. *Mol Biol Evol* 2011; **28**: 2439–2442.
- 6 Zwart SP. The ecological impact of high-performance computing in astrophysics. *Nature Astronomy* 2020; **4**: 819–822.

ANNEX: Justification for Fossil Calibrations

For nodes without a maximum justification, the maximum is constrained to be the 2.5% quantile of the fitted ST/SN density in an ancestral node. This is done to avoid truncation artefacts between fossil calibration and fitted densities. Calibrations integrate geochronological updates as of September 2021.

Sort ID	Crown group	Dating step	Min (Ma)	Max (Ma)	Justification
1	Mammalia	1	164.1	252.2	<p>Node Calibrated. Divergence of monotremes, marsupials, and placentals, following Tarver et al. ¹.</p> <p>Fossil taxon and specimen. Bathonian australosphenidans such as <i>Ambondro mahabo</i> (UA 10602 University of Antananarivo, Madagascar; Flynn et al. ²).</p> <p>Phylogenetic justification. Puttick et al. ³ compared application of the Mk model in MrBayes to implied and equal-weights parsimony, and supported the interpretation of Jenkins et al. ⁴ and Luo et al. ⁵ that Triassic haramiyids fall outside of crown Mammalia.</p> <p>Minimum Age. 164.1 Ma.</p> <p>Maximum Age. 252.2 Ma.</p> <p>Age Justification. <i>Ambondro</i> comes from the upper part of the Isalo "Group" (middle Jurassic, Bathonian) of Madagascar ²), dated as generally Bathonian, so we select the top of the Bathonian as the hard minimum calibration date, 165.3 Ma \pm 1.1 Myr, or 164.1 Ma ⁶. Following Tarver et al. ¹ we revise our maximum calibration to allow for the possibility that the monotreme stem lineage really does extend into the upper Triassic ^{7,8}. Specifically, the soft maximum is set at the Permian-Triassic boundary, dated at the base of the Induan, 251.9 Ma \pm 0.3 Myr ⁹ or 252.2 Ma.</p> <p>Discussion. Our calibration for this node contrasts to suggestions (e.g., ^{7,8,10}) that Triassic <i>Thomasia</i> and <i>Haramiyavia</i> are closely related to multituberculates and monotremes, which, in turn, implies membership of these Triassic species within crown Mammalia. We follow Luo et al. ⁵, Benton et al. ¹¹, Puttick et al. ³ and Huttenlocker et al. ¹² in excluding haramiyids from crown Mammalia and in using <i>Ambondro</i> for the minimum calibration.</p>

2	Theria	1	121.56	169.4	<p>Node calibrated. Divergence of marsupial and placental mammals.</p> <p>Fossil taxon and specimen. <i>Sinodelphys szalayi</i>.</p> <p>Phylogenetic justification. Resolved on stem to Placentalia, within Theria, by Bi et al. 2018¹³.</p> <p>Minimum age. 121.56 Ma.</p> <p>Maximum age. 169.4 Ma.</p> <p>Age justification. Fossils from the Jehol biota of northeast China come from Barremian to Aptian-age deposits, although there is some ambiguity about their age¹⁴. Here we take the youngest age estimate from tuffs overlying the main fossil-bearing layers, dated to 121.96 Ma \pm 0.5 Myr¹⁵, thus 121.56 Ma. We conservatively use the age of the Barremian to define the ages of Jehol specimens, which has an upper margin of 125.0 Ma. Given the possibility that southern, tribosphenic mammals such as <i>Ambondro</i> are therian (cf.¹⁶), we set the soft maximum age for Theria in the Bathonian, 168.2 Ma \pm 1.2 Myr so 169.4 Ma⁶.</p> <p>Discussion. Luo et al.¹⁷ hypothesized that <i>Juramaia sinensis</i> from the late Jurassic was the geologically oldest therian mammal, more closely related to crown placentals than to other mammals and therefore eutherian (see also Bi et al.¹³). Some subsequent analyses have corroborated this result^{5,8}, but others have not, placing <i>Juramaia</i> instead on the stem to Theria (e.g.,¹⁰). Other candidates for the oldest crown therians include <i>Sinodelphys</i>¹⁸ and <i>Eomaia</i>¹⁹ originally argued to be on the stems to Marsupialia and Placentalia, respectively. Again, <i>Eomaia</i> in more recent studies has been placed on the therian stem^{10,20}, and <i>Sinodelphys</i> appears more consistently on the stem leading to either Placentalia¹³ or Marsupialia^{5,8,21}. Krause et al.¹⁰ reconstruct <i>Sinodelphys</i> as a metatherian in at least their Bayesian topologies (their figs. S2, S4), although not with MP (their figs. S1, S3) or in Krause et al.²². Overall, <i>Sinodelphys</i> enjoys better support as a crown therian¹² than other taxa and we thus use it as a minimum constraint for Theria.</p>
3	Placentalia	1	61.66	162.5	<p>Node calibrated. The human-tenrec split is equivalent to the origin of the clade comprising Boreoeutheria (Laurasiatheria and Euarchontoglires) and Atlantogenata (Xenarthra and Afrotheria). Following Benton et al.¹¹ but with the geochronology revised following²³ and⁶.</p>
4	Euarchontoglires	1	61.66	162.5	<p>Node calibrated. Euarchontoglires is composed of two clades, the Archonta and the Glires. Primates belong to the former, Rodentia to the latter, the common ancestor of which corresponds to the origin of Euarchontoglires. Following Benton et al.¹¹ but with the geochronology revised following²³ and⁶.</p>

5	Primates	1	56	66.09	Node calibrated. Crown-group Primates, or Euprimates, encompass living forms plus the extinct adapoids and omomyoids; the latter are more closely related to extant lemuriforms than to anthropoids ²⁴⁻²⁶ . Following Benton et al. ¹¹ with the exception that the soft-maximum constraint, defined as the base of the Paleocene, is revised to 66.04 Ma \pm 0.05 Myr ²⁷ , so 66.09 Ma.
6	Anthropoidea	1	33.9	66.09	Node calibrated. Last common ancestor of platyrrhine and catarrhine primates. Following Benton et al. ¹¹ with the exception that the soft-maximum constraint, defined as the base of the Paleocene, is revised to 66.04 Ma \pm 0.05 Myr ²⁷ , so 66.09 Ma.
7	Catarrhini	1	24.44	33.9	Node calibrated. The common ancestor of Old World monkeys (Cercopithecoidea) and apes (Hominoidea), which together form crown Catarrhini. Following Benton et al. ¹¹ with the exception that the soft-maximum constraint, defined on the base of the Oligocene, is dated to 33.9 Ma ²³ .
8	Hominidae	1	11.65	33.9	Node calibrated. Last common ancestor of great apes, including human, chimp, gorilla, and orangutan. Following Benton et al. ¹¹ with the exception that the minimum age constraint is revised The Chinji Formation of Pakistan corresponds to magnetic polarity chron 5Ar, estimated to be ca. 12 Ma before present ²⁸ . This correlates to the Serravallian stage, the top of which is dated to 11.65 Ma ²⁹ .
9	Homininae	1	5.33	33.9	<p>Node calibrated. Divergence of the human-chimp lineage from that of gorillas.</p> <p>Fossil taxon and specimen. <i>Chororapithecus abyssinicus</i> CHO-BT 4 from the Beticha locality, Chorora Fm, Ethiopia.</p> <p>Phylogenetic justification. Suwa et al.³⁰ identify shared, derived characters of their dental fossils with the lineage of <i>Gorilla</i>.</p> <p>Minimum age. 5.33 Ma.</p> <p>Maximum age. 33.9 Ma.</p> <p>Age justification. Katoh et al.³¹ revised the geological context of this find, and concluded that it is not middle Miocene as originally reported, but upper Miocene, between 7-9 Ma in age, overlapping with the Tortonian and Messinian. The latter has an upper bound of 5.33 Ma²⁹. The soft maximum is as for catarrhines, above.</p> <p>Discussion. The fossil lineage of habitually bipedal hominins is much better than that for great apes, and also has an oldest occurrence in the late Miocene (e.g., Brunet et al.³²). No hominin fossils are known from deposits correlating with a marine stage older than the Messinian.</p>
10	Hominini	1	6.5	10	Node calibrated. Chimpanzee-human. Following Benton et

					al. ¹¹ .
11	Cercopithecinae	1	5.33	33.9	<p>Node calibrated. Divergence of vervet monkeys (<i>Chlorocebus</i>) from baboons and macaques (<i>Macaca</i> and <i>Papio</i>).</p> <p>Fossil taxon and specimen. <i>Macaca libyca</i>, YPM 21551 (Benefit et al. ³³: fig. 2) from Wadi Natrun, Egypt.</p> <p>Phylogenetic justification. Referred to the same genus as the living macaque by Benefit et al. ³³.</p> <p>Minimum age. 5.33 Ma.</p> <p>Maximum age. 33.9 Ma.</p> <p>Age justification. Cercopithecine fossils are known from As-Sahabi (Libya), Menacer (Algeria), Wadi Natrun (Egypt), and Toros-Menalla (Chad). All are late Miocene in age and overlap with the Messinian, with an upper bound of 5.33 Ma ²⁹. The soft maximum date is as for Catarrhini, above.</p> <p>Discussion. Cercopithecine fossils have been reported from the late Miocene of Europe ³⁴ and North Africa ³³. Following Raaijmakers et al. (³⁵: fig. 3), the record of <i>Macaca</i> is slightly older than that of baboons, but Benefit et al. ³³ summarize fossils of both lineages from North Africa. The lineage of vervet monkeys appears to be limited to the Plio-Pleistocene.</p>
12	Papionini	1	5.33	33.9	<p>Node calibrated. Divergence of baboons (e.g., <i>Papio</i>) from macaques (<i>Macaca</i>).</p> <p>Fossil taxon and specimen. <i>Macaca libyca</i>, YPM 21551 (Benefit et al. ³³: fig. 2) from Wadi Natrun, Egypt.</p> <p>Phylogenetic justification. As for cercopithecines, above.</p> <p>Minimum age. 5.33 Ma.</p> <p>Soft maximum age. 33.9 Ma.</p> <p>Age justification. As for catarrhines.</p>
13	Strepsirhini	1	33.9	66.09	<p>Node calibrated. The crown clade comprising lemurs, lorises, galagos, and other extant primates that possess a toothcomb ³⁶. Following Benton et al. ¹¹ with the exception that we use the base of the Paleocene as the soft maximum, as for Primates, above.</p>
14	Glires	1	56	162.5	<p>Node calibrated. The last common ancestor of Rodentia and Lagomorpha. Following Benton et al. ¹¹ with the exception that the soft-maximum constraint, defined as the base of the Oxfordian, is revised to 161.5 Ma \pm 1.0 Myr ⁶, so 162.5 Ma.</p>

15	Rodentia	1	56	66.09	<p>Node calibrated. The common ancestor of the three major extant rodent clades: Muroidea (mouse-related), Sciuromorpha (squirrel-related), and Ctenohystrica (guinea-pig related). Following Benton et al.¹¹ with the exception that the soft maximum constraint, defined on the base of the Paleocene, is revised to 66.04 Ma \pm 0.05 Myr²⁷, so 66.09 Ma.</p>
16	Nonsquirrel rodentia	1	48.07	59.24	<p>Node calibrated. The divergence of Myomorpha+ Ctenohystrica to the exclusion of Sciuromorpha (Fabre et al.^{37, 38}; high-level taxa defined in Asher et al.³⁸). We acknowledge that there is uncertainty regarding the initial divergence within Rodentia (cf. Myomorpha reconstructed as sister to Ctenohystrica-Sciuromorpha in Swanson et al.³⁹).</p> <p>Fossil taxon and specimen. Chapattimyidae such as <i>Birbalomys sondaari</i> (Geological Survey of Pakistan, Howard University Collection, H-GSP 92161 of Thewissen et al.⁴⁰) from the Kuldana Formation of the Ganda Kas area, Pakistan.</p> <p>Phylogenetic justification. Phylogenetic analysis by Marivaux et al.⁴¹ placed Eocene chapattimyids within the Ctenohystrica, close to hystricognaths and to the exclusion of diatomyids. They are therefore nested within the unnamed crown clade comprising Myomorpha and Ctenohystrica.</p> <p>Minimum age. 48.07 Ma.</p> <p>Maximum age. 59.24 Ma.</p> <p>Age justification. The Kuldana Formation of Pakistan has been dated as early–middle Eocene, and ages may differ in different regions of northern India, and mammals occur in different horizons. <i>Birbalomys</i> is noted as occurring at 51 Ma by Marivaux et al.^(41, p. 132), thus well within the Ypresian. Hence, we assign a minimum constraint for rodents excluding Sciuromorpha at the top of the Ypresian marine stage, hence 48.07 Ma²³. The soft maximum constraint might be taken as equivalent to the age of <i>Paramys</i> and <i>Franimys</i> from the late Paleocene (base of the Thanetian) of North America and Europe, 59.24 Ma²³.</p> <p>Discussion. Fossils associated with the mouse-related stem group are younger, including Eocene dipodids such as <i>Ulkenulastomys</i>, <i>Blentosomys</i>, and <i>Aksyiromys</i> from the Obayla Svita of the Zaysan Basin, Kazakhstan⁴². Lucas⁴³ assigned a younger, Irđinmanhan age to this site based on biostratigraphic comparisons, changing its previous stratigraphic interpretation from early Eocene to the base of the middle Eocene.</p>

17	Dipodidae-Muroidea	1	41.03	59.24	<p>Node calibrated. Divergence of dipodid from muroid(i.e., within the mouse-related clade) rodents.</p> <p>Fossil taxon and specimen. <i>Aksyiromys dalos</i>, IZ-NAS-RK 34/181 (Emry et al. ⁴⁴: fig. 3A).</p> <p>Phylogenetic justification. Following Fabre et al. ³⁷ and Asher et al. ³⁸, dipodids (jerboas, birch mice, et al.) comprise the sister taxon to Muroids. Marivaux et al. ⁴¹ reconstruct <i>Aksyiromys</i> as sister taxon to fossil dipodids (e.g., <i>Primisminthus</i>) and cricetids (e.g., <i>Pappocricetodon</i>), the latter a putative member of Muroidea.</p> <p>Minimum age. 41.03 Ma.</p> <p>Maximum age. 59.24 Ma.</p> <p>Age justification. Lucas ⁴³ and Emry ⁴⁵ note that the age of the fossils described by Shevyreva ⁴² is within the Irdivmanhan ALMA, as are their fossils from the Shinzaly fauna of eastern Kazakhstan ⁴⁴. The marine equivalent is likely the Lutetian, with an upper bound of 41.03 Ma ²³. The soft maximum is as for rodents minus the squirrel related clade, above.</p> <p>Discussion. Shevyreva ⁴² described <i>Aksyiromys</i>, <i>Ulkenulastomys</i>, and "<i>Blentosomys</i>" from middle Eocene deposits of Kazakhstan. dos Reis et al. ⁴⁶ used <i>Ulkenulastomys</i> as a minimum calibration point for this clade. Emry et al. ⁴⁴ described <i>Aksyiromys</i> as a zapodine dipodid rodent from the Shinzaly fauna of eastern Kazakhstan, equivalent in age to Obayla Svita, Zaysan Basin, Kazakhstan, where Shevyreva ⁴² first described <i>Aksyiromys</i>. Emry ⁴⁵ noted that <i>Blentosomys</i> is likely a junior synonym of <i>Aksyiromys</i>. Because their description is more accessible in the literature than that of Shevyreva ⁴², and because of their publication of good quality figures with associated specimen numbers, we base our minimum calibration on <i>Aksyiromys</i> as described by Emry et al. ⁴⁴, rather than other fossil dipodids of the same age.</p>
18	Murinae	1	7.25	15.99	<p>Node calibrated. Divergence of <i>Mus</i> from <i>Rattus</i>. Following Benton et al. ¹¹; note that their summary age constraints did not match their justification - we follow their justification and revise the age constraints following ²⁹.</p>
19	Lagomorpha	1	48.07	66.09	<p>Node calibrated. The common ancestor of leporids (rabbits and hares) and ochotonids (pikas). Following Benton et al. ¹¹ but with the geochronology revised following ²³.</p>

20	Euungulata	1	50.7	66.09	<p>Node calibrated. Common ancestor of Perissodactyla and Artiodactyla. Following calibration for crown-Artiodactyla in Benton et al. ¹¹ but with the geochronology revised following ²³.</p> <p>Discussion. dos Reis et al. ⁴⁶ took <i>Lambdaotherium</i> as the basis for a 62.5 Ma minimum date for perissodactyls, based on Benton et al. ⁴⁷. However, the 62.5 Ma date from Benton et al. ⁴⁷ derived from a topology ("Zooamata", or Carnivora-Perissodactyla) that is no longer supported by larger datasets (¹: figs S1, S3) and which was based on a carnivoran calibration: <i>Proticis</i> (Torrejonian NALMA). Instead, the 21.4 gigabase alignment of Tarver et al. (¹: fig. S1) supports an artiodactyl-perissodactyl clade, or Euungulata. Two Paleocene genera often associated with perissodactyls are worth mention: <i>Radinskya</i> and <i>Lambdaotherium</i> as possible minimum calibration points. Neither Holbrook ⁴⁸ nor Rose et al. ⁴⁹ unequivocally support <i>Radinskya</i> in a close sister-taxon relationship with perissodactyls. Rose et al. ⁴⁹ does support <i>Lambdaotherium</i> within tapiromorphs; Beard ⁵⁰ emphasizes its affinities to perissodactyls, but the description of a Gashatan ALMA (Thanetian) specimen by Meng et al. (⁵¹: 176) is more circumspect: "other than its possible perissodactyl affinities, the fragmentary material precludes definitive taxonomic placement." There are many records of slightly younger, early Eocene perissodactyls (e.g., <i>Homogalax</i>, <i>Hyracotherium</i>) and among the best material is <i>Cambaytherium</i> from the Cambay Shale, India (ca. 54.5 Ma ⁴⁹). These correlate with the Ypresian, the top of which is 47.8Ma. The record of archaeocete whales (<i>Himalayacetus</i>, described below) is likely younger in absolute terms, but is found in deposits with intercalated marine deposits (NP zones 11-12, 52.4 Ma), and thus can be correlated with the marine record at an older age than early Eocene Asian and North American records of perissodactyls.</p>
21	Artiodactyla	1	50.7	66.09	<p>Node calibrated. Common ancestor of ruminants, tylopods, and "Suiformes", including the now well-established hippo-whale clade. Following Benton et al. ¹¹ but with the geochronology revised following ²³.</p>
22	Cetruminantia	1	50.7	66.09	<p>Node calibrated. Divergence of the common ancestor of ruminants and cetaceans, excluding suids and tylopods. Following the calibration for Whippomorpha-Ruminantia in Benton et al. ¹¹ but with the geochronology revised following ²³.</p>
23	Bovidae	1	15.99	27.29	<p>Node calibrated. The branching between the cow (<i>Bos</i>) and sheep (<i>Ovis</i>) is an intrafamilial split within the Family Bovidae. <i>Bos</i> is a member of the Tribe Bovini, and <i>Ovis</i> is a member of the Tribe Caprini, which belong respectively to the subfamilies Bovinae and Antilopinae ⁵². Following the calibration for Bovinae-Antilopinae in Benton et al. ¹¹ but with the geochronology revised following ²⁹.</p>
24	Carnivora	1	37.71	66.09	<p>Node calibrated. Common ancestor of Caniformia (dogs, bears, raccoons, seals) and Feliformia (cats, mongooses, hyaenas), excluding stem carnivoramorphans sensu Wesley Hunt and Flynn ⁵³. Following Benton et al. ¹¹ but</p>

					with the geochronology revised following ²³ .
25	Caniformia	1	37.71	66.09	<p>Node calibrated. Divergence of canids (dogs) and arctoids (musteloids, ursids, pinnipeds).</p> <p>Fossil taxon and specimen. <i>Hesperocyon gregarius</i> (SMNH P1899.6; ⁵⁴) from the Cypress Hills Formation, Duchesnian NALMA, Lac Pelletier local fauna, Saskatchewan.</p> <p>Phylogenetic justification. As for Carnivora.</p> <p>Minimum age. 37.71 Ma.</p> <p>Maximum age. 66.09 Ma.</p> <p>Age justification. As for Carnivora.</p>
26	Chiroptera	1	48.07	66.09	<p>Node calibrated. Divergence of Yinpterochiroptera and Yangochiroptera.</p> <p>Fossil taxon and specimen. <i>Eppsinycotis anglica</i> ⁵⁵, BMNH M13776 from the Lessness Shell Bed, Blackheath Beds, Abbey Wood, Ypresian.</p> <p>Phylogenetic justification. As summarized by Eiting & Gunnell ⁵⁶, the stem lineage of chiropterans extends to the basal Eocene of Europe ⁵⁷, Australia ⁵⁸. <i>Eppsinycotis</i> from the early Eocene of the UK may be related to emballonurids ⁵⁵; <i>Honrovits</i> from the early Eocene of Wyoming may be related to natalids ⁵⁹; <i>Witwatia</i> and <i>Dizzya</i> from the early Eocene of Tunisia may be vespertilionoids ^{60,61}. We choose <i>Eppsinycotis</i> as the minimum constraint as it is represented by a well preserved jaw ⁵⁵.</p> <p>Minimum age. 48.07 Ma.</p> <p>Maximum age. 66.09 Ma.</p> <p>Age justification. The three oldest records for modern bat groups cited above all correspond to the Ypresian in age, which has an upper bound of 48.07 Ma ²³. The absence of any chiropterans during the Paleocene may point to a soft maximum constraint at the base of the Danian, 66.04 Ma ± 0.05 Myr ²³, so 66.09 Ma.</p> <p>Discussion. Smith et al. ⁶² estimate that the earliest records of modern families are middle Eocene, and we agree that the evidence in the above cases is uncertain. Nonetheless, the presence of multiple identifications of modern groups in the early Eocene, as noted above, implies that crown Chiroptera existed at this time.</p>
27	Lipotyphla	1	61.66	162.5	<p>Node calibrated. common ancestor of modern soricids, talpids, erinaceids, and <i>Solenodon</i>. Following the calibration for crown-Lipotyphla in Benton et al. ¹¹ but with the geochronology revised following ²³ and ⁶.</p>

28	Xenarthra	1	48.07	162.5	Node calibrated. Divergence of cingulates (armadillos) from Pilosa (i.e., sloths and anteaters). Following Benton et al. ¹¹ but with the geochronology revised following ²³ and ⁶ .
29	Afrotheria	1	56	162.5	Node calibrated. Last common ancestor of proboscideans and tenrecids (i.e., all extant afrotheres). Following Benton et al. ¹¹ but with the geochronology revised following ²³ and ⁶ .
30	Paenungulata	1	56	162.5	<p>Node calibrated. Common ancestor of <i>Loxodonta</i> and <i>Procavia</i>.</p> <p>Fossil taxon and specimen. The extinct proboscidean <i>Eritherium azzouzor</i> (MNHN PM69, Paris) from the Sidi Chennane quarries, phosphate bed IIa, lower bone-bed, Ouled Abdoun Basin of Morocco, regarded as upper Paleocene (early Thanetian ⁶³).</p> <p>Phylogenetic justification. See Afrotheria.</p> <p>Minimum age. 56 Ma.</p> <p>Soft maximum age. 162.5 Ma.</p> <p>Age justification. See Afrotheria.</p> <p>Discussion. The topology within paenungulates is less certain than most other inter-ordinal branches among mammals. Several recent studies support a proboscidean-hyrax clade to the exclusion of sirenians ^{64,65}; others support a proboscidean-sirenian clade to the exclusion of hyracoids ^{66,67}. Either way, the fossil record of Proboscidea remains the oldest, well-documented fossil lineage in Afrotheria.</p>
31	Marsupialia	1	48.07	127.2	Node calibrated. Divergence of crown marsupials. Following Benton et al. ¹¹ but with the geochronology revised following ²³ and ²⁷ .

32	Eometatheria	1	23.04	56	<p>Node calibrated. Divergence of dasyuromorphs (e.g., <i>Sarcophilus</i>) and diprotodonts (e.g., <i>Macropus</i>), i.e., the origin of crown Australasian australidelphians.</p> <p>Fossil taxon and specimen. <i>Perikoala robustus</i>, SAM P26552 from Turtle Quarry, Etadunna Fm., west side of Lake Palankarina, South Australia ⁶⁸.</p> <p>Phylogenetic justification. Black et al. ⁶⁹ reconstruct <i>Perikoala</i> closer to <i>Phascolarctos</i> than <i>Vombatus</i> (but did not test its affinities widely throughout marsupials). Combined with the identification by Wooburne et al. ⁶⁸ of features diagnostic of vombatiforms, we accept their identification of this taxon within Diprotodontia.</p> <p>Minimum age. 23.04 Ma.</p> <p>Maximum age. 56.0 Ma.</p> <p>Age justification. Woodburne et al. ⁷⁰, as summarized in Mitchell et al. ⁷¹, noted the presence of crown diprotodonts including likely pseudocheirids and phascolarctids from Zone A of the Etadunna Fm. Megirian et al. ⁷² assign an age of 24.9-25.3 Ma, equivalent to the Chattian, the top of which is 23.04 Ma ²³. Following Mitchell et al. ⁷¹, no crown australidelphian lineages are evident at Murgon (early Eocene, = Tingamarra local fauna), which samples the early Eocene at ca. 55Ma, justifying a soft maximum defined by the base of the Ypresian at 56.0 Ma ²³.</p> <p>Discussion. Other crown australidelphians from Riversleigh could also serve as the minimum, including a potorine ("<i>Kyeema mahoneyi</i>") and a pseudocheirid from the Etadunna Faunal Zone "A" ^{73,74}. The term Eometatheria dates to Simpson ⁷⁵, who used it as we do, to encapsulate Australasian marsupials. The term was subsequently used by Kirsch ⁷⁶ and Asher et al. ⁷⁷ to imply Australasian marsupials excluding peramelians, based on the now overturned idea ^{71,78,79} that peramelians are the basal-most australidelphians. Given this somewhat complicated history, Beck ⁷⁹ and Mitchell et al. ⁷¹ used the taxon "Eomarsupialia" for this clade (australidelphians excluding <i>Dromiciops</i>) instead. Arguably, however, the importance of precedent and minimizing the introduction of novel taxa would favor retaining older terms that have been used to delineate broadly similar (and in the case of Simpson ⁷⁵ identical) groups ⁸⁰. Although the content of Eometatheria has changed over time, this is also true of other high-level taxa (e.g., Primates, Dinosauria); we therefore prefer Eometatheria over alternatives to indicate the crown clade of Australasian australidelphian marsupials.</p>
----	--------------	---	-------	----	---

33	Cingulata	2	34.85	56.0	<p>Node calibrated. Common ancestor of dasypodids and other cingulates.</p> <p>Fossil taxon and specimen. Dasypodid petrosal (PVL 6245) from the middle Member of the Geste Formation, Antofagasta de la Sierra, Catamarca Province, Argentina Babot et al. ⁸¹.</p> <p>Phylogenetic justification. Ciancio et al. ⁸² discuss <i>Prostegotherium</i> with dermal remains from the Vacan (early Casamayoran) as a member of Dasypodinae, but this ID as a crown cingulate is I think not yet bolstered by a phylogenetic analysis. Babot et al. ⁸¹ do undertake a phylogenetic analysis and place a petrosal from the slightly younger Barrancan (late Casamayoran) Geste Fm closer to Dasypus than other cingulate genera.</p> <p>Minimum age. 34.85 Ma.</p> <p>Soft maximum. Age: 56.0 Ma.</p> <p>Age justification. The Geste Formation is conventionally interpreted as late Eocene (Barrancan subage of Casamayoran South American Land Mammal Age; SALMA ⁸¹); however, this age interpretation is not clearly established ⁸¹. Detrital zircons from Geste Formation establish a 37 Ma maximum age interpretation and a bracket of 37.3 Ma \pm 1.5 Myr to 35.4 Ma \pm 0.55 Myr ⁸³.</p> <p>The soft maximum is established on the Eocene (Itaboraian) of Itaborai, Brasil ⁸⁴ based on presence of xenarthrans but absence of any undisputed crown taxa. Also relevant is absence of any xenarthra from localities older than Itaborai (e.g., Paleocene Tiupampa; see Woodburne et al. ⁸⁴: table 1). Woodburne et al. ⁸⁴ and Speijer et al. ²³ consider the Itaboraian SALMA to be Ypresian, its base equating to 56.0 Ma ²³.</p>
----	-----------	---	-------	------	---

34	Chlamyphoridae	2	33.9	56.0	<p>Node calibrated. Common ancestor of tolypeutines-chlamyphorines and euphractines.</p> <p>Fossil taxon and specimen. <i>Glyptatelus</i>, e.g., scutes assigned to <i>G. fractus</i> including MACN 10949⁸⁵. Following McKenna et al.⁸⁶ (fig. 1), the jaw fragment AMNH 29483 is not <i>Glyptatelus</i> but likely the folivoran <i>Pseudoglyptodon</i> (see below).</p> <p>Phylogenetic justification. <i>Riostegotherium</i> is not convincingly a dasypodine but it is more conservatively regarded as a stem cingulate. Delsuc et al.⁸⁷ reconstruct glyptodonts within crown cingulates, closer to tolypeutines-chlamyphorines than to dasypodines or euphractines. <i>Pseudoglyptodon</i> from the Abanico Fm of Chile⁸⁶ is likely a stem folivoran (see below), but this is still younger (Tingurrician) than Mustersan fossils like <i>Glyptatelus</i>. McKenna et al.⁸⁶ assigned a jaw fragment Simpson thought was <i>Glyptatelus</i> (cingulate, AMNH 29483) to <i>Pseudoglyptodon</i> (folivoran) so affinities of that specimen remain ambiguous (although the part-skull assigned to <i>Pseudoglyptodon</i> by McKenna et al.⁸⁶ does appear to be a stem folivoran). Hence, Mustersan dermal scutes and fossil teeth are the oldest indicators of glyptodonts and therefore non-dasypodid cingulates.</p> <p>Minimum age. 33.9 Ma.</p> <p>Soft maximum age. 56.0 Ma.</p> <p>Age justification. Eocene (Mustersan SALMA), Musters Fm, Patagonia^{85,87}. The 2012 Geologic Timescale interprets the Mustersan SALMA to straddle Bartonian-Priabonian boundary, with a minimum age c. 33.9 Ma²³. The soft maximum constraint follows that of Cingulata.</p>
35	Pilosa	2	31.17	56	<p>Node calibrated. Common ancestor of folivorans (sloths) and vermilinguans (anteaters).</p> <p>Fossil taxon and specimen. <i>Pseudoglyptodon chilensis</i>, SGO PV 2995⁸⁶ (fig. 3).</p> <p>Phylogenetic justification. Folivoran ID of <i>Pseudoglyptodon</i> from McKenna et al.⁸⁶ is supported by Slater et al.⁸⁸ and Gaudin and Croft⁸⁹.</p> <p>Minimum age. 31.17 Ma.</p> <p>Maximum age. 56.0 Ma.</p> <p>Age justification. <i>Pseudoglyptodon chilensis</i> was recovered from volcanoclastic strata within the Abanico Fm., Chile, and is considered early Oligocene in age as it forms part of the Tinguirirican fauna and its associated South American Land Mammal Age (SALMA)⁸⁶. The minimum age constraint is established based on Ar40/Ar39 dating from within the Tinguirirican SALMA stratotype, the youngest range being 31.34 Ma \pm 0.17 Myr⁹⁰, providing a minimum constraint of 31.17 Ma. The soft maximum constraint follows that of Cingulata.</p>

36	Folivora	2	15.99	56	<p>Node calibrated. Common ancestor of megalonychid sloths (including <i>Choloepus</i>) and <i>Bradypus</i>.</p> <p>Fossil taxon and specimen. <i>Imagocnus zaza</i>, holotype MNHNH P 3014 (MacPhee & Iturralde-Vinent ⁹¹: fig. 1).</p> <p>Phylogenetic justification. <i>Octodontotherium</i> and <i>Desadognathus</i> from Salla (Bolivia) may be stem folivorans rather than <i>Choloepus</i> sister taxa (following discussion in Slater et al. ⁸⁸). Pujos et al. (⁹²: fig. 5) show a consensus tree with <i>Octodontotherium</i> closer to <i>Choloepus</i> than <i>Bradypus</i>, but this was not an original phylogenetic analysis (and neither <i>Octodontotherium</i> nor <i>Desadognathus</i> are mentioned by Gaudin and Croft ⁸⁹). Thus, we interpret <i>Imagocnus</i> as the oldest definitive crown folivoran.</p> <p>Minimum age. 15.99 Ma.</p> <p>Maximum age. 56.0 Ma.</p> <p>Age justification. The holotype of <i>Imagocnus zaza</i> was recovered from the Lagunitas Fm., Domo de Zaza, Cuba ⁹¹. As a majority of the remains recovered were found in float that cannot be constrained stratigraphically, the minimum constraint is based on the age of the Formation, believed to be Burdigalian (Miocene) based on foraminifera indicative of the Miogypsina-Soritiidae zone (<i>Miopypsina antillea</i>, <i>Heterostegina antillea</i>, and <i>Sorites marginalis</i>) ⁹³. MacPhee et al. ⁹³ also attempted to date 4 shelly horizons using Sr87/Sr86 analysis but decided the results were inconsistent as stratigraphically older horizons produced younger dates than the youngest horizons. The minimum age is thus the Upper Burdigalian-Lower Langhian boundary, dated at 15.97 Ma ²⁹.</p> <p>The soft maximum constraint follows that of Cingulata.</p>
----	----------	---	-------	----	--

37	Vermilingua	2	17.36	56	<p>Node calibrated. Common ancestor of <i>Cyclopes</i> and myrmecophagines (<i>Myrmecophaga-Tamandua</i>).</p> <p>Fossil taxon and specimen. <i>Protamandua rothi</i> from the Santacrucian of Argentina, represented by a partial skull (YPM-VPPU 15267) and postcrania (e.g., astragalus MACN-A 10901b and calcaneus MACN-A 11530; see Bargo et al. ⁹⁴; fig. 13.2).</p> <p>Phylogenetic justification. Following Gaudin & Bramhan (⁹⁵; fig. 1) and Bargo et al. (⁹⁴; fig. 13.1), <i>Protamandua</i> comprises the sister taxon of myrmecophagines (extant <i>Myrmecophaga</i> and <i>Tamandua</i>) to the exclusion of <i>Cyclopes</i>. Skeletal elements now recognized as <i>Protamandua</i> were first assigned by Ameghino ⁹⁶ to multiple species but later recognized as a single species (and perhaps individual) by Hirschfeld ⁹⁷.</p> <p>Minimum age. 17.36 Ma.</p> <p>Maximum age. 56.0 Ma.</p> <p>Age justification. These remains of <i>Protamandua rothi</i> were collected south of the Río Coyle correlated to the lower fossiliferous levels (FL 1-7) of the Estancia La Costa Member of the Santa Cruz Formation, which is generally considered to be of Miocene age ⁹⁸. Tephra analysis using Ar40/Ar39 methods suggest FL 1-7 are part of a conformable sequence and that there is no temporal distinction between FL 3 and 7 ⁹⁹. Ar40/Ar39 dating of tephra sample CO from above FL 1-7, correlated across the Estancia La Costa Member fossil localities (Puesto Estancia La Costa, Cañadón Silva, and Estancia La Costa) was dated as 17.41 Ma \pm 0.05 Myr ¹⁰⁰, thus making the minimum age 17.36 Ma.</p> <p>The soft maximum constraint floors that of Cingulata.</p>
38	<i>Chrysochloris asiatica</i> - other chrysochlorids	2	3.6	33.9	<p>Node calibrated. Divergence of <i>Chrysochloris asiatica</i> from other chrysochlorids.</p> <p>Oldest crown fossil. Following Asher & Avery ¹⁰¹, two Pliocene chrysochlorids from Langebaanweg, South Africa (<i>Chrysochloris bronneri</i> and <i>C. arenosa</i>) are more closely related to the extant <i>C. asiatica</i> than to other extant chrysochlorids. Other extinct chrysochlorids such as <i>Chlorotalpa spelea</i> from Sterkfontein and <i>Amblysomus hamiltoni</i> from Makapansgat, South Africa ¹⁰¹⁻¹⁰³ may also be crown taxa, but likely post-date the Pliocene.</p> <p>Minimum age. 3.6 Ma.</p> <p>Maximum age. 33.9 Ma.</p> <p>Age justification. <i>Chrysochloris arenosa</i> and <i>C. bronneri</i> are from early Pliocene deposits at Langebaanweg, South Africa. Most fossils from this locality were not recovered in-situ and represent at least some time-averaging. Nonetheless, they are generally regarded as early Pliocene and thus older than fossils recovered from South African hominid sites. Hence the minimum constraint for crown chrysochlorids would be the Langebaanweg fossils, correlating to Zanclean with a top of 3.6Ma. We propose a soft maximum in the late Eocene given the abundance of African mammal fossils during that time but absence of uncontroversial crown chrysochlorids elsewhere ^{101,104}.</p>

39	Macroscelidea	2	23.04	56	<p>Node calibrated. Divergence of <i>Rhynchocyon</i> from other macroscelidids.</p> <p>Oldest crown fossil. <i>Oligorhynchocyon songwensis</i>, RRBP 08086 (left p4) from the Songwe Member of Nsungwe Formation.</p> <p>Minimum age. 23.04 Ma.</p> <p>Maximum age. 56.0 Ma.</p> <p>Age justification. Stevens et al. ¹⁰⁵ describe an isolated lower premolar from Tanzania, 25.2 Ma in age and diagnostic to Rhynchocyoninae. This falls within the Chattian marine stage the upper margin of which is 23.04 Ma ²³. As the soft maximum, we propose the base of the Eocene (Ypresian) dated to 56.0 Ma ²³. Various localities near and above the Paleocene-Eocene boundary have yielded numerous remains of afrotherians ^{63,106} without evidence for crown macroscelideans.</p>
40	Proboscidea	2	5.33	23.04	<p>Node calibrated. Common ancestor of <i>Elephas</i> and <i>Loxodonta</i>, following Benton et al. ¹¹ but with the geochronology revised following ²⁹ and ²³.</p>
41	Sirenia	2	41.03	66.09	<p>Node calibrated. Common ancestor of <i>Dugong</i> and <i>Trichechus</i>. Following ¹¹ excepting (i) that we use the top rather than base of the Lutetian to define the minimum age constraint, (ii) we include the dating errors in defining the soft maximum constraint, and (iii) with the geochronology revised following ²³.</p>
42	Hyracoidea	2	5.33	33.9	<p>Node calibrated. Divergence of <i>Dendrohyrax</i> from other hyracoid genera.</p> <p>Oldest crown fossil. <i>Dendrohyrax validus</i> ¹⁰⁷. Pickford & Hlusko ¹⁰⁷ describe many specimens of <i>Dendrohyrax cf. validus</i> from Lemudong'o, Narok, Kenya., one of which is KNM-NK 36534 (left mandible with p4-m2)).</p> <p>Minimum age. 5.33 Ma.</p> <p>Maximum age. 33.9 Ma.</p> <p>Age justification. According to Pickford & Hlusko ¹⁰⁷, fossils from Lemudong'o Locality 1, including <i>Dendrohyrax</i>, are ca. 6.1 Ma old. This is within the Messinian marine stage with an upper bound of 5.33 Ma ²⁹. <i>Heterohyrax auricampensis</i> from Berg Aukas, Namibia is presumably contemporaneous (see Rasmussen et al. ¹⁰⁸). Max bound would be better constrained by lack of crown hyracoid spp. in north African localities. As the soft maximum, we propose the base of the Oligocene, corresponding to the Rupelian ²³. Numerous localities from near this age show no evidence of the divergence of extant hyracoid genera.</p>
43	Paucituberculata (Caenolestidae)	2	0	15.97	<p>Node calibrated. Divergence of <i>Caenolestes</i>, <i>Rhyncholestes</i> and <i>Lestoros</i>.. Following Emerling et al. ¹⁰⁹.</p>

44	Didelphidae	2	11.608	28.1	Node calibrated. Divergence of didelphine and caluromyine marsupials. Following Emerling et al. ¹⁰⁹ .
45	Dasyuromorphia	2	15.97	-	Node calibrated. Divergence of <i>Thylacinus</i> from other dasyuromorphs. Following Emerling et al. ¹⁰⁹ .
46	Peramelidae	2	4.36	23.8	Node calibrated. Divergence of <i>Peroryctes</i> from other peramelids. Following Emerling et al. ¹⁰⁹ .
47	Vombatiformes	2	25.5	-	Node calibrated. Divergence of phascolarctids from other vombatiformes. Following Emerling et al. ¹⁰⁹ .
48	Phalangeridae- Burramyidae	2	25	-	Node calibrated. Divergence of <i>Phalanger</i> from <i>Burramys</i> . Following Emerling et al. ¹⁰⁹ .
49	Petauridae - Pseudocheiridae	2	25.5	-	Node calibrated. Divergence of <i>Petaurus</i> from <i>Pseudocheirus</i> . Following Emerling et al. ¹⁰⁹ .
50	Macropodoidea (=Macropodidae + Potoroidae)	2	24.7	-	Node calibrated. Divergence of <i>Macropus</i> from <i>Potorous</i> . Following Emerling et al. ¹⁰⁹ .
51	Platyrrhini	2	20.45	37.7	<p>Node calibrated. Divergence of cebids from other South American monkeys (Platyrrhini).</p> <p>Fossil taxon and specimen. <i>Panamacebus transitus</i>, left upper M1 (UF 280128) from Lirio Norte, Panama Canal area, Panama ¹¹⁰.</p> <p>Phylogenetic justification. Bloch et al. ¹¹⁰ resolved <i>Panamacebus transitus</i> as a member of crown-Cebinae based on parsimony analysis of a morphological dataset.</p> <p>Minimum age. 20.45 Ma.</p> <p>Maximum age. 37.7 Ma.</p> <p>Age justification. Bloch et al. (2016) report a “a precisely dated 20.9-Ma layer in the Las Cascadas Formation in the Panama Canal Basin, Panama” as the source of <i>Panamacebus</i>. This is just within the Aquitanian marine stage with an upper bound of 20.45 Ma. As a soft maximum we suggest the late Eocene, a time by which a number of localities globally have yielded abundant primate remains, but as yet without evidence for crown platyrrhines.</p>

52	Primates	2	64.645	-	<p>Node calibrated. Divergence of dermopterans from primates.</p> <p>Fossil taxon and specimen. <i>Purgatorius</i> UCMP 197509 isolated astragalus attributed to <i>Purgatorius</i> by Chester et al. ¹¹¹ from the late Puercan Garbani Channel fauna, northeastern Montana, USA.</p> <p>Phylogenetic justification. Chester et al. (2015: fig. 2) place <i>Purgatorius</i> within a dermopteran-scandentian-primate clade.</p> <p>Minimum age. 64.645 Ma.</p> <p>Age justification. The late Puercan Garbani Channel fauna <i>Purgatorius</i> occurs within Puercan 2-3 ¹¹², the top of which falls within Chron C28r ²³, the top of which is dated to 64.645 Ma ²³.</p>
53	Scandentia	2	38	66.0	<p>Node calibrated. Divergence of <i>Tupaia</i> from <i>Ptilocercus</i>, following Emerling et al. ¹⁰⁹.</p>
54	Suina	2	34.7	-	<p>Node calibrated. Divergence of <i>Tayassu</i> from <i>Sus</i>.</p> <p>Fossil taxon and specimen(s). <i>Perchoerus probus</i>; UMPE 0031: mandible fragment with m2-m3 and UMPE: upper canine from the Municipality of Santiago Yolomécatl, Tlaxiaco basin, northwestern Oaxaca, southern Mexico ¹¹³.</p> <p>Phylogenetic justification. <i>Perchoerus probus</i> has been classified as either a crown tayassuid, suid or stem suoid in whole-scale analyses of Cetartiodactyla ^{114,115}, however in suoid-level analyses ^{114,116,117} <i>Perchoerus</i> is nested within Tayassuidae due to a suite of cranial characters ¹¹⁸.</p> <p>Minimum age. 34.7 Ma.</p> <p>Age justification. The minimum age constraint is based on the age of the Santiago Yolomécatl fauna. K-Ar dating of overlying volcanic rocks and the presence of <i>Miohippus assinoboimensis</i> suggest the fauna is late Miocene in age, equivalent to the Chadronian North American Land Mammal Age ¹¹³. K-Ar dating of the Cañada María Andesite overlying the mudstone outcrops from which the remains of the Santiago Yolomécatl fauna were recovered produced dates of 35.7 Ma ±1.0 Myr at the base and 32.9 Ma ±0.9 Myr further up the volcanic sequence ¹¹³. The minimum age constraint therefore is 34.7 Ma.</p>

55	Whippomorpha	2	50.7	-	<p>Node calibrated. Clade containing Cetacea and Hippopotamidae according to ¹¹⁹.</p> <p>Fossil taxon and specimen. <i>Himalayacetus subathensis</i>; Holotype: specimen 2003, left dentary with molar teeth M2-3, Roorkee University Vertebrate Paleontology Laboratory (RUSB); from oyster-rich limestone near the base of the Subathu Formation, type section in Kuthar Nala, Simla Hills, Lesser Himalaya Range, Himachal Pradesh, India ¹²⁰.</p> <p>Phylogenetic justification. <i>Himalayacetus subathensis</i> is a representative of the extinct cetacean suborder Archaeoceti based on the absence of auditory specialisations within a small mandibular canal present in the type dentary and its possession of Pakicetus-like teeth ¹²⁰.</p> <p>Minimum age. 50.7 Ma.</p> <p>Age justification. <i>Himalayacetus subathensis</i> was found in zone IIIc from (Mathur 1978), associated with <i>Nummulites atacicus</i> from shallow benthic zone SB8 (zones II-IV) ¹²⁰. The minimum age constraint therefore is correlated to the top of nanoplankton zone NP11-12, which gives an updated minimum age constraint of 50.7 Ma (Benton, et al. 2015).</p>
----	--------------	---	------	---	---

56	Cetacea	2	36.13	56	<p>Node calibrated. The crown cetacean clade consisting of the suborders Odontoceti and Mysticeti to the exclusion of the extinct Archaeoceti¹²¹.</p> <p>Fossil taxon and specimen. <i>Mystacodon selenensis</i>; Holotype: MUSM 1917, partial skeleton including cranium, mandibles, teeth, cervical, thoracic, lumbar and caudal vertebrae, ribs, partial right and left forelimbs, and left innominate from the Yumaque Formation, Playa Media Luna, southern part of Pisco Basin, southern coast of Peru¹²².</p> <p>Phylogenetic justification. <i>Mystacodon</i> possesses derived mysticete characters including: a dorsoventrally thin lateral edge of maxilla on the rostrum, the presence of an antorbital process of the maxilla, the presence of a maxillary infraorbital plate, and triangular supraoccipital shield¹²². As a result <i>Mystacodon</i> is considered the oldest mysticete, part of the basal-most mysticete family Llanocetidae¹²³. This group is characterised by large cheek teeth with two separate roots, and strong labial and lingual enamel ornament (uncertain in <i>Mystacodon</i>)¹²³.</p> <p>Minimum age. 36.13 Ma.</p> <p>Maximum age. 56 Ma.</p> <p>Age justification. The <i>Mystacodon selenensis</i> holotype was discovered 77 metres above the base of the Yumaque Formation, correlated to calcareous nanofossil zone NP19/20 of¹²⁴ in¹²². This corresponds to the <i>Isthmolithus recurvus</i> Partial Range Zone CNE18, with an estimated age range of 37.46-36.13 Ma¹²⁵. The availability of this marine correlation for this fossil enables us to forego use of the corresponding marine stage (Ypresian). This gives a minimum age constraint of 36.13 Ma. We follow Benton et al.¹¹ in establishing the soft maximum constraint on the presence of a diverse, early Eocene artiodactyl record, including archaeocetes but no crown cetaceans during the Ypresian. Thus, the base of the Eocene serves as a soft maximum for the odontocete-mysticete divergence, dated at 56.0 Ma²³.</p>
----	---------	---	-------	----	---

57	Mysticeti	2	15.99	-	<p>Node calibrated. Clade consisting of the most recent common ancestor of the living baleen whale families Balaenidae, Balaenopteridae, Cetotheriidae, and Eschrichtiidae ¹²⁶.</p> <p>Fossil taxon and specimen. <i>Morenocetus parvus</i>; Holotype: MLP 5-11, incomplete cranium including the left periotic and incomplete right periotic in articulation with the basicranium but lacking the rostrum from El Castillo locality, Gaiman Formation, southern margin of the Lower Valley of the Chubut River, Chubut Province, central Patagonia, Argentina ^{127,128}.</p> <p>Phylogenetic justification. An unnamed stem balaenid from New Zealand dated to approximately 28 Ma was previously thought to be the oldest balaenid ¹²⁹, however recent analyses have reported it outside Balaenidae ¹²⁸. Instead <i>Morenocetus parvus</i> is now considered the oldest representative of Balaenidae, the oldest lineage of crown Mysticeti ¹²⁸. Identified as a balaenid due to the posterior margin of the zygomatic process of the squamosal and the lateral edge of the occipital forming a continuous lateral skull border, an anterolaterally directed zygomatic process of the squamosal, a squamosal that is higher dorsoventrally than long anteroposteriorly, and the body of the periotic lateral to the pars cochlearis is laterally and ventrally hypertrophied ¹²⁸.</p> <p>Minimum age. 15.99 Ma.</p> <p>Age justification. The lower Cerro Castillo beds of the lower part of the Gaiman Formation are considered Aquitanian-Burdigalian in age ¹²⁸. An Early Miocene age is supported by the Colhuehuapian mammal fauna from the underlying Trelew member of the Sarmiento Formation since it is dated to 21.0-20.5 Ma in age at Gran Barranca, Chubut Province, central Patagonia, Argentina ^{128,130}. The overlying Gaiman Formation shouldn't be older than this estimate, and the presence of marine vertebrates (fishes and penguins) indicate an early Miocene (Burdigalian) age ¹²⁸. The minimum constraint is then defined on the Burdigalian-Langhian boundary and the base of the Burdigalian, dated at 15.99 Ma ²⁹.</p>
----	-----------	---	-------	---	--

58	Odontoceti	2	23.04	<p>- Node calibrated. Clade consisting of the most recent common ancestor of the living toothed whale families Delphinidae, Monodontidae, Phocoenidae, Iniidae, Pontoporiidae, Platanistidae, Lipotidae, Kogiidae, Physteridae, and Zhiphidae.</p> <p>Fossil taxon and specimen. <i>Arktocara yakataga</i>; type specimen: USNM 214830, incomplete skull lacking the rostrum anterior of the antorbital notches, tympanoperiotics, dentition and mandibles from Poul Creek Formation, Yakutat City and Borough, Alaska, United States of America ¹³¹.</p> <p>Phylogenetic justification. <i>Arktocara yakataga</i> belongs in Platanistoidea since the width of its maxilla is exceeds 50% of the width of the rostrum at the antorbital notch and it possesses affinities with members of Allodelphinidae that possess unequivocal synapomorphies of Platanistoidea ¹³¹. Phylogenetic analysis supports this by placing <i>Arktocara</i> as the sister taxon to Allodelphis, meaning <i>Arktocara yakataga</i> is the oldest allodelphinid and oldest crown odontocete ¹³¹.</p> <p>Minimum age. 23.04 Ma.</p> <p>Age justification. The <i>Arktocara yakataga</i> holotype (USNM 214830) was recovered from an unknown locality 400-500 metres below the top of the Poul Creek Formation ¹³¹. The Poul Creek Formation is constrained to approximately 40-20 Ma in age, so, using a broadcast time of ~20 Ma and a thickness of ~2 km for the Poul Creek Formation, a constant rate of sedimentation gives an approximate age of 25 Ma to USNM 214830 (Late Eocene-Early Miocene) ¹³¹. USNM 214830 is therefore Chattian in age (but with a possible species range extending into the Rupelian ¹³¹). The minimum age constraint is therefore 23.04 Ma ²³.</p>
----	------------	---	-------	--

59	Delphinida	2	15.99	-	<p>Node calibrated. Clade consisting of the most recent common ancestor of the living delphinoid odontocete families Lipotidae, Iniidae, Phocoenidae, Monodontidae and Delphinidae ¹³².</p> <p>Fossil taxon and specimen. <i>Kentriodon pernix</i>; Type specimen: USNM 8060, fairly complete skeleton with skull, mandibles, tympanic bullae, periotics, right thyrohyal of the hyoids, and cervical and dorsal vertebrae in their natural positions; the left side displays 10 mostly incomplete ribs, an incomplete vertebral column with 7 cervicals, 10 dorsals, 4 lumbar with 3 transverse processes of others, 10 caudals with 1 epiphysis of another, and 4 chevrons; the right side displays 6 articulated and 4 disarticulated ribs; forelimbs are missing ; from greenish sandy clay of Shattuck's zone 5, Calvert formation, Chesapeake bay, Chesapeake Beach, Calvert County, Maryland, Virginia, United States of America ¹³³.</p> <p>Phylogenetic justification. <i>Kentriodon pernix</i> shares various anatomical similarities with the living porpoise genus <i>Sotalia</i> as described by ¹³³.</p> <p>Minimum age. 15.99 Ma.</p> <p>Age justification. Referred materials USNM 10670 (skull) and USNM 11400 (atlas) suggest that the stratigraphic range of <i>Kentriodon pernix</i> extends between zones 3 to 10 of the Calvert Formation ¹³³. The minimum age constraint is therefore based on the minimum age of zone C3 since it is the earliest stratigraphic occurrence of the <i>Kentriodon pernix</i>. Zone C3 has Sr87/Sr86 ages of 19.2-18.6 Ma with the best estimated range being 18.8-18.4 Ma ¹³⁴. This makes the minimum age constraint 18.4 Ma.</p>
60	Phocoenidae-Monodontidae	2	7.6	-	<p>Node calibrated. Divergence between porpoises (Phocoenidae) and narwhals (Monodontidae).</p> <p>Fossil taxon and specimen. <i>Salumiphocaena stocktoni</i>; Type specimen: UCMP 34576, a skull from Dacelite Quarry, Valmonte Diatomite Member, Monterey Formation, Palos Verdes Peninsula, California, United States of America ^{135,136}.</p> <p>Phylogenetic justification. <i>Salumiphocaena stocktoni</i> is considered the most basal phocoenid ¹³⁷.</p> <p>Minimum age. 7.6 Ma.</p> <p>Age justification. The minimum age constraint is based on the earliest recorded appearance of <i>Salumiphocaena stocktoni</i> in the Late Miocene Monterey Formation ¹³⁷. Barnes ¹³⁶ described the age of the holotype to be between 11-10 Ma, while Xiong et al. ¹³⁸ suggested 11.2-10 Ma, Chen et al. ¹³⁹ suggested 11.2-10 Ma \pm 1.138 Myr, and Galatius et al. ¹⁴⁰ suggested 11.2-7.246 Ma. However, the upper bound on the Valmonte Diatomite is constrained by the <i>Thalassiosira antiqua</i> Zone ¹⁴¹, the upper bound on which is 7.2 Ma ²⁹.</p>

61	Hippopotamidae	2	7.74	-	<p>Node calibrated. Divergence of <i>Hippopotamus</i> from <i>Hexaprotodon</i>.</p> <p>Fossil taxon and specimen. <i>Cororatherium roobii</i>; Holotype: CHO-BT 68, partial right upper unerupted molar from Beticha locality, 3 km south of Chorora type locality, Chorora Formation, southern Afar Depression, Ethiopia ¹⁴².</p> <p>Phylogenetic justification. <i>Cororatherium roobii</i> displays a hippopotamine trigonid defined by lacking a developed metacristid, an enlarged endometacristid and a postprotocristid reduced compared to the postparacristid, supporting a placement within the subfamily Hippopotaminae ¹⁴². Phylogenetic analysis utilising the ¹⁴³ data matrix recovers <i>Cororatherium roobii</i> as the basal-most hippopotamine based on various other dental characters.</p> <p>Minimum age. 7.74 Ma.</p> <p>Age justification. The minimum age constraint is based on the age of the Beticha locality. This was dated to between 8.02 Ma and 7.74 Ma through single crystal step-heating Ar40-Ar39 analysis undertaken by ³¹, though the remains are stated to be closer to 8.0 Ma in age ^{31,142}.</p>
62	Giraffidae	2	14	-	<p>Node calibrated. Divergence of <i>Okapia</i> from <i>Giraffa</i> ^{144,145}.</p> <p>Fossil taxon and specimen. <i>Giraffokeryx punjabiensis</i>; PC-GCUF 163/19 (Pakistan Palaeontology Research Center, Faisalabad, Pakistan), partial skull roof with horn cores and incomplete upper dentition ¹⁴⁶.</p> <p>Phylogenetic justification. Danowitz et al. ¹⁴⁵ follow Hamilton ¹⁴⁷ and Solounias ¹⁴⁸ in identifying <i>Giraffokeryx punjabiensis</i> as an ingroup member of the <i>Giraffa-Okapia</i> clade based on the presence of ossicones ¹⁴⁹, among other characters (shortened back of skull, posteriorly positioned orbits, flexed skull, brachycephalic skulls, cheek teeth with high crowns).</p> <p>Minimum age: 14 Ma.</p> <p>Age justification. Samiullah et al. ¹⁴⁶ describe cranial fossils of <i>G. punjabiensis</i> from the Chinji Fm. of Pakistan, dated to the middle Miocene, between 11.2 and 14.2 Ma. This would indicate a marine equivalent of either (from oldest to youngest) the Langhian, Serravallian, or Tortonian marine stages. The top of the youngest (Tortonian) is 7.25 Ma in age. However, Barry et al. ¹⁵⁰ suggest that <i>G. punjabiensis</i> from the Chinji Fm. has a first appearance of 14 Ma, which we accept.</p>

63	Bovini	2	10.2	-	<p>Node calibrated. Bovini is the clade consisting of all extant and extinct species that share a common ancestor more closely related to Bovini than <i>Pseudoryx nghetinhensis</i> ¹⁵¹. This node is equivalent to the Bovini + <i>Pseudoryx</i> clade when only considering extant taxa ¹⁵¹.</p> <p>Fossil taxon and specimen. <i>Selenoportax vexillarius</i>; Holotype: AMNH 19748, cranium with right and left horn cores from Hasnot, Jhelum district, Punjab province, Nagri Formation, Siwalik Group, northern Pakistan ¹⁵².</p> <p>Phylogenetic justification. <i>Selenoportax vexillarius</i> is the oldest bovid species to display derived morphological characters associated with the early evolution of Bovini according to Bibi ¹⁵¹. These bovine synapomorphies include a great basal divergence of the horns, a low and wide cranium with an enlarged mastoid region, and the absence of a textured dorsal cranial depression present in fossil and living Boselaphini ¹⁵³. The consideration of this taxon as a representative of stem Bovini however is due to poorly developed bovine dental synapomorphies such as the complication of occlusal enamel surfaces, tall and wide entostyles and ectostylids involved in occlusion, and increased crown height ¹⁵¹.</p> <p>Minimum age. 10.2 Ma.</p> <p>Age justification. The minimum age constraint is based on the species range of <i>Selenoportax vexillarius</i>, dated to be 10.2-9.8 Ma in age based on magnetostratigraphic dating of localities associated with the first and last occurrences of <i>Selenoportax vexillarius</i> ¹⁵⁴. The minimum age constraint is therefore set as 10.2 Ma since it is the earliest recorded appearance of <i>Selenoportax vexillarius</i> ¹⁵⁴.</p>
64	Tragelaphini	2	5.49	-	<p>Node calibrated. The clade is defined by the most recent common ancestor of <i>Tragelaphus scriptus</i> and all living bovids more closely related to it than to <i>Boselaphus tragocamelus</i> or <i>Bos primigenius</i> ¹⁵¹.</p> <p>Fossil taxon and specimen. <i>Tragelaphus moroitu</i>; Holotype: ALA-VP-2/2, frontlet with almost complete left horn core, proximal half of right horn core, and occipital fragment from the Asa Koma Member, Adu-Asa Formation, Middle Awash, Ethiopia ¹⁵⁵.</p> <p>Phylogenetic justification. <i>Tragelaphus moroitu</i> possesses all the synapomorphies of Tragelaphini: horn cores rising upright, spiralling 270°, with three keels and a triangular cross-section throughout the core, with weak anteroposterior compression basally if at all, and simple mesodont teeth with relatively long premolar rows ¹⁵¹. <i>Tragelaphus moroitu</i> however lacks any autapomorphies or apomorphies that ally it with any of the living lineages of tragelaphins, therefore it is considered ancestral to all tragelaphin lineages ¹⁵¹.</p> <p>Minimum age. 5.49 Ma.</p> <p>Age justification. Bibi ¹⁵¹ suggested deriving the minimum age constraint from the age of the Asa Koma Member. The Wittl Mixed Magmatic Tuff (WMMT, MA96-30) near the top of the Asa Koma Member was dated using Ar40/Ar39 dating methods, yielding an age of 5.57 Ma ±0.08 Myr ¹⁵⁶, resulting in a minimum age constraint of 5.49 Ma.</p>

65	Reduncini	2	5.111	-	<p>Node calibrated. The clade is defined by the most recent common ancestor of <i>Redunca redunca</i> and <i>Kobus kob</i> ¹⁵¹.</p> <p>Fossil taxon and specimen. <i>Redunca ambae</i>; Holotype: AME-VP-1/42, cranium from the Kuseralee Member, Sagantole Formation, Middle Awash, Ethiopia ¹⁵⁵.</p> <p>Phylogenetic justification. <i>Redunca ambae</i> is the first appearance of <i>Redunca</i> in the fossil record and thus the first crown reduncin ¹⁵¹.</p> <p>Minimum age. 5.111 Ma.</p> <p>Age justification. The minimum age constraint is based on the minimum age of the Kuseralee Member. Basalt sample MA92-15 from the Gawto Member basalts overlying the Kuseralee Member was dated to 5.177 Ma \pm 0.066 Myr in age using Ar40/Ar39 step heating methods ¹⁵⁷. The minimum age constraint therefore is set at 5.111 Ma.</p>
66	Hippotragini-Alcelaphini	2	6.48	-	<p>Node calibrated. Divergence of Hippotragini and Alcelaphini ¹⁵¹.</p> <p>Fossil taxon and specimen. <i>Tchadotragus sudrei</i>; Holotype: TM12-97-23, near complete skull lacking premaxillae, right nasal, zygomatic arches, and most of auditory region from the anthracotheriid unit of Toros-Menalla, Djurab region, northern Chad ¹⁵⁸.</p> <p>Phylogenetic justification. <i>Tchadotragus sudrei</i> possesses typical hippotragine features including long slender, curved horn cores, weak cranial flexure, large frontal sinuses, and hippotragine-like dentition ¹⁵⁸. It is thus considered a basal member of the tribe predating the <i>Oryx-Praedamalis</i> split ¹⁵⁸.</p> <p>Minimum age. 6.48 Ma.</p> <p>Age justification. The minimum age constraint is based on the minimum age constraint of the anthracotheriid unit. Be¹⁰/Be⁹ atmospheric cosmogenic nuclide dating of the anthracotheriid unit resulted in a mean authigenic age of 6.88 Ma \pm 0.40 Myr above the ash tuff layer at TM 254 ¹⁵⁹. The minimum age constraint is based on the Be¹⁰/Be⁹ authigenic mean above TM 254 and so is set as 6.48 Ma.</p>

67	Alcelaphini	2	5.05	-	<p>Node calibrated. This clade is defined by the most recent common ancestor of <i>Alcelaphus buselaphus</i>, <i>Connochaetes gnou</i>, <i>Damaliscus pygargus</i>, and <i>Beatragus hunteri</i> ¹⁵¹.</p> <p>Fossil taxon and specimen. <i>Damalacra neanica</i>; Holotype: L7257, complete skull with horn cores and upper dentitions comprising P3-M3 on the right and broken M1-M3 on the left from bed 3aS, 'E' Quarry, Pelletal Phosphorite Member (PPM), Varswater Formation, Langebaanweg, South Africa ¹⁶⁰.</p> <p>Phylogenetic justification. <i>Damalacra neanica</i> is recognised as an alcelaphine based on a suite of cranial and dental characters as highlighted by Gentry ¹⁶⁰. This placement in crown Alcelaphini has been supported by morphological and molecular analyses done by Vrba ¹⁶¹ and Faith et al. ¹⁶².</p> <p>Minimum age. 5.05 Ma.</p> <p>Age justification. The minimum age constraint is based on the minimum age of the Muishond Fontein Pelletal Phosphorite Members (MPPM). The fossils from the MPPM are considered slightly younger than sea level cycle T7 since they occur within a small interval between 26-30 metres above sea level (asl) within the Varswater Formation, which starts approximately 15 metres asl ¹⁶³. This gives an age estimate of 5.15 Ma \pm 0.1 Myr ¹⁶³, establishing the minimum age constraint at 5.05 Ma.</p>
68	Caprinae	2	8.9	-	<p>Node calibrated. Clade that consists of all extant and extinct species that share a more recent common ancestor (MRCA) with <i>Capra ibex</i> than <i>Pantholops hodgsonii</i> ¹⁵¹.</p> <p>Fossil taxon and specimen. <i>Aragoral mudejar</i>; Holotype: RO-2268, MPZ 96/54, frontal fragment with two horn cores from La Roma 2, Alfambra, Teruel, Aragón, Spain ^{164,165}.</p> <p>Phylogenetic justification. <i>Aragoral mudejar</i> is considered a member of Caprini due to the presence of hystodonty, reduced premolar rows, horn cores with well-developed pedicular sinuses, and short and robust metacarpals ¹⁶⁶. The greatly shortened and wide metacarpals is synapomorphy of Caprini ¹⁶⁷, however the simple frontal sinuses in the pedicel and horn core base are a synapomorphy of the Caprini + Alcelaphini + Hippotragini clade justifying the consideration of <i>Aragoral Mudejar</i> as a stem caprine ¹⁵¹.</p> <p>Minimum age. 8.9 Ma.</p> <p>Age justification. The minimum age constraint is based on the minimum age of the La Roma 2 locality, which is upper Vallesian in age ¹⁶⁶. This locality is correlated to Mammal Neogene zone MN10 and dated to 8.9 Ma using bio- and magnetostratigraphy ^{168,169}.</p>

69	Cervidae	2	17.235	28.4	<p>Node calibrated. Clade consisting of all extant and extinct species that share a more recent common ancestor with Cervidae than any other living ruminant ¹⁵¹.</p> <p>Fossil taxon and specimen. <i>Procervulus praelucidus</i>; Specimens: BSPG 1937 II 16841, BSPG 1937 II 16803, BSPG 1937 II 16794, BSPG 1937 II 16852, antlers from Wintershof-West, Germany ^{170,171}.</p> <p>Phylogenetic justification. <i>Procervulus praelucidus</i> is classified as a cervid as it possesses antlers with a proximal permanent pedicel and an upper deciduous antler ¹⁵¹. <i>Procervulus praelucidus</i> is however considered a stem taxon as it retains the conserved character of antler burrs, suggesting a different method of antler development to the crown clade ¹⁵¹.</p> <p>Minimum age. 17.235 Ma.</p> <p>Maximum age. 28.4 Ma.</p> <p>Age justification. The minimum age constraint is based on the minimum age of the type locality of Wintershof-West. This locality is the type locality for the Mammal Neogene zone MN3 ¹⁶⁹, the top of which is dated to 17.235 Ma ¹⁷². Due to a lack of phylogenetic resolution between late Oligocene ruminants and their living relatives Bibi ¹⁵¹ suggests utilising a soft maximum age constraint of 28.4 Ma.</p>
70	stem-Moschidae	2	19.5	-	<p>Node calibrated. Divergence of moschids from other pecoran artiodactyls.</p> <p>Fossil taxon and specimen. <i>Dremotherium feignouxii</i>; MNHN SG. 4304 (Museum national d'Histoire naturelle, Paris, France) and StG. 548 (Centre de Conservation et d'Etudes des Collections Lyon), from early Miocene deposits, Saint-Gérard-le-Puy, France ¹⁷³.</p> <p>Phylogenetic justification. <i>Dremotherium feignouxii</i>; was identified as a stem-Moschidae based on a morphological (skeletal) phylogenetic analysis by Janis and Scott ¹⁷⁴ and this interpretation has been followed to justify calibrations for stem-Moschidae in Bibi ¹⁵¹ and Zusano et al. ¹⁴⁴.</p> <p>Minimum age. 19.5 Ma.</p> <p>Age justification. Saint-Gérard-le-Puy is a suite of localities, the stratigraphy of which is not very well constrained. However. Costeur ¹⁷³ asserts an early Miocene age, Aquitanian, European Land Mammal Zone MN2. The MN2-3 boundary has been dated to 19.3 Ma ¹⁶⁹.</p>

71	Neobalaeninae	2	23.04	33.9	<p>Node calibrated. Divergence of <i>Caperea</i> (pygmy right whale) from Balaenopteridae ¹⁷⁵.</p> <p>Fossil taxon and specimen. <i>Mauicetus parki</i>; OU 22545 (Otago University), from the Otekaike Limestone at Hakataramea Valley, South Canterbury, New Zealand ¹⁷⁶.</p> <p>Phylogenetic justification. Both Marx and Fordyce ¹⁷⁷ and Lloyd and Slater ¹⁷⁸ resolved <i>Mauicetus parki</i> as the oldest representative of Balaenopteridae and, therefore, Neobalaeninae, based on total evidence and supertree methods.</p> <p>Minimum age. 23.04 Ma.</p> <p>Maximum age. 33.9 Ma.</p> <p>Age justification. Integrated biostratigraphy and isotope stratigraphy has established that the top of the Otekaike Limestone falls fully within the Chattian ¹⁷⁹, the top of which is dated to 23.04 ²³.</p>
72	Balaenopteridae	2	7.3	-	<p>Node calibrated. Divergence of crown Balaenopteridae (<i>Balaenoptera</i>, <i>Eschrichtius</i>, <i>Megaptera</i>).</p> <p>Fossil taxon and specimen. <i>Incakujira anillodefuego</i> GNMH Fs-098-1 (Gamagori Natural History Museum, Gamagori, Japan) from <i>Cosmopolitodus</i>-bearing horizons of the Pisco Formation, Aguada de Lomas, near Puerto de Lomas, approximately 80 km south of Nazca, Peru.</p> <p>Phylogenetic justification. Resolved as the oldest member of crown-Balaenopteridae by Marx and Kohno ¹⁸⁰ based on a total evidence analysis.</p> <p>Minimum age. 7.3 Ma.</p> <p>Age justification. Marx and Kohno ¹⁸⁰ quote a 7.3 Ma minimum constraint based on Sr isotope dating.</p>
73	Physeteroidea	2	13.82	-	<p>Node calibrated. Divergence of <i>Kogia</i> and <i>Physeter</i> ¹⁷⁸.</p> <p>Oldest crown fossil. <i>Idiophyseter merriami</i>; UCMP V75114 (University of California Museum of Paleontology, Berkeley, California) at Locality Templeton 2, San Luis Obispo County, California ¹⁸¹.</p> <p>Phylogenetic justification. Collareta et al. ¹⁸² identified <i>Idiophyseter merriami</i> as the oldest member of the crown-clade defined by extant <i>Kogia</i> and <i>Physeter</i> based on a morphological phylogenetic analysis.</p> <p>Minimum age. 13.82 Ma.</p> <p>Age justification. The Palaeobiology Database asserts a Langhian age for <i>Idiophyseter merriami</i>, the top of which is dated to 13.82 Ma ²⁹.</p>

74	Perissodactyla	2	55.5	66.09	Node calibrated. The clade comprised of Equidae, Tapiridae and Rhinocerotidae. Following Emerling et al. ¹⁰⁹ with the exception that the soft-maximum constraint, defined as the base of the Paleocene, is revised to 66.04 Ma \pm 0.05 Myr ²⁷ , so 66.09 Ma.
75	Ceratomorpha	2	48.078	66.09	<p>Node calibrated. Divergence of tapirids from rhinocerotids.</p> <p>Fossil taxon and specimen: <i>Cambaylophus</i>. IITR/SB/VLM 760, right maxilla fragment from the Cambay Shale, Vastan Lignite Mine, western India ¹⁸³.</p> <p>Phylogenetic justification. Kapur & Bajpai ¹⁸³ reconstruct <i>Cambaylophus</i> as a tapiroid. Its relation to modern tapirids to the exclusion of rhinocerotids is also reflected in the analysis of Bai et al. ¹⁸⁴.</p> <p>Minimum age. 48.078 Ma.</p> <p>Age justification. Kapur & Bajpai ¹⁸³ cite data from isotope stratigraphy and dinoflagellate biostratigraphy supporting the interpretation that Vastan fossils are between 54.5 (PETM) and 53.7 Ma (9 ETM2) in age. This provides for a minimum constraint defined on the Ypresian-Lutetian boundary which is dated at 48.07 Ma. The soft maximum, defined as the base of the Paleocene, is revised to 66.04 Ma \pm 0.05 Myr ²⁷, so 66.09 Ma.</p>
76	Prionodontidae-Felidae	2	28.1	66.09	Node calibrated. Divergence of Prionodontidae from Felidae. Following Emerling et al. ¹⁰⁹ with the exception that the soft-maximum constraint, defined as the base of the Paleocene, is revised to 66.04 Ma \pm 0.05 Myr ²⁷ , so 66.09 Ma.
77	Herpestidae-Eupleridae	2	15.97	33.9	Node calibrated. The clade comprised of mongooses and Malagasy mongooses ⁶⁴ . Following Emerling et al. ¹⁰⁹ .

78	Mustelidae-Procyonidae	2	26.42	-	<p>Node calibrated. The split between mustelids (weasels) and procyonids (raccoons) ¹⁸⁵.</p> <p>Fossil taxon and specimen. <i>Pseudobassaris riggsi</i>; Holotype: YPM-PU 11455, skull from the Phosphorites du Quercy, France ¹⁸⁶.</p> <p>Phylogenetic justification. <i>Pseudobassaris riggsi</i> is considered the oldest known procyonid since it possesses procyonid suprameatal fossae and epitympanic recesses of the middle-ear ^{186,187}. <i>Pseudobassaris riggsi</i> is also stratigraphically older than the oldest known mustelid, <i>Plesictis plesictis</i> ¹⁸⁵.</p> <p>Minimum age. 26.42 Ma.</p> <p>Age justification. <i>Pseudobassaris riggsi</i> is from French localities Belgarric 1 and Belgarrit 4A and so the minimum age constraint is based on the minimum age of these localities ¹⁸⁷. These localities are correlated with European Paleogene reference levels MP 24 and MP 25 ¹⁸⁵ the upper range of which is constrained with Chron C25r ¹⁸⁸; the upper bound of Chron C25r is dated to 26.42 Ma, providing the minimum age constraint.</p>
79	Feliformia	2	19.535	-	<p>Node calibrated. Most recent common ancestor of Felidae (cats), Prionodontidae (Asiatic lisangs), Herpestidae (mongooses), Eupleridae (Malagasy mongooses), Hyaenidae (Hyaenas) and Viverridae (civets and genets).</p> <p>Fossil taxon and specimen. <i>Proailurus lemanensis</i>; Holotype: MNHN SG 3509, skull from Saint-Gérard-le-Puy, France ¹⁸⁹.</p> <p>Phylogenetic justification. <i>Proailurus lemanensis</i> is placed within Feliformia based on its possession of an anteriorly positioned middle lacerate foramen (extreme in its case) ¹⁹⁰, and was further identified as a felid based on a derived petrosal morphology that incorporates a uniquely bony flange on the medial border of the promontorium (a feature that is suppressed and/or reoriented in living felids) ^{191,192}. However, under more recent analysis <i>Proailurus lemanensis</i> falls outside Felidae and nests within Eupleridae, though it is still considered a feliform ¹⁹³.</p> <p>Minimum age. 19.535 Ma.</p> <p>Age justification. The minimum age constraint is based on the age of the early Miocene Saint-Gérard-le-Puy locality ¹⁹⁴, correlated to Mammal Neogene zone MN2 ¹⁸⁹. The top of this zone is correlated to chron C6r ¹⁷², dated to 19.535 Ma ²³.</p>

80	Viverrinae- Genettinae	2	20.44	-	<p>Node calibrated. Most recent common ancestor of <i>Genetta</i> and <i>Viverra</i> ¹⁹⁵.</p> <p>Fossil taxon and specimen. <i>Herpestides antiquus</i>; Specimen: MGL SG 3066, cranium and associated lower jaw from unknown locality, Sant Gérard, Allier basin, France ¹⁹⁶.</p> <p>Phylogenetic justification. Basicranial morphology of the auditory region has patterns similar to those found in living viverrids ¹⁹⁶, however based on the differences in peculiarities of the dental morphotypes of Hemigalinae and Paradoxurinae ¹⁹⁷ hypothesize <i>Herpestides</i> is a representative of a viverrine and genettine fossil lineage.</p> <p>Minimum age. 20.44 Ma.</p> <p>Age justification. Though the specific locality from which the 12 basicrania analysed by Hunt Jr ¹⁹⁶ is unknown the regional geology is considered of Aquitanian age. The minimum age constraint is therefore based on the minimum age of the Aquitanian, dated to 20.45 Ma ²⁹.</p>
81	Lobodontini	2	5.05	-	<p>Node calibrated. Common ancestor of <i>Ommatophoca</i>, <i>Lobodon</i>, <i>Leptonychotes</i> and <i>Hydruga</i> ¹⁹⁸.</p> <p>Fossil taxon and specimen. <i>Homiphoca capensis</i>; Holotype: SAM-PQI-15695, rostral segment of partial skull from the Muishond Fontein Pelletal Phosphorite Members (MPPM), Varswater Formation, Langebaanweg, republic of South Africa ¹⁹⁹.</p> <p>Phylogenetic justification. A phylogenetic analysis utilising 6 skulls attributed to <i>Homiphoca capensis</i> from the Varswater Formation resulted in the taxon nesting within Lobodontini ¹⁹⁹.</p> <p>Minimum age. 5.05 Ma.</p> <p>Age justification. The minimum age constraint is based on the minimum age of the Muishond Fontein Pelletal Phosphorite Members (MPPM). The MPPM is considered to be of early Pliocene Zanclean age ²⁰⁰, as the member overlies sea level cycle T7 within the Varswater Formation ²⁰¹. This gives a central age estimate of 5.15 Ma \pm0.1 Myr for the MPPM ²⁰¹, setting the minimum age constraint at 5.05 Ma.</p>

82	Phocidae	2	13.82	-	<p>Node calibrated. Divergence between the subfamilies Monachinae and Phocinae ¹⁹⁸.</p> <p>Fossil taxon and specimen. <i>Monotherium? wymani</i>; Holotype: MCZ 8741, left and right temporal bones from Shockoe creek ravine near the base of Church Hill, Calvert Formation, Richmond, Virginia, United States of America ²⁰².</p> <p>Phylogenetic justification. <i>Monotherium? wymani</i> is considered the oldest known monachine phocid according to ²⁰³⁻²⁰⁶.</p> <p>Minimum age. 13.82 Ma.</p> <p>Age justification. The Calvert Formation spans an interval of time from the early to middle Miocene (Aquitania-Langhian) ²⁰², however Deméré et al. ²⁰⁵ cite <i>Monotherium? wymani</i> as exclusively Langhian in age, and phocid remains from zone 10 of the Calvert Formation outcropping at the Calvert Cliffs in Maryland are cited as early middle Miocene age ²⁰². The minimum age constraint is therefore defined by the upper bound of the Langhian, dated at 13.82 Ma ²⁹.</p>
83	Otarioidea	2	15.97	-	<p>Node calibrated. Divergence between the families Otariidae (fur seals and sea lions) and Odobenidae (walruses) ¹⁹⁸.</p> <p>Fossil taxon and specimen. <i>Proneotherium repenningi</i>; Holotype: USNM 205334, nearly complete skull with all teeth except left I1, right P1, left P4, and right and left M1-2; missing part of right zygomatic arch from the "Iron Mountain bed", Astoria Formation, Lincoln County, Oregon, United States of America ²⁰⁷.</p> <p>Phylogenetic justification. A phylogenetic analysis utilising 24 cranial, dental and postcranial characters done by ²⁰⁷ supports the monophyly of Odobenidae with the genera <i>Proneotherium</i> and <i>Prototaria</i> as sister taxa and basal members of the group. Because of this <i>Proneotherium repenningi</i> can be considered the oldest odobenid taxon to date ^{205,208}.</p> <p>Minimum age. 15.99 Ma.</p> <p>Age justification. <i>Proneotherium repenningi</i> is of Burdigalian age ²⁰⁵, the top of which is dated to 15.99 Ma ²⁹.</p>

84	Pinnipedia	2	20.45	27.29	<p>Node calibrated. Divergence between the super families Otarioidea (Otariidae+Odobenidae) and Phocoidea (Desmatophocidae+Phocidae).</p> <p>Fossil taxon and specimen. <i>Desmatophoca brachycephala</i>; Holotype: LACM 120199, incomplete cranium with crowns of left I1-3, parts of both canines, lacking other teeth and parts of the rostrum, and the right dorsolateral part of the braincase from locality LACM 4584, Astoria Formation, east of Knappton, Pacific County, Washington State, United States of America ²⁰⁹.</p> <p>Phylogenetic justification. <i>Desmatophoca brachycephala</i> is the oldest records of crown-Pinnipedia ²⁰⁶.</p> <p>Minimum age. 20.45 Ma.</p> <p>Maximum age. 27.29 Ma.</p> <p>Age justification. <i>Desmatophoca brachycephala</i> is of Aquitanian age ²⁰⁵, the top of which is dated to 20.45 Ma ²⁹. The presence of stem pinnipeds such as <i>Enaliarctos tedfordi</i> extends no further than the late Oligocene Chattian age ^{64,206,210}. The soft maximum age constraint is thus set to the base of the Chattian age, dated at 27.29 Ma ²³.</p>
85	Hipposideridae-Rhinolophidae	2	38	56	<p>Node calibrated. Divergence of Hipposideridae-Rhinolophidae. Following Emerling et al. ¹⁰⁹.</p>
86	Megadermatidae-Craseonycteridae	2	33.9	47.8	<p>Node calibrated. Divergence of megadermatids from craseonycterids. Following Emerling et al. ¹⁰⁹.</p>
87	Molossidae - Vespertilionidae + Miniopteridae	2	38	56	<p>Node calibrated. Divergence of Molossidae from Vespertilionidae + Miniopteridae. Following Emerling et al. ¹⁰⁹.</p>
88	Natalidae - Vespertilionidae + Miniopteridae + Molossidae	2	38	56	<p>Node calibrated. Divergence of Natalidae from Molossidae plus Vespertilionidae plus Miniopteridae. Following Emerling et al. ¹⁰⁹.</p>

89	Sciuromorpha	2	41.03	59.24	<p>Node calibrated. Common ancestor of the glirid-<i>Apodontia</i>-sciurid clade within Sciuromorpha.</p> <p>Fossil taxon and specimen. <i>Eoglriravus wildi</i>; Specimen: WDC-C-MG202, articulated skeleton from Messel, Germany (Storch and Seiffert 2007).</p> <p>Phylogenetic justification: <i>Eoglriravus wildi</i> is thought to be the earliest appearance of the suborder Gliridae²¹¹, since It possesses occlusal tooth morphology that links Eocene/Oligocene Glirid genera with Eocene ischyromyids²¹².</p> <p>Minimum age. 41.03 Ma.</p> <p>Maximum age. 59.24 Ma.</p> <p>Age justification. The minimum age constraint is based on the age of the Messel Formation. The Messel Formation is early-middle Eocene in age, correlated with Mammal Paleogene (MP) zone 11²¹². This suggests that the Messel Formation is Lutetian in age and therefore the minimum age is set by the age of the Lutetian-Bartonian boundary²¹². This is dated to 41.03 Ma²³, giving a minimum age constraint of 40.7 Ma. The soft maximum age is based on the presence of <i>Paramys</i> in Thanetian age deposits. The base of the Thanetian is dated to 59.24 Ma²³ and serves as the soft maximum constraint.</p>
90	Abrocomidae	2	1.778	13.82	<p>Node calibrated. Most recent common ancestor of Abrocomidae (<i>Abrocoma</i>+<i>Cuscomys</i>).</p> <p>Fossil taxon and specimen. <i>Abrocoma</i> sp.; MMP 1059-M: fragment of left maxillary with DP4-M1 from Punta San Andrés, San Andrés Formation²¹³; and MACN 19722: right mandible with incisor and dp4-m2 from Santa Isabel, San Andrés Formation, between S2 and S3²¹⁴.</p> <p>Phylogenetic justification. <i>Abrocoma</i> is the oldest crown member of Abrocomidae (<i>Abrocoma</i>+<i>Cuscomys</i>)²¹⁵.</p> <p>Minimum age. 1.778 Ma.</p> <p>Maximum age. 9.112 Ma.</p> <p>Age justification. The fossiliferous unit from which the San Andrés Formation rodents are recovered from is part of the Sanandresian substage of the upper Marplatan South American Land Mammal Age (SALMA)²¹³. West²¹⁶ suggests that the Marplatan extends up until the end of chron C2, dated to 1.775 Ma by²⁹. Verzi et al.²¹⁷ noted paleontological evidence for divergence within abrocomids through the middle and late Miocene, prior to the divergence of <i>Abrocoma</i> from <i>Cuscomys</i> (Verzi et al.²¹⁷: fig. 10). We therefore define the soft maximum on the middle Miocene (base Serravallian), dated to 13.82 Ma²⁹.</p>

91	Monotremata	2	24.459	133.2	<p>Node calibrated. Divergence of <i>Platypus</i> from echidnas.</p> <p>Fossil taxon and specimen. <i>Obdurodon insignis</i> SAM P18087 and AMNH 97228, (right upper molars) from University of California, Riverside Loc. RV-7247, SAM Quarry North, Unit 2 of Etadunna Formation, west side of Lake Palankarinna, South Australia ²¹⁸.</p> <p>Minimum age. 24.459 Ma.</p> <p>Soft maximum age. 133.2 Ma.</p> <p>Age justification. Woodburne et al. ⁷³ identify Unit 2 of Etadunna Formation as falling within magnetozone C7r which is age constrained by the base of the succeeding C7n.2n, dated to 24.459 Ma ²³. Given the possibility that Cretaceous fossils such as <i>Teinolophos</i> from Flat Rocks, Australia, might be crown monotremes, more closely related to the extant <i>Ornithorhynchus</i> than to <i>Tachyglossus</i>, we use the maximum age of the Flat Rocks site to establish the soft maximum constraint. The age of the Flat Rocks site (Strzelecki Group) is usually considered Barremian-Aptian (e.g. ²¹⁹). However, the age of the Flat Rocks site has been subject to detailed palynological characterization finding that it falls fully within the range of the spore <i>Pilosporites notensis</i> ²²⁰, the FAD of which coincides with the base of the <i>Foraminisporis wonhaggiensis</i> Zone, <i>Dictyosporites speciosus</i> Zone and its <i>Cyclosporites hughesii</i> subzone ²²⁰. The <i>Foraminisporis wonhaggiensis</i> Zone is interpreted to have a Hauterivian to Barremian age (Partridge (2011) in Holdgate, et al. ²²¹). A soft maximum can therefore be established on the base of the Hauterivian 132.6 Ma \pm 0.6 Myr ²⁷, thus 133.2 Ma.</p>
92	Tachyglossidae	2	2.58	133.2	<p>Node calibrated. Common ancestor of <i>Tachyglossus</i> and <i>Zaglossus</i>.</p> <p>Fossil taxon and specimen. Postcranial elements of tachyglossids from Chinchilla Sands ²²², no specimen numbers given.</p> <p>Phylogenetic Justification. "<i>Zaglossus</i>" (<i>Megalibgwilia</i>) <i>robustus</i> from the Miocene of Gulgong, NSW may constrain age of crown echidnas, but this taxon is now referred to <i>Megalibgwilia robustus</i> and is not clearly demonstrated to be closer to <i>Zaglossus</i> than <i>Tachyglossus</i>. Following Pian et al. ²²³ there are no unequivocal pre-Pliocene echidnas and, following Musser ²²², the oldest are <i>Tachyglossus</i> sp. from Pliocene of Chinchilla Sands.</p> <p>Minimum age. 2.58 Ma.</p> <p>Maximum age. 133.2 Ma.</p> <p>Age justification. The Chinchilla Sand fluvial deposits near the town of Chinchilla, on the Darling Downs, Queensland. No direct dates have been obtained for this deposit but Tedford et al. ²²⁴ and Mackness et al. ²²⁵ in Dawson ²²⁶ argue for an early to middle Pliocene age interpretation based on correlation. Hence, we use the date of the Pliocene-Pleistocene boundary to inform the minimum age interpretation of this fossil, dated to 2.58 Ma ²²⁷. The soft maximum follows that of Monotremata.</p>

References for “Justification for Fossil Calibrations”

- 1 Tarver, J. E. *et al.* The interrelationships of placental mammals and the limits of phylogenetic inference. *Genome Biology and Evolution* **8**, 330-344, doi:10.1093/gbe/evv261 (2016).
- 2 Flynn, J. J., Parrish, J. M., Rakotosamimanana, B., Simpson, W. F. & Wyss, A. R. A Middle Jurassic mammal from Madagascar. *Nature* **401**, 57-60 (1999).
- 3 Puttick, M. N. *et al.* Uncertain-tree: discriminating among competing approaches to the phylogenetic analysis of phenotype data. *Proceedings of the Royal Society B: Biological Sciences* **284**, 20162290, doi:10.1098/rspb.2016.2290 (2017).
- 4 Jenkins, F. A., Gatesy, S. M., Shubin, N. H. & Amaral, W. W. Haramiyids and Triassic mammalian evolution. *Nature* **385**, 715-718 (1997).
- 5 Luo, Z. X., Gatesy, S. M., Jenkins, F. A., Amaral, W. W. & Shubin, N. H. Mandibular and dental characteristics of Late Triassic mammaliaform Haramiyavia and their ramifications for basal mammal evolution. *Proceedings National Academy of Sciences* **112**, E7101–E7109, doi:10.1073/pnas.1519387112 (2015).
- 6 Hesselbo, S. P., Ogg, J. G., Ruhl, M., Hinnov, L. A. & Huang, C. J. in *Geologic Time Scale 2020* 955-1021 (2020).
- 7 Zheng, X., Bi, S., Wang, X. & Meng, J. A new arboreal haramiyid shows the diversity of crown mammals in the Jurassic period. *Nature* **500**, 199-202, doi:10.1038/nature12353 (2013).
- 8 Bi, S., Wang, Y., Guan, J., Sheng, X. & Meng, J. Three new Jurassic euharamiyidan species reinforce early divergence of mammals. *Nature* **514**, 579-584, doi:10.1038/nature13718 (2014).
- 9 Li, M. *et al.* Astronomical tuning of the end-Permian extinction and the Early Triassic Epoch of South China and Germany. *Earth and Planetary Science Letters* **441**, 10-25, doi:10.1016/j.epsl.2016.02.017 (2016).
- 10 Krause, D. W. *et al.* First cranial remains of a gondwanatherian mammal reveal remarkable mosaicism. *Nature* **515**, 512-517, doi:10.1038/nature13922 (2014).
- 11 Benton, M. J. *et al.* Constraints on the timescale of animal evolutionary history. *Palaeontologia Electronica* **18**, 1-106 (2015).
- 12 Huttenlocker, A. K., Grossnickle, D. M., Kirkland, J. I., Schultz, J. A. & Luo, Z. X. Late-surviving stem mammal links the lowermost Cretaceous of North America and Gondwana. *Nature* **558**, 108-112, doi:10.1038/s41586-018-0126-y (2018).
- 13 Bi, S. *et al.* An Early Cretaceous eutherian and the placental–marsupial dichotomy. *Nature*, doi:10.1038/s41586-018-0210-3 (2018).
- 14 Meng, J., Hu, Y., Li, C. & Wang, Y. The mammal fauna in the Early Cretaceous Jehol Biota: implications for diversity and biology of Mesozoic mammals. *Geological Journal* **41**, 439-463 (2006).
- 15 Ogg, J. G., Agterberg, F. P. & Gradstein, F. M. in *A geologic time scale 2004* (eds F. M. Gradstein, J. G. Ogg, & A. Smith) 344-383 (Cambridge University Press, 2004).

- 16 Woodburne, M. O., Rich, T. H. & Springer, M. S. The evolution of tribospheny and the antiquity of mammalian clades. *Molecular Phylogenetics and Evolution* **28**, 360-385 (2003).
- 17 Luo, Z. X., Yuan, C. X., Meng, Q. J. & Ji, Q. A Jurassic eutherian mammal and divergence of marsupials and placentals. *Nature* **476**, 442-445, doi:10.1038/nature10291 (2011).
- 18 Luo, Z. X., Ji, Q., Wible, J. R. & Yuan, C. X. An early Cretaceous tribosphenic mammal and metatherian evolution. *Science* **302**, 1934-1940 (2003).
- 19 Ji, Q. *et al.* The earliest known eutherian mammal. *Nature* **416**, 816-822 (2002).
- 20 O'Leary, M. A. *et al.* The placental mammal ancestor and the post-K-Pg radiation of placentals. *Science* **339**, 662-667, doi:10.1126/science.1229237 (2013).
- 21 Yuan, C.-X., Ji, Q., Meng, Q.-J., Tabrum, A. R. & Luo, Z.-X. Earliest evolution of multituberculate mammals revealed by a new Jurassic fossil. *Science* **341**, 779-783 (2013).
- 22 Krause, D. W. *et al.* Skeleton of a Cretaceous mammal from Madagascar reflects long-term insularity. *Nature* **581**, 421-427, doi:10.1038/s41586-020-2234-8 (2020).
- 23 Speijer, R. P., Pălike, H., Hollis, C. J., Hooker, J. J. & Ogg, J. G. in *Geologic Time Scale 2020* 1087-1140 (2020).
- 24 Silcox, M. T., Bloch, J. I., Sargis, E. J. & Boyer, D. M. in *The rise of placental mammals : origins and relationships of the major extant clades* (eds K.D. Rose & J.D. Archibald) 127-144 (Johns Hopkins University Press, 2005).
- 25 Bloch, J. I., Silcox, M. T., Boyer, D. M. & Sargis, E. J. New Paleocene skeletons and the relationship of plesiadapiforms to crown-clade primates. *Proceedings of the National Academy of Sciences, USA* **104**, 1159-1164 (2007).
- 26 Seiffert, E. R., Perry, J. M., Simons, E. L. & Boyer, D. M. Convergent evolution of anthropoid-like adaptations in Eocene adapiform primates. *Nature* **461**, 1118-1121, doi:10.1038/nature08429 (2009).
- 27 Gale, A. S. *et al.* in *Geologic Time Scale 2020* 1023-1086 (2020).
- 28 Kappelman, J. *et al.* The earliest occurrence of Sivapithecus from the Middle Miocene of Chinji Formation of Pakistan. *Journal of Human Evolution* **21**, 61-73 (1991).
- 29 Raffi, I. *et al.* in *Geologic Time Scale 2020* 1141-1215 (2020).
- 30 Suwa, G., Kono, R. T., Katoh, S., Asfaw, B. & Beyene, Y. A new species of great ape from the late Miocene epoch in Ethiopia. *Nature* **448**, 921-924 (2007).
- 31 Katoh, S. *et al.* New geological and palaeontological age constraint for the gorilla-human lineage split. *Nature* **530**, 215-218, doi:10.1038/nature16510 (2016).
- 32 Brunet, M., Guy, F., Pilbeam, D., Mackay, H. T., Likius, A., Djimboumbaye, A., *et al.* . A new hominid from the upper Miocene of Chad, central Africa. *Nature* **418**, 145-151 (2002).
- 33 Benefit, B. R., McCrossin, M., Boaz, N. T. & Pavlakis, P. New fossil cercopithecoids from the Late Miocene of As Sahabi, Libya. *Garyounis Scientific Bulletin Special Issue* **5**, 265-282 (2008).
- 34 Alba, D. M. *et al.* First joint record of Mesopithecus and cf. Macaca in the Miocene of Europe. *J*

- Hum Evol* **67**, 1-18, doi:10.1016/j.jhevol.2013.11.001 (2014).
- 35 Raaum, R. L., Sterner, K. N., Noviello, C. M., Stewart, C. B. & Disotell, T. R. Catarrhine primate divergence dates estimated from complete mitochondrial genomes: concordance with fossil and nuclear DNA evidence. *J Hum Evol* **48**, 237-257, doi:10.1016/j.jhevol.2004.11.007 (2005).
 - 36 Fleagle, J. G. *Primate adaptation and evolution*. (Academic Press, 1999).
 - 37 Fabre, P.-H., Hautier, L., Dimitrov, D. & Douzery, E. A glimpse on the pattern of rodent diversification: a phylogenetic approach. *BMC Evol Biol* **12**, 88 (2012).
 - 38 Asher, R. J., Smith, M. R., Rankin, A. & Emry, R. J. Congruence, fossils and the evolutionary tree of rodents and lagomorphs. *Royal Society Open Science* **6**, doi:10.1098/rsos.190387 (2019).
 - 39 Swanson, M. T., Oliveros, C. H. & Esselstyn, J. A. A phylogenomic rodent tree reveals the repeated evolution of masseter architectures. *Proceedings. Biological sciences / The Royal Society* **286**, 20190672, doi:10.1098/rspb.2019.0672 (2019).
 - 40 Thewissen, J. G. M., Williams, E. M., Roe, L. J. & Hussain, S. T. Skeletons of terrestrial cetaceans and the relationship of whales to artiodactyls. *Nature* **413**, 277-281 (2001).
 - 41 Marivaux, L., Vianey-Liaud, M. & Jaeger, J.-J. High-level phylogeny of early Tertiary rodents: dental evidence. *Zoological Journal of the Linnean Society* **142**, 105-134 (2004).
 - 42 Shevyreva, N. S. in *Flora i fauna Zaysanskoi vpadiny [Flora and fauna of Zaysan Basin]* (ed L. K. Gabuniya) 77–114 (Akademiya Nauk Gruzinskoy SSR, 1984).
 - 43 Lucas, S. G. in *Late Paleocene–Early Eocene climatic and biotic events in the marine and terrestrial records* (eds M. P. Aubry, S. G. Lucas, & W. A. Berggren) 451-500 (Columbia University Press, 1998).
 - 44 Emry, R. J., Tyutkova, L. A., Lucas, S. G. & Wang, B. Rodents of the middle Eocene Shinhualy fauna of Eastern Kazakhstan. *Journal of Vertebrate Paleontology* **18**, 218-227 (1998).
 - 45 Emry, R. J. The Middle Eocene North American myomorph rodent *Elymys*, her Asian sister *Aksyiromys*, and other Eocene myomorphs. *Bulletin of the Carnegie Museum of Natural History* **39**, 141-150 (2007).
 - 46 dos Reis, M. *et al.* Phylogenomic datasets provide both precision and accuracy in estimating the timescale of placental mammal phylogeny. *Proceedings of the Royal Society B: Biological Sciences* **279**, 3491-3500, doi:10.1098/rspb.2012.0683 (2012).
 - 47 Benton, M. J., Donoghue, P. C. J. & Asher, R. J. in *The timetree of Life* (eds S. B. Hedges & S. Kumar) 35-86 (Cambridge University Press, 2009).
 - 48 Holbrook, L. T. On the skull of *Radinskya* (Mammalia) and its phylogenetic position. *Journal of Vertebrate Paleontology* **34** (2014).
 - 49 Rose, K. D. *et al.* Early Eocene fossils suggest that the mammalian order Perissodactyla originated in India. *Nat Commun* **5**, 5570, doi:10.1038/ncomms5570 (2014).
 - 50 Beard, K. C. East of Eden: Asia is an important center of taxonomic origination in mammalian evolution. *Bulletin of the Carnegie Museum of Natural History* **34**, 5-39 (1998).
 - 51 Meng, J., Zhai, R. J. & Wyss, A. R. The late Paleocene Bayan Ulan fauna of Inner Mongolia,

- China. *Bulletin of the Carnegie Museum of Natural History* **34**, 148-185 (1998).
- 52 Hassanin, A. *et al.* Pattern and timing of diversification of Cetartiodactyla (Mammalia, Laurasiatheria), as revealed by a comprehensive analysis of mitochondrial genomes. *C R Biol* **335**, 32-50, doi:10.1016/j.crv.2011.11.002 (2012).
 - 53 Wesley-Hunt, G. D. & Flynn, J. J. Phylogeny of the Carnivora: Basal relationships among the carnivoramorphans, and assessment of the position of 'Miacoidea' relative to Carnivora. *Journal of Systematic Palaeontology* **3**, 1-28, doi:10.1017/s1477201904001518 (2005).
 - 54 Bryant, H. The Carnivora of the Lac Pelletier Lower Fauna (Eocene: Duchesnean), Cypress Hills Formation, Saskatchewan. *Journal of Paleontology* **66**, 847-855 (1992).
 - 55 Hooker, J. J. A primitive emballonurid bat (Chiroptera, Mammalia) from the earliest Eocene of England. *Palaeovertebrata* **25**, 287-300 (1996).
 - 56 Eiting, T. P. & Gunnell, G. F. Global completeness of the bat fossil record. *Journal of Mammalian Evolution* **16**, 151-173, doi:10.1007/s10914-009-9118-x (2009).
 - 57 Tabuce, R., Telles Antunes, M. & Sigé, B. A new primitive bat from the earliest Eocene of Europe. *Journal of Vertebrate Paleontology* **29**, 627-630 (2009).
 - 58 Hand, S., Novacek, M., Godthelp, H. & Archer, M. First Eocene bat from Australia. *Journal of Vertebrate Paleontology* **14**, 375-381, doi:10.1080/02724634.1994.10011565 (1994).
 - 59 Beard, K. C., Sigé, B. & Krishtalka, L. A primitive vespertilionoid bat from the early Eocene of central Wyoming. *Comptes rendus de l'Académie des sciences. Série 2, Mécanique, Physique, Chimie, Sciences de l'univers, Sciences de la Terre* **314**, 735-741 (1992).
 - 60 Sigé, B. Morphologie dentaire lactéale d'un Chiroptère de l'Éocène inférieur-moyen d'Europe. *Geobios* **24**, 231-236 (1991).
 - 61 Ravel, A. *et al.* New philisids (Mammalia, Chiroptera) from the Early–Middle Eocene of Algeria and Tunisia: new insight into the phylogeny, palaeobiogeography and palaeoecology of the Philisidae. *Journal of Systematic Palaeontology* **13**, 691-709, doi:10.1080/14772019.2014.941422 (2014).
 - 62 Smith, T., Habersetzer, J., Simmons, N. B. & Gunnell, G. F. in *Evolutionary History of Bats: Fossils, Molecules and Morphology* (eds G. F. Gunnell & N. B. Simmons) 23-66 (Cambridge University Press, 2012).
 - 63 Gheerbrant, E. Paleocene emergence of elephant relatives and the rapid radiation of African ungulates. *Proceedings of the National Academy of Sciences* **106**, 10717-10721, doi:10.1073/pnas.0900251106 (2009).
 - 64 Meredith, R. W. *et al.* Impacts of the Cretaceous Terrestrial Revolution and KPg extinction on mammal diversification. *Science* **334**, 521-524, doi:10.1126/science.1211028 (2011).
 - 65 McCormack, J. E. *et al.* Ultraconserved elements are novel phylogenomic markers that resolve placental mammal phylogeny when combined with species-tree analysis. *Genome Res* **22**, 746-754, doi:10.1101/gr.125864.111 (2012).
 - 66 Asher, R. J. A web-database of mammalian morphology and a reanalysis of placental phylogeny. *BMC Evol Biol* **7**, 108, doi:10.1186/1471-2148-7-108 (2007).

- 67 Springer, M. S. *et al.* Interordinal gene capture, the phylogenetic position of Steller's sea cow based on molecular and morphological data, and the macroevolutionary history of Sirenia. *Mol Phylogenet Evol* **91**, 178-193, doi:10.1016/j.ympev.2015.05.022 (2015).
- 68 Woodburne, M. O., Pledge, N. S. & Archer, M. in *Possums and Opossums: Studies in Evolution* (ed M. Archer) 581-602 (Surrey Beatty and Sons, 1987).
- 69 Black, K. H., Archer, M. & Hand, S. J. New Tertiary koala (Marsupialia, Phascolarctidae) from Riversleigh, Australia, with a revision of phascolarctid phylogenetics, paleoecology, and paleobiodiversity. *Journal of Vertebrate Paleontology* **32**, 125-138 (2012).
- 70 Woodburne, M. O. *et al.* Land mammal biostratigraphy and magnetostratigraphy of the Etadunna Formation (late Oligocene) of South Australia. *Journal of Vertebrate Paleontology* **13**, 483-515, doi:10.1080/02724634.1994.10011527 (1994).
- 71 Mitchell, K. J. *et al.* Molecular phylogeny, biogeography, and habitat preference evolution of marsupials. *Mol Biol Evol* **31**, 2322-2330, doi:10.1093/molbev/msu176 (2014).
- 72 Megirian, D., Prideaux, G., Murray, P. & Smit, N. An Australian land mammal age biochronological scheme. *Paleobiology* **36**, 658-671 (2010).
- 73 Woodburne, M. O. *et al.* Land mammal biostratigraphy and magnetostratigraphy of the Etadunna Formation (late Oligocene) of South Australia. *Journal of Vertebrate Palaeontology* **13**, 483-515 (1993).
- 74 Janis, C. M. *et al.* Palaeoecology of Oligo-Miocene macropodoids determined from craniodental and calcaneal data. *Memoirs of Museum Victoria* **74**, 209-232 (2016).
- 75 Simpson, G. G. The Argyrolagidae, extinct South American marsupials. *Bulletin of the Museum of Comparative Zoology* **139**, 1-86 (1970).
- 76 Kirsch, J. A. W., Lapointe, F.-J. & Springer, M. S. DNA-hybridisation studies of marsupials and their implications for metatherian classification. *Australian Journal of Zoology* **45**, 211-280 (1997).
- 77 Asher, R. J., Horovitz, I. & Sanchez-Villagra, M. R. First combined cladistic analysis of marsupial mammal interrelationships. *Mol Phylogenet Evol* **33**, 240-250, doi:10.1016/j.ympev.2004.05.004 (2004).
- 78 Phillips, M. J., McLenachan, P. A., Down, C., Gibb, G. C. & Penny, D. Combined mitochondrial and nuclear DNA sequences resolve the interrelations of the major Australasian marsupial radiations. *Syst Biol* **55**, 122-137, doi:10.1080/10635150500481614 (2006).
- 79 Beck, R. M. An 'ameridelphian' marsupial from the early Eocene of Australia supports a complex model of Southern Hemisphere marsupial biogeography. *Naturwissenschaften* **99**, 715-729 (2012).
- 80 Asher, R. J. & Helgen, K. M. Nomenclature and placental mammal phylogeny. *BMC Evolutionary Biology* **10**, 102 (2010).
- 81 Babot, J., López, D. A. G. & Gaudin, T. J. The most ancient xenarthran petrosal: morphology and evolutionary significance. *Journal of Vertebrate Paleontology* **32**, 1186-1197, doi:10.1080/02724634.2012.686466 (2012).
- 82 Ciancio, M., Herrera, C., Aramayo, A., Payrola, P. & Babot, M. Diversity of cingulates (Mammalia, Xenarthra) in the middle-late Eocene of Northwestern Argentina. *Acta Palaeontologica Polonica*

- 61**, doi:10.4202/app.00208.2015 (2016).
- 83 DeCelles, P. G., Carrapa, B. & Gehrels, G. E. Detrital zircon U-Pb ages provide provenance and chronostratigraphic information from Eocene synorogenic deposits in northwestern Argentina. *Geology* **35**, doi:10.1130/g23322a.1 (2007).
 - 84 Woodburne, M. O. *et al.* Revised timing of the South American early Paleogene land mammal ages. *Journal of South American Earth Sciences* **54**, 109-119, doi:10.1016/j.jsames.2014.05.003 (2014).
 - 85 Simpson, G. G. *Menatherium*, Eocene mammal from France. *American Journal of Science* **246**, 165, doi:10.2475/ajs.246.3.165 (1948).
 - 86 McKenna, M. C., Wyss, A. R. & Flynn, J. J. Paleogene pseudoglyptodont xenarthrans from central Chile and Argentine Patagonia. *American Museum Novitates* **3536**, 1-18 (2006).
 - 87 Delsuc, F. *et al.* The phylogenetic affinities of the extinct glyptodonts. *Current biology : CB* **26**, R155-156, doi:10.1016/j.cub.2016.01.039 (2016).
 - 88 Slater, G. J. *et al.* Evolutionary Relationships among Extinct and Extant Sloths: The Evidence of Mitogenomes and Retroviruses. *Genome Biol Evol* **8**, 607-621, doi:10.1093/gbe/evw023 (2016).
 - 89 Gaudin, T. J. & Croft, D. A. Paleogene Xenarthra and the evolution of South American mammals. *Journal of Mammalogy* **96**, 622-634, doi:10.1093/jmammal/gyv073 (2015).
 - 90 Flynn, J. J., Wyss, A. R., Croft, D. A. & Charrier, R. The Tinguiririca Fauna, Chile: biochronology, paleoecology, biogeography, and a new earliest Oligocene South American Land Mammal 'Age'. *Palaeogeography, Palaeoclimatology, Palaeoecology* **195**, 229-259, doi:10.1016/s0031-0182(03)00360-2 (2003).
 - 91 MacPhee, R. D. & Iturralde-Vinent, M. First Tertiary land mammal from Greater Antilles: an Early Miocene sloth. *3094* (1994).
 - 92 Pujos, F., Gaudin, T. J., De Iuliis, G. & Cartelle, C. Recent Advances on Variability, Morpho-Functional Adaptations, Dental Terminology, and Evolution of Sloths. *Journal of Mammalian Evolution* **19**, 159-169, doi:10.1007/s10914-012-9189-y (2012).
 - 93 MacPhee, R. D., Iturralde-Vinent, M. & Gaffney, E. S. Domo de Zaza, an Early Miocene vertebrate locality in south-central Cuba, with notes on the tectonic evolution of Puerto Rico and the Mona Passage. *American Museum Novitates* **3394**, 1-42 (2003).
 - 94 Bargo, M. S., Toledo, N. & Vizcaíno, S. F. in *Early Miocene paleobiology in Patagonia. High latitude paleocommunities of the Santa Cruz Formation* (eds S. F. Vizcaíno, R. F. Kay, & M. S. Bargo) 216-242 (Cambridge University Press, 2012).
 - 95 Gaudin, T. J. & Branham, D. G. The phylogeny of the Myrmecophagidae (Mammalia, Xenarthra, Vermilingua) and the relationship of Eurotamandua to the Vermilingua. *Journal of Mammalian Evolution* **5**, 237-265 (1998).
 - 96 Ameghino, F. Nuevas especies de mamíferos cretáceos y terciarios de la República Argentina. *Anales Soc. Cient. Arg.* **56-58** (1904).
 - 97 Hirschfeld, S. E. A new fossil anteater (Edentata, Mammalia) from Colombia, S.A. and evolution of the Vermilingua. *Journal of Paleontology* **50**, 419-432 (1976).

- 98 Kay, R. F., Vizcaíno, S. F. & Bargo, M. S. in *Early Miocene paleobiology in Patagonia: High-latitude paleocommunities of the Santa Cruz Formation* (eds S. F. Vizcaíno, R. F. Kay, & M. S. Bargo) 331-365 (Cambridge University Press, 2012).
- 99 Fleagle, J. G. *et al.* in *Early Miocene paleobiology in Patagonia: High-latitude paleocommunities of the Santa Cruz Formation* (eds S. F. Vizcaíno, R. F. Kay, & M. S. Bargo) 41-58 (Cambridge University Press, 2012).
- 100 Perkins, M. E. *et al.* in *Early Miocene paleobiology in Patagonia: High-latitude paleocommunities of the Santa Cruz Formation* (eds S. F. Vizcaíno, R. F. Kay, & M. S. Bargo) 23-40 (Cambridge University Press, 2012).
- 101 Asher, R. J. & Avery, D. M. New golden moles (Afrotheria, Chrysochloridae) from the early Pliocene of South Africa. *Paleontologia Electronica* **13**, 13.11.13A (2010).
- 102 Butler, P. M. Macroscelidea, Insectivora, and Chiroptera from the Miocene of East Africa. *Palaeovertebrata* **14**, 117-200 (1984).
- 103 Broom, R. On two Pleistocene golden moles. *Annals of the Transvaal Museum* **20**, 215-216 (1941).
- 104 Asher, R. J. Recent additions to the fossil record of tenrecs and golden moles. *Afrotherian Conservation* **15**, 4-13 (2019).
- 105 Stevens, N. J., O'Connor, P. M., Mtelela, C. & Roberts, E. M. Macroscelideans (Myohyracinae and Rhynchocyoninae) from the late Oligocene Nsungwe formation of the Rukwa Rift Basin, southwestern Tanzania. *Historical Biology*, 1-7, doi:10.1080/08912963.2021.1938565 (2021).
- 106 Tabuce, R. New remains of *Chambius kasserinensis* from the Eocene of Tunisia and evaluation of proposed affinities for Macroscelidea (Mammalia, Afrotheria). *Historical Biology* **30**, 251-266, doi:10.1080/08912963.2017.1297433 (2017).
- 107 Pickford, M. & Hlusko, L. J. Late Miocene procaviid hyracoids (Hyracoidea: *Dendrohyrax*) from Lemudong'o, Kenya. *Kirtlandia* **56**, 106-111 (2007).
- 108 Rasmussen, D. T. & Gutiérrez, M. in *Cenozoic mammals of Africa* (eds L. Werdelin & W. J. Sanders) 123-146 (University of California Press, 2010).
- 109 Emerling, C. A., Huynh, H. T., Nguyen, M. A., Meredith, R. W. & Springer, M. S. Spectral shifts of mammalian ultraviolet-sensitive pigments (short wavelength-sensitive opsin 1) are associated with eye length and photic niche evolution. *Proceedings. Biological sciences / The Royal Society* **282**, doi:10.1098/rspb.2015.1817 (2015).
- 110 Bloch, J. I. *et al.* First North American fossil monkey and early Miocene tropical biotic interchange. *Nature* **533**, 243-246, doi:10.1038/nature17415 (2016).
- 111 Chester, S. G., Bloch, J. I., Boyer, D. M. & Clemens, W. A. Oldest known euarchontan tarsals and affinities of Paleocene Purgatorius to Primates. *Proceedings of the National Academy of Sciences* **112**, 1487-1492 (2015).
- 112 Clemens, W. A. Purgatorius (Plesiadapiformes, Primates?, Mammalia), a Paleocene immigrant into northeastern Montana: stratigraphic occurrences and incisor proportions. *Bulletin of Carnegie Museum of Natural History* **2004**, 3-13 (2004).

- 113 Jiménez-Hidalgo, E., Smith, K. T., Guerrero-Arenas, R. & Alvarado-Ortega, J. The first Late Eocene continental faunal assemblage from tropical North America. *Journal of South American Earth Sciences* **57**, 39-48, doi:10.1016/j.jsames.2014.12.001 (2015).
- 114 Orliac, M., Boisserie, J.-R., MacLatchy, L. & Lihoreau, F. Early Miocene hippopotamids (Cetartiodactyla) constrain the phylogenetic and spatiotemporal settings of hippopotamid origin. *Proceedings of the National Academy of Sciences* (2010).
- 115 Frantz, L. *et al.* The evolution of Suidae. *Annu Rev Anim Biosci* **4**, 61-85, doi:10.1146/annurev-animal-021815-111155 (2016).
- 116 Liu, L. *Chinese fossil Suoidea: Systematics, evolution, and paleoecology*. (University of Helsinki, 2003).
- 117 Boisserie, J. R., Lihoreau, F. & Brunet, M. The position of hippopotamidae within cetartiodactyla. *Proceedings of the National Academy of Sciences of the United States of America* **102**, 1537-1541 (2005).
- 118 Prothero, D. R. The early evolution of the North American peccaries (Artiodactyla: Tayassuidae). *Museum of Northern Arizona Bulletin* **65**, 509-541 (2009).
- 119 Waddell, P. J., Okada, N. & Hasegawa, M. Towards resolving the interordinal relationships of placental mammals. *Systematic Biology* **48**, 1-5 (1999).
- 120 Bajpai, S. & Gingerich, P. D. A new Eocene archaeocete (Mammalia, Cetacea) from India and the time of origin of whales. *Proceedings of the National Academy of Sciences, USA* **95**, 15464-15468 (1998).
- 121 Fordyce, R., Perrin, W., Würsig, B. & Thewissen, J. Encyclopedia of marine mammals. (2009).
- 122 Lambert, O. *et al.* Earliest mysticete from the Late Eocene of Peru sheds new light on the origin of Baleen Whales. *Current biology : CB* **27**, 1535-1541 e1532, doi:10.1016/j.cub.2017.04.026 (2017).
- 123 Fordyce, R. E. & Marx, F. G. Gigantism precedes filter feeding in baleen whale evolution. *Current biology : CB* **28**, 1670-1676 e1672, doi:10.1016/j.cub.2018.04.027 (2018).
- 124 Martini, E. in *Second Planktonic Conference*,. 739–785.
- 125 Agnini, C. *et al.* Biozonation and biochronology of Paleogene calcareous nannofossils from low and middle latitudes. *Newsletter in Stratigraphy* **47**, 131-181 (2014).
- 126 Tsai, C. H. & Fordyce, R. E. Archaic baleen whale from the Kokoamu Greensand: earbones distinguish a new late Oligocene mysticete (Cetacea: Mysticeti) from New Zealand. *Journal of the Royal Society of New Zealand* **46**, 117-138, doi:10.1080/03036758.2016.1156552 (2016).
- 127 Cabrera, A. Cetáceos fósiles del Museo de La Plata. *Revista del Museo de la Plata* **29**, 363-411 (1926).
- 128 Bueno, M. R., Fernández, M. S., Cozzuol, M. A., Cuitiño, J. I. & Fitzgerald, E. M. G. The early Miocene balaenid *Morenocetus parvus* from Patagonia (Argentina) and the evolution of right whales. *PeerJ*, e4148, doi:10.7717/peerj.4148 (2017).
- 129 Fordyce, R. E. Oligocene origin of skim-feeding right whales: a small archaic balaenid from New

- Zealand. *Journal of Vertebrate Paleontology* **22**, 54(A) (2002).
- 130 Dunn, R. E. *et al.* A new chronology for middle Eocene-early Miocene South American Land Mammal Ages. *Geological Society of America Bulletin* **125**, 539-555, doi:10.1130/b30660.1 (2012).
 - 131 Boersma, A. T. & Pyenson, N. D. *Arktocara yakataga*, a new fossil odontocete (Mammalia, Cetacea) from the Oligocene of Alaska and the antiquity of Platanistoidea. *PeerJ* **4**, e2321, doi:10.7717/peerj.2321 (2016).
 - 132 Geisler, J. H., McGowen, M. R., Yang, G. & Gatesy, J. A supermatrix analysis of genomic, morphological, and paleontological data from crown Cetacea. *BMC Evolutionary Biology* **11**, 112 (2011).
 - 133 Kellogg, R. *Kentriodon pernix*, a Miocene porpoise from Maryland. *Proceedings of the U. S. National Museum* **69**, 1-72 (1927).
 - 134 Browning, J. V. *et al.* Quantification of the effects of eustasy, subsidence, and sediment supply on Miocene sequences, mid-Atlantic margin of the United States. *Geological Society of America Bulletin* **118**, 567-588, doi:10.1130/b25551.1 (2006).
 - 135 Wilson, L. E. A delphinid (Mammalia, Cetacea) from the Miocene of Palos Verdes Hills, California. *University of California Publications in Geological Sciences* **103**, 1-34 (1973).
 - 136 Barnes, L. G. Evolution, taxonomy and antitropical distributions of the porpoises Phocoenidae, Mammalia). *Marine Mammal Science* **1**, 149-165 (1985).
 - 137 Fajardo-Mellor, L., Berta, A., Brownell, R. L., Boy, C. C. & Natalie P. Goodall, R. The phylogenetic relationships and biogeography of true porpoises (Mammalia: Phocoenidae) based on morphological data. *Marine Mammal Science* **22**, 910-932, doi:10.1111/j.1748-7692.2006.00080.x (2006).
 - 138 Xiong, Y., Brandley, M. C., Xu, S., Zhou, K. & Yang, G. Seven new dolphin mitochondrial genomes and a time-calibrated phylogeny of whales. *BMC Evol Biol* **9**, 20, doi:10.1186/1471-2148-9-20 (2009).
 - 139 Chen, Z., Xu, S., Zhou, K. & Yang, G. Whale phylogeny and rapid radiation events revealed using novel retroposed elements and their flanking sequences. *BMC Evolutionary Biology* **11**, 314 (2011).
 - 140 Galatius, A. *et al.* Raising your voice: evolution of narrow-band high-frequency signals in toothed whales (Odontoceti). *Biological Journal of the Linnean Society* **126**, 213-224 (2019).
 - 141 Rowell, H. C. in *The Monterey Formation and related siliceous rocks of California* (eds R. E. Garrison *et al.*) 56-70 (SEPM, 1981).
 - 142 Boisserie, J.-R. *et al.* Basal hippopotamines from the upper Miocene of Chorora, Ethiopia. *Journal of Vertebrate Paleontology* **37**, doi:10.1080/02724634.2017.1297718 (2017).
 - 143 Lihoreau, F., Boisserie, J. R., Manthi, F. K. & Ducrocq, S. Hippos stem from the longest sequence of terrestrial cetartiodactyl evolution in Africa. *Nat Commun* **6**, 6264, doi:10.1038/ncomms7264 (2015).
 - 144 Zurano, J. P. *et al.* Cetartiodactyla: Updating a time-calibrated molecular phylogeny. *Mol*

- Phylogenet Evol* **133**, 256-262, doi:10.1016/j.ympev.2018.12.015 (2019).
- 145 Danowitz, M., Vasilyev, A., Kortlandt, V. & Solounias, N. Fossil evidence and stages of elongation of the *Giraffa camelopardalis* neck. *R Soc Open Sci* **2**, 150393, doi:10.1098/rsos.150393 (2015).
- 146 Samiullah, K. *et al.* A new discovery of a *Giraffokeryx* skull and associated fossil assemblage of Ruminants from the Middle Miocene deposits of the Siwaliks. *Historical Biology*, 1-25, doi:10.1080/08912963.2021.1946529 (2021).
- 147 Hamilton, W. R. Fossil giraffes from the Miocene of Africa and a revision of the phylogeny of the Giraffoidea. *Philosophical Transactions of the Royal Society B-Biological Sciences* **283**, 165-229 (1973).
- 148 Solounias, N. I. in *The evolution of artiodactyls* (eds D. R. Prothero & S. E. Foss) 257-277 (Johns Hopkins University Press, 2007).
- 149 Solounias, N. & Moelleken, S. M. C. Evidence for the presence of ossicones in *Giraffokeryx punjabiensis*. *Journal of Mammalogy* **72**, 215-217 (1991).
- 150 Barry, J. C., Johnson, N. M., Raza, S. M. & Jacobs, L. L. Neogene mammalian faunal change in southern Asia: correlations with climatic, tectonic, and eustatic events. *Geology* **13**, 637-640 (1985).
- 151 Bibi, F. A multi-calibrated mitochondrial phylogeny of extant Bovidae (Artiodactyla, Ruminantia) and the importance of the fossil record to systematics. *BMC Evolutionary Biology* **13**, 1-15 (2013).
- 152 Pilgrim, G. E. & Brown, B. Siwalik antelopes and oxen in the American Museum of Natural History. *Bulletin of the American Museum of Natural History* **72**, 729-874 (1937).
- 153 Bibi, F. Origin, paleoecology, and paleobiogeography of early Bovini. *Palaeogeography, Palaeoclimatology, Palaeoecology* **248**, 60-72, doi:10.1016/j.palaeo.2006.11.009 (2007).
- 154 Badgley, C. *et al.* Ecological changes in Miocene mammalian record show impact of prolonged climatic forcing. *Proc Natl Acad Sci U S A* **105**, 12145-12149, doi:10.1073/pnas.0805592105 (2008).
- 155 Haile-Selassie, Y., Vrba, E. S. & Bibi, F. in *Ardipithecus kadabba: Late Miocene Evidence from the Middle Awash, Ethiopia* (eds Y. Haile-Selassie & G. WoldeGabriel) 277-330 (University of California Press, 2007).
- 156 WoldeGabriel, G. *et al.* Geology and palaeontology of the Late Miocene Middle Awash valley, Afar rift, Ethiopia. *Nature* **412**, 175-178 (2001).
- 157 Renne, P. R., WoldeGabriel, G., Hart, W. K., Heiken, G. & White, T. D. Chronostratigraphy of the Miocene–Pliocene Sagantole Formation, Middle Awash Valley, Afar rift, Ethiopia. *GSA Bulletin* **111**, 869-885 (1999).
- 158 Geraads, D. *et al.* New hippotragini (Bovidae, Mammalia) from the Late Miocene of Toros-Menalla (Chad). *Journal of Vertebrate Paleontology* **28**, 231-242, doi:10.1671/0272-4634(2008)28[231:Nhbmft]2.0.Co;2 (2008).
- 159 Lebatard, A. E. *et al.* Cosmogenic nuclide dating of *Sahelanthropus tchadensis* and *Australopithecus bahrelghazali*: Mio-Pliocene hominids from Chad. *Proc Natl Acad Sci U S A*

- 105**, 3226-3231, doi:10.1073/pnas.0708015105 (2008).
- 160 Gentry, A. W. Fossil Bovidae (Mammalia) from Langebaanweg, South Africa. *Annals of the South African Museum* **79**, 213-337 (1980).
- 161 Vrba, E. S. New fossils of Alcelaphini and Caprinae (Bovidae: Mammalia) from Awash, Ethiopia, and phylogenetic analysis of Alcelaphini. *Palaeont. afr.* **34**, 127-198 (1997).
- 162 Faith, J. T., Choiniere, J. N., Tryon, C. A., Peppe, D. J. & Fox, D. L. Taxonomic status and paleoecology of Rusingoryx atopocranion (Mammalia, Artiodactyla), an extinct Pleistocene bovid from Rusinga Island, Kenya. *Quaternary Research* **75**, 697-707, doi:10.1016/j.yqres.2010.11.006 (2017).
- 163 Roberts, D. L. *et al.* Regional and global context of the Late Cenozoic Langebaanweg (LBW) palaeontological site: West Coast of South Africa. *Earth-Science Reviews* **106**, 191-214, doi:10.1016/j.earscirev.2011.02.002 (2011).
- 164 Adrover, R., Alcalá, L., Paricio, J., Mein, P. & Moissenet, F. Dos nuevos yacimientos de vertebrados terciarios continentales: La Roma II (Alfambra, Teruel) y Búnker de Valdecebro (Teruel). *Teruel* **67**, 7-21 (1982).
- 165 Alcalá, L. *Macromammíferous neógenos de la fose de Alfambra-Teruel*. (Instituto de Estudios Terulenses-Museo Nacional de Ciencias Naturales, 1994).
- 166 Alcalá, L. & Morales, J. A primitive caprine from the Upper Vallesian of La Roma 2 (Alfambra, Teruel, Aragon, Spain). *Comptes Rendus de l'Académie des Sciences - Series IIA - Earth and Planetary Science* **324**, 947-953 (1997).
- 167 Vrba, E. S. & Schaller, G. *Antelopes, deer, and relatives: fossil record, behavioral ecology, systematics, and conservation*. (Yale University Press, 2000).
- 168 Van Dam, J. A. *et al.* The upper Miocene mammal record from the Teruel-Alfambra region (Spain). The MN system and continental stage/age concepts discussed. *Journal of Vertebrate Paleontology* **21**, 367-385, doi:10.1671/0272-4634(2001)021[0367:Tummr]2.0.Co;2 (2001).
- 169 Hilgen, F. J., Lourens, L. J. & Van Dam, J. A. in *The Geologic Times Scale 2012* (eds F. M. Gradstein, J. G. Ogg, M. Schmitz, & G. Ogg) 923-978 (Elsevier, 2012).
- 170 Rössner, G. E. Odontologische und schädelanatomische Untersuchungen an Procervulus (Cervidae, Mammalia). *Münchner geowissenschaftliche Abhandlungen, Reihe A* **29**, 1-127 (1995).
- 171 Rössner, G. E. Systematics and palaeoecology of Ruminantia (Artiodactyla, Mammalia) from the Miocene of Sandelzhausen (southern Germany, Northern Alpine Foreland Basin). *Paläontologische Zeitschrift* **84**, 123-162, doi:10.1007/s12542-010-0052-2 (2010).
- 172 Agustí, J. *et al.* A calibrated mammal scale for the Neogene of Western Europe. State of the art. *Earth-Science Reviews* **52**, 247-260, doi:[https://doi.org/10.1016/S0012-8252\(00\)00025-8](https://doi.org/10.1016/S0012-8252(00)00025-8) (2001).
- 173 Costeur, L. A partial skull of *Dremotherium feignouxii* from the Aquitanian of France (MN2, Saint-Gérard-le-Puy, Allier). *Acta Geologica Slovaca* **3**, 105-111 (2011).
- 174 Janis, C. M. & Scott, K. M. The interrelationships of higher ruminant families: with special emphasis on the members of the Cervoidea. *American Museum Novitates* **2893**, 1-85 (1987).

- 175 Fordyce, R. E. & Marx, F. G. The pygmy right whale *Caperea marginata*: the last of the cetotheres. *Proceedings. Biological sciences / The Royal Society* **280**, 20122645, doi:10.1098/rspb.2012.2645 (2013).
- 176 Fordyce, E. New specimen of archaic baleen whale *Mauicetus parki* (Late Oligocene, New Zealand) elucidates early crown-mysticeti. *Journal of Vertebrate Paleontology* **25**, 58A-58A (2005).
- 177 Marx, F. G. & Fordyce, R. E. Baleen boom and bust: a synthesis of mysticete phylogeny, diversity and disparity. *R Soc Open Sci* **2**, 140434, doi:10.1098/rsos.140434 (2015).
- 178 Lloyd, G. T. & Slater, G. J. A total-group phylogenetic metatree for Cetacea and the importance of fossil data in diversification analyses. *Syst Biol*, doi:10.1093/sysbio/syab002 (2021).
- 179 Graham, I. J., Morgans, H. E., Waghorn, D. B., Trotter, J. A. & Whitford, D. J. Strontium isotope stratigraphy of the Oligocene-Miocene Otekaike Limestone (Trig Z section) in southern New Zealand: age of the Duntroonian/Waitakian Stage boundary. *New Zealand Journal of Geology and Geophysics* **43**, 335-347 (2000).
- 180 Marx, F. G. & Kohno, N. A new Miocene baleen whale from the Peruvian desert. *R Soc Open Sci* **3**, 160542, doi:10.1098/rsos.160542 (2016).
- 181 Kellogg, R. Two physeteroid whales from California. *Contributions to Palaeontology from the Carnegie Institution of Washington* **348**, 1-35 (1925).
- 182 Collareta, A., Lambert, O., de Muizon, C., Urbina, M. & Bianucci, G. *Koristocetus pescei* gen. et sp. nov., a diminutive sperm whale (Cetacea: Odontoceti: Kogiidae) from the late Miocene of Peru. *Fossil Record* **20**, 259-278, doi:10.5194/fr-20-259-2017 (2017).
- 183 Kapur, V. V. & Bajpai, S. Oldest South Asian tapiromorph (Perissodactyla, Mammalia) from the Cambay Shale Formation, western India, with comments on its phylogenetic position and biogeographic implications. *The Palaeobotanist* **64**, 95-103 (2015).
- 184 Bai, B., Meng, J., Janis, C. M., Zhang, Z. Q. & Wang, Y. Q. Perissodactyl diversities and responses to climate changes as reflected by dental homogeneity during the Cenozoic in Asia. *Ecology and Evolution* **10**, 6333-6355 (2020).
- 185 Sato, J. J. *et al.* Deciphering and dating the red panda's ancestry and early adaptive radiation of Musteloidea. *Molecular Phylogenetics and Evolution* **53**, 907-922 (2009).
- 186 Wolsan, M. & Lange-Badré, B. An arctomorph carnivoran skull from the Phosphorites du Quercy and the origin of procyonids. *Acta Palaeontologica Polonica* **41**, 277-298 (1996).
- 187 Sato, J. J. *et al.* Phylogenetic relationships and divergence times among mustelids (Mammalia: Carnivora) based on nucleotide sequences of the nuclear interphotoreceptor retinoid binding protein and mitochondrial cytochrome b genes. *Zoological Science* **20**, 243-264 (2003).
- 188 Vandenberghe, N., Hilgen, F. J. & Speijer, R. P. in *The geologic timescale 2012* (eds F. M. Gradstein, J. G. Ogg, M. Schmitz, & G. Ogg) 855-921 (Elsevier, 2012).
- 189 Werdelin, L., Yamaguchi, N., Johnson, W. E. & O'Brien, S. J. Phylogeny and evolution of cats (Felidae). *Biology and conservation of wild felids*, 59-82 (2010).
- 190 Flynn, J. J. & Wesley-Hunt, G. D. in *The rise of placental mammals: origins and relationships of*

- the major extant clades* (eds K. D. Rose & J. D. Archibald) 175-198 (Johns Hopkins University Press, 2005).
- 191 Hunt Jr, R. M. Evolution of the aeluroid Carnivora. Diversity of the earliest aeluroids from Eurasia (Quercy, Hsanda-Gol) and the origin of felids. *American Museum novitates*; no. 3252. (1998).
 - 192 Barycka, E. Evolution and systematics of the feliform Carnivora. *Mammalian Biology* **72**, 257-282 (2007).
 - 193 Phillips, M. J. & Fruciano, C. The soft explosive model of placental mammal evolution. *BMC Evol Biol* **18**, 104, doi:10.1186/s12862-018-1218-x (2018).
 - 194 Janis, C. M., Damuth, J. & Theodor, J. M. Miocene ungulates and terrestrial primary productivity: where have all the browsers gone? *Proceedings of the National Academy of Sciences* **97**, 7899-7904 (2000).
 - 195 Patou, M.-L. *et al.* Phylogenetic relationships of the Asian palm civets (Hemigalinae & Paradoxurinae, Viverridae, Carnivora). *Molecular Phylogenetics and Evolution* **47**, 883-892 (2008).
 - 196 Hunt Jr, R. M. Evolution of the aeluroid Carnivora. Viverrid affinities of the Miocene carnivoran Herpestides. *American Museum novitates*; no. 3023. (1991).
 - 197 Gaubert, P. & Cordeiro-Estrela, P. Phylogenetic systematics and tempo of evolution of the Viverrinae (Mammalia, Carnivora, Viverridae) within feliformians: implications for faunal exchanges between Asia and Africa. *Molecular Phylogenetics and Evolution* **41**, 266-278 (2006).
 - 198 Fulton, T. L. & Strobeck, C. Multiple fossil calibrations, nuclear loci and mitochondrial genomes provide new insight into biogeography and divergence timing for true seals (Phocidae, Pinnipedia). *Journal of Biogeography* **37**, 814-829 (2010).
 - 199 Govender, R. Preliminary phylogenetics and biogeographic history of the Pliocene seal, *Homiphoca capensis* from Langebaanweg, South Africa. *Transactions of the Royal Society of South Africa* **70**, 25-39 (2015).
 - 200 Govender, R. Fossil cetaceans from Duinefontein (Koeberg) an early Pliocene site on the southwestern Cape, South Africa. *Palaeontologia Electronica* **22**, 1-21 (2019).
 - 201 Roberts, D. L. *et al.* Regional and global context of the Late Cenozoic Langebaanweg (LBW) palaeontological site: West Coast of South Africa. *Earth-Science Reviews* **106**, 191-214 (2011).
 - 202 Dewaele, L., Lambert, O. & Louwye, S. A critical revision of the fossil record, stratigraphy and diversity of the Neogene seal genus *Monotherium* (Carnivora, Phocidae). *R Soc Open Sci* **5**, 171669, doi:10.1098/rsos.171669 (2018).
 - 203 Ray, C. E. Geography of phocid evolution. *Systematic Zoology* **25**, 391-406 (1976).
 - 204 Repenning, C., Ray, C. & Grigorescu, D. (Oregon State University Press, Corvallis, OR, 1979).
 - 205 Deméré, T. A., Berta, A. & Adam, P. J. Chapter 3: Pinnipedimorph evolutionary biogeography. *Bulletin of the American Museum of Natural History*, 32-76 (2003).
 - 206 Yonezawa, T., Kohno, N. & Hasegawa, M. The monophyletic origin of sea lions and fur seals (Carnivora; Otariidae) in the Southern Hemisphere. *Gene* **441**, 89-99 (2009).

- 207 Deméré, T. A. & Berta, A. A reevaluation of *Proneotherium repenningi* from the Miocene Astoria Formation of Oregon and its position as a basal odobenid (Pinnipedia: Mammalia). *Journal of Vertebrate Paleontology* **21**, 279-310 (2001).
- 208 Berta, A. in *Encyclopedia of marine mammals* 712-722 (Elsevier, 2018).
- 209 Barnes, L. G. An early Miocene pinniped of the genus *Desmatophoca* (Mammalia: Otariidae) from Washington. *Contributions in Science* **382**, 1-20 (1987).
- 210 Berta, A. New *Enaliarctos* (Pinnipedimorpha) from the Oligocene and Miocene of Oregon and the role of "enaliarctids" in pinniped phylogeny. (1991).
- 211 Norris, R. Phylogenetic relationships and divergence times in rodents based on both genes and fossils. (2009).
- 212 Storch, G. & Seiffert, C. Extraordinarily preserved specimen of the oldest known glirid from the middle Eocene of Messel (Rodentia). *Journal of Vertebrate Paleontology* **27**, 189-194 (2007).
- 213 Verzi, D. H. & Quintana, C. A. The caviomorph rodents from the San Andrés Formation, east-central Argentina, and global Late Pliocene climatic change. *Palaeogeography, Palaeoclimatology, Palaeoecology* **219**, 303-320 (2005).
- 214 Teruggi, M. E., Andreis, R. R., Mazzoni, M. M., Dalla Salda, L. H. & Spalletti, L. A. in *Anales del LEMIT*.
- 215 Patterson, B. D. & Upham, N. S. A newly recognized family from the Horn of Africa, the Heterocephalidae (Rodentia: Ctenohystrica). *Zoological Journal of the Linnean Society* **172**, 942-963 (2014).
- 216 West, A. R. *Multidisciplinary investigations on the origins and evolution of the extinct ungulate order Notoungulata (Mammalia: Placentalia) and the extinct muskox genus Bootherium (Mammalia: Artiodactyla: Bovidae)*. (Columbia University, 2017).
- 217 Verzi, D. H., Olivares, A. I., Morgan, C. C. & Álvarez, A. Contrasting phylogenetic and diversity patterns in octodontoid rodents and a new definition of the family Abrocomidae. *Journal of Mammalian Evolution* **23**, 93-115 (2016).
- 218 Woodburne, M. O. & Tedford, R. H. The first Tertiary monotreme from Australia. *American Museum Novitates* **2588**, 1-11 (1975).
- 219 Poropat, S. F. *et al.* Early Cretaceous polar biotas of Victoria, southeastern Australia—an overview of research to date. *Alcheringa: An Australasian Journal of Palaeontology* **42**, 157-229, doi:10.1080/03115518.2018.1453085 (2018).
- 220 Seegets-Villiers, D. E. & Wagstaff, B. E. Morphological variation of stratigraphically important species in the genus *Pilosisorites* Delcourt & Sprumont, 1955 in the Gippsland Basin, southeastern Australia. *Memoirs of Museum Victoria* **74**, 81-91 (2016).
- 221 Holdgate, G. R., Wallace, M. W. & Forbes, S. Pre-Cenozoic geology of the Latrobe Valley Area—onshore Gippsland Basin, S.E. Australia. *Australian Journal of Earth Sciences*, 1-22, doi:10.1080/08120099.2015.1085901 (2015).
- 222 Musser, J. M. in *Evolution and biogeography of Australasian vertebrates* (eds J. Merrick, M. Archer, G. Hickey, & M. S. Y. Lee) 523-550 (Auscipub, 2006).

- 223 Pian, R., Archer, M., Hand, S. J., Beck, R. M. & Cody, A. The upper dentition and relationships of the enigmatic Australian Cretaceous mammal *Kollikodon ritchiei*. *Memoirs of Museum Victoria* **74**, 97-105 (2016).
- 224 Tedford, R., Wells, R. & Barghoorn, S. Tirari formation and contained faunas, Pliocene of the Lake Eyre basin, South Australia. *Beagle: Records of the Museums and Art Galleries of the Northern Territory, The* **9**, 173-193 (1992).
- 225 Mackness, B., Wroe, S., Muirhead, J., Wilkinson, C. & Wilkinson, D. First fossil bandicoots from the Pliocene. *Australian Mammalogy* **22**, 133-136 (2000).
- 226 Dawson, L. A new Pliocene tree kangaroo species (Marsupialia, Macropodinae) from the Chinchilla Local Fauna, southeastern Queensland. *Alcheringa* **28**, 267-273 (2004).
- 227 Gibbard, P. L. & Head, M. J. in *Geologic Time Scale 2020* Vol. 2 (eds F. M. Gradstein, J. G. Ogg, Schmitz, M. D., & G. M. Ogg) 1217-1255 (Elsevier, 2020).